Role of host-derived ADAM-9 in tumor invasion and metastasis of malignant melanoma

A dissertation
Submitted in partial fulfillment of the requirements for the award of
Doctor of Philosophy Degree
in the Faculty of Natural Science
University of Cologne

Submitted by

Ngum Anna Abety
from Bafou-Djuttitsa, Cameroon

Cologne 2012

For my Father

"I thank God every time I remember you. In all my prayers for you, I always pray with joy."

<div align="right">*Philippians 1:3-4*</div>

Table of content

Abstract

A Disintegrin And Metalloproteases (ADAMs) represents a family of transmembrane proteins with a distinct multidomain structure including a metalloprotease, disintegrin, and cysteine-rich domain. These proteins function in adhesion, regulation of cell signaling by proteolysis of cell surface proteins and their receptors. ADAM-9 is a protease that cleaves membrane-bound proteins such as VCAM-1, TNF-α, as well as extracellular matrix proteins like fibronectin and laminin-111. ADAM-9 also contains adhesive domains that are involved in cell adhesion and migration. In human and murine melanoma, ADAM-9 is expressed by both tumor and stroma cells at the tumor-stroma border. The significance of this expression is however not clear. To explore the functional role of ADAM-9 produced by the host in melanoma progression, B16F1 murine melanoma cells were injected in the flank of *Adam-9*$^{-/-}$ and wild type animals. Tumors developed in *Adam-9*$^{-/-}$ mice were significantly larger compared to wild type animals and displayed significant increase in tumor cell proliferation accompanied by decrease in apoptosis. Using co-culture systems of primary fibroblasts and B16F1 melanoma cells, we could detect increased melanoma cell proliferation when cultured in the presence of supernatants from *Adam-9*$^{-/-}$ but not wild type fibroblasts. Among the proteins secreted in strongly enhanced amounts from *Adam-9*$^{-/-}$ fibroblasts, was tissue inhibitor of metalloproteinases-1 (TIMP-1). Neutralization of TIMP-1 in *Adam-9*$^{-/-}$ fibroblasts supernatant using specific antibodies abolished the induced B16F1 proliferation. Besides TIMP-1, soluble TNF-α and TNFR1 were also up-regulated in *Adam-9*$^{-/-}$ fibroblasts supernatants. Using various *in vitro* approaches, we could demonstrate that neutralization of TNF-α in *Adam-9*$^{-/-}$ fibroblast resulted in reduced B16F1 cell apoptosis. In addition, by RNA and proteomic analysis, we found altered expression of extracellular matrix proteins at the tumor-stroma border of tumors from *Adam-9*$^{-/-}$ animals compared to wild type, which likely contributes to the melanoma phenotype observed in *Adam-9*$^{-/-}$ animals. Interestingly, we identified collagen type I as a new substrate of ADAM-9. In summary, our results indicate that loss of ADAM-9 in stromal fibroblasts results in altered release of soluble factors, which in turn affect melanoma cell proliferation and apoptosis.

Zusammenfassung

Die A Disintegrin and Metalloproteases (ADAMs) sind Transmembranproteine und weisen eine Multidomänen-Struktur mit einer Metalloprotease-, einer Disintegrin- und einer Cystein-reichen Domäne auf. ADAMs vermitteln Zelladhäsion und sind an zellulärer Signaltransduktion durch die Proteolyse von Oberflächenproteinen und deren Rezeptoren beteiligt. ADAM-9 ist eine aktive Protease, welche membrangebundene Proteine, wie z.B. VCAM-1 und TNF-α sowie Proteine der extrazellllulären Matrix wie Fibronectin und Laminin-111 prozessiert. ADAM-9 vermittelt ebenfalls Zelladhäsion und -migration. In humanen und murinen Melanomen wurde gezeigt, dass ADAM-9 an der Tumor-Stroma-Grenze sowohl in stromalen als auch in Tumorzellen lokalisiert ist. Die Bedeutung der ADAM-9 Expression für das Tumorwachstum ist unklar. Um die Funktion der Expression von ADAM-9 in Stromazellen für die Melanomentwicklung zu analysieren, wurden B16F1 Melanomzellen in die Flanke von *Adam-9$^{-/-}$* und Wildtyp Tieren injiziert. Tumore die in *Adam-9$^{-/-}$* Mäusen entstanden, waren signifikant größer als die in Wildtyp-Tieren und wiesen eine signifikant erhöhte Tumorzellproliferation und eine erniedrigte Apoptose auf. In Kokultur-Systemen mit primären Fibroblasten und B16F1 Melanomzellen konnten wir eine erhöhte Proliferation der Melanomzellen durch Inkubation mit Überständen von *Adam-9$^{-/-}$* Fibroblasten, aber nicht von Wildtyp-Zellen, feststellen. Wir konnten zeigen, dass *Adam-9$^{-/-}$* Fibroblasten unter anderem erhöhte Menge des TIMP-1 (tissue inhibitor of metalloproteinases) sekretieren. Die Neutralisation von TIMP-1 in Überständen von *Adam-9$^{-/-}$* Fibroblasten durch spezifische Antikörper führte zur aufhebung der erhöhten Proliferation der Melanom Zellen. Neben TIMP-1 waren auch lösliches TNF-α (tumornekrosefaktor-α) und TNFR1 erhöht in Überständen von *Adam-9$^{-/-}$* Fibroblasten nachzuweisen. Durch verschiedene *in vitro* Experimente konnten wir zeigen, dass die Neutralisation von TNF-α in *Adam-9$^{-/-}$* Fibroblasten zu einer reduzierten Apoptose der B16F1 Zellen führt. Zusätzlich konnten wir mit Hilfe von RNA- und Proteomarrays eine veränderte Expression von Proteinen der extrazellluären Matrix in der Tumor-Stroma-Grenze von *Adam-9$^{-/-}$* im Vergleich zu Wildtyp-Tieren feststellen. Diese Veränderungen könnten zu erhöhte Tumorwachstum in *Adam-9$^{-/-}$* Tieren beitragen. Interessanterweise konnten wir Kollagen Typ I als neues Substrat für ADAM-9 identifizieren. Zusammenfassend haben unsere Ergebnisse gezeigt, dass der Verlust von ADAM-9 in stromalen

Fibroblasten zu einer veränderten Freisetzung löslicher Faktoren führt, welche die Melanomzellproliferation und- apoptose beeinflussen.

1　Introduction

1.1　Malignant melanoma

1.1.1　Origin of melanoma

Melanoma is the most serious form of skin cancer that originates from melanocytes (Bandarchi et al., 2010). During embryonic development, melanocytes from the neural-crest migrate into the skin where their survival, proliferation and differentiation are under control of several tissue factors (Herlyn et al., 2000). Gene mutations, altered production of growth factors and loss of adhesion molecules, contribute to the disruption of pathways involved in the regulation of melanocytes homeostasis and lead to malignant transformation (Schopfer et al., 2007). One of the initial events of transformation is the loss of intercellular contacts with keratinocytes, which release melanocytes from the regulatory control of these cells; this is followed by increased melanocyte proliferation and formation of nevus. Nevi are regarded as benign formations. Malignant transformation of melanocytes or nevi leads to exponential growth within the epidermis, also known as radial-growth-phase (RGP) melanoma. From the RGP, melanoma can invade the underlying dermal tissue thus initiating the vertical-growth-phase (VGP) ultimately leading to metastatic spread (figure 1) (Schopfer et al., 2007). According to histological and clinical features, human melanoma can be classified into four main subtypes. 1) Superficial spreading melanoma (SSM), which is the most common type and is located at the intraepidermal compartment. 2) Nodular melanoma (NMM), the second most common type forms raised nodules and have no radial phase. 3) Lentigo maligna melanoma (LMM) is flat in appearance and occurs on sun-exposed skin. 4) Acral lentiginous melanoma (ALM) is common on the palms of the hand, the soles of the feet and nail bed (Clark et al., 1984; Bandarchi et al., 2010).

Transformation of a nevus into a melanoma has been hypothesized to be as a result of accumulation of genetic alterations, some of which are caused by exposure to UV light, this includes mutations in molecules of signaling pathways regulating cell survival and proliferation such as Ras/Raf/MEK/ERK and PI3K/AKT (Cohen et al., 2002; Satyamoorthy et al., 2003). The most common mutation in the Ras/Raf/MEK/ERK pathway is a mutation in BRAF, which is found in about 50% of melanomas (Davies et al., 2002). The substitution of glutamic acid with valine at position 600 (V600E) is the most common BRAF mutation and leads to constitutive ERK signaling. RAS is also a target for gain-of-function mutations in melanoma.

NRAS, one of the three human Ras genes, is mutated in approximately 30% of melanomas with the substitution of glutamine with leucine at position 61 being the most common (Davies et al., 2002).

1.1.2 Melanoma invasion

Upon transformation, tumor progression into the tissue greatly depends on the cross talk with neighboring cells and matrix components. During malignant transformation, down-regulation of E-cadherin in transformed melanonocytes allows their escape from keratinocytes control. Following this event, N-cadherin is up-regulated (Hsu et al., 1996) allowing the melanoma cells to switch their communication partners from keratinocytes to fibroblasts. In addition to cell-cell communication, soluble factors produced by the melanoma cells can induce fibroblasts to secrete growth factors, cytokines, matrix proteins, and proteases to generate a tumor-promoting microenvironment (Tang et al., 1994; Hsu et al., 2000). Melanoma cells produce several factors with stroma-inducing potential, for example basic fibroblast growth factor (bFGF) and vascular endothelial growth factor (VEGF) (Mueller and Fusenig 2004). Stimulated fibroblasts are also a rich source of soluble factors such as stromal cell-derived factor 1 (SDF-1) which stimulates tumor cell proliferation (Kalluri and Zeisberg 2006). Several cell biological processes are activated in this microenvironment, which leads to the growth and progression of melanoma cells into the host tissue. The activity of several proteolytic enzymes in the tumor microenvironment has been shown to be pivotal in promoting melanoma cell invasion by degradation of matrix components or shedding of cellular receptors (Hofmann et al., 2000). Several protease families are involved in melanoma invasion, these include serine proteases, matrix metalloproeases (MMPs) and more recently also the family of A disintegrin and metalloproteases (ADAMs) (Egebald and Werb 2002; Mochizuli and Okada 2007).

Matrix metalloproteinases (MMPs) are zinc-dependent endopeptidases which are capable of degrading extracellular matrix proteins, but also process bioactive molecules (Visse and Nagase 2003). MMPs produced by tumor or stromal cells participate in melanoma progression by degrading basement membrane, remodeling the ECM and releasing ECM- and membrane-bound growth factors (McGuire et al., 2003). These processes in turn influence cell proliferation, migration, invasion, and metastasis (reviewed by Zigrino and Mauch 2011). MMPs also affect inflammation

and angiogenesis during melanoma progression. For example, the early stage of inflammation during melanoma growth is delayed in *Mmp-12* knockout mice (Balbin et al., 2003). Furthermore, endothelial cells secrete MMPs to degrade blood vessel basement membrane and ECM components but also generate endogenous angiogenic inhibitors like endostatin from collagen XVIII (Stetler-Stevenson et al., 1999).
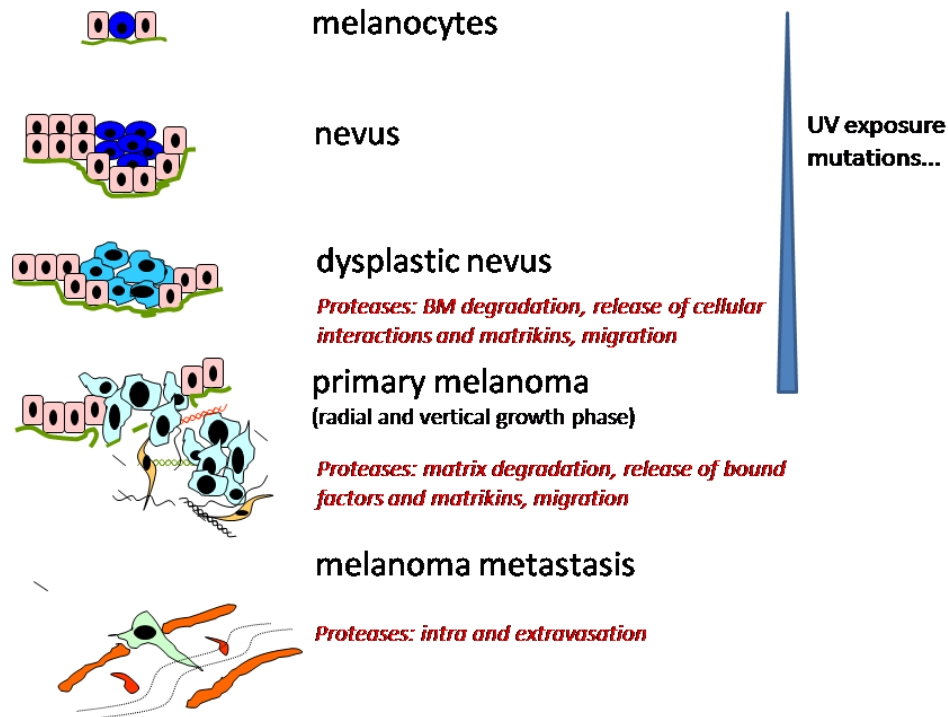
Figure 1 Transformation of melanocytes to melanoma. Benign transformation of melanocytes leads to formation of melanocytic nevi which progress into dysplastic nevi. The progression into a malignant radial or vertical growth melanoma is characterized by the activity of several proteolytic enzymes. These proteases contribute to cellular functions leading to malignant cell progression through the tissue and intravasation of melanoma cells into blood and lymph vessels. (From Zigrino and Mauch, Melanoma Development: Proteases in Melanoma 2011, Springer).

Another example of proteolytic enzymes implicated in melanoma progression are the serine proteases. The serine proteases plasmin and urokinase plasminogen activator (uPA) are involved in cleaving ECM proteins and activate MMPs in the extracellular space (Nagase 1997). It is thought that through their role in activating MMP-2 and -14, serine proteases may play a role in the vertical growth phase transition of melanoma (Antonicelli et al., 2007). In recent years, another group of proteases has become interesting in melanoma progression, namely the ADAMs.

ADAMs are membrane-bound proteins involved in proteolysis and cell adhesion (White 2003). ADAM-9 and -10 were shown to be up-regulated in melanoma while ADAM-9 was shown to mediate cellular contact between fibroblasts and melanoma cells while ADAM-10 was found to increase melanoma cell migration *in vitro* (Zigrino et al., 2011, Lee et al., 2010). Another member, ADAM-15, was shown to be down-regulated in melanoma metastasis as compared to primary melanoma (Ungerer et al., 2010). The specific role of ADAMs in melanoma however, is presently not yet clear.

1.2   ADAM proteases

1.2.1   ADAM domain structure and function

The ADAMs are multidomain, type I transmembrane proteins that together with the ADAMs containing thrombospondin motifs (ADAMTS), form the adamalysin subfamily under the metzincin family of metalloproteases. Members of the ADAM family are characterized by a conserved domain structure including, a signal peptide, prodomain, metalloprotease, disintegrin, cysteine-rich, epidermal growth factor-like domain, transmembrane domains and a cytoplasmic tail (figure 2) (Seals and Courtneidge 2003). ADAMs may exist in two forms, membrane-bound and soluble, which derive from alternative splicing.

The signal peptide at the N-terminus is important in directing ADAM proteins to the secretory pathway (Vitale and Denecke 1999). ADAMs may contain a zinc-binding motif coordinated by three histidine residues (HExxHxxGxxHD) within their metalloproteinase domain. However, only 13 of the circa 22 identified mammalian ADAMs contain the catalytic consensus sequence and are thought to be catalytically active (Duffy et al., 2011). The prodomain chaperones the proper folding of ADAM proteins (Milla et al., 1999) and keeps the metalloprotease site inactive by forming a supramolecular complex, the so-called "cysteine-switch". The "cysteine-switch" is formed between a conserved cysteine residue in the prodomain and the active zinc ion in the metalloprotease domain. This keeps the protein inactive until the prodomain is removed by proprotein convertases or organomercurials, cleaving at a conserved Rx(R/K)R site (Roghani et al. 1999; Howard et al. 2000)**.** The removal of the prodomain occurs in the trans-Golgi network (Van Wart and Birkedal-Hansen 1990).
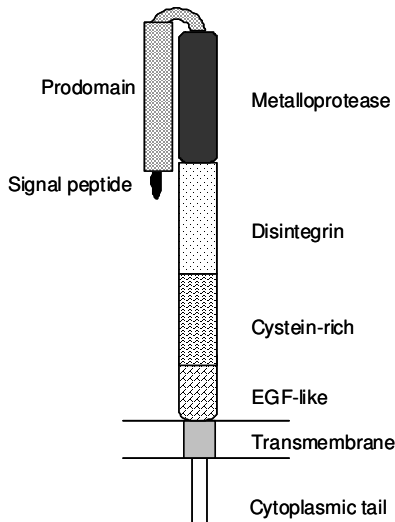
Figure 2. Schematic representation of the general domain structure of membrane-bound ADAM protein. ADAMs are activated intracellularly by removal of the prodomain. ADAMs appear on the cell surface in the activated form anchored to the plasma membrane by the transmembrane domain.

ADAMs proteolytic activity has been associated with ectodomain shedding. One of the best studied examples of shedding is that of TNF-α originally described by Black et al., (1997). Using genetic mouse models Horiuchi et al., (2007) showed that shedding of TNF-α *in vivo* is primarily mediated by ADAM-17. Another example is the involvement of ADAM proteases in regulation of notch signaling. ADAM-10 (kuzbanian, in Drosophila) and ADAM-17 have been implicated in the ectodomain shedding of the notch receptor leading to intramembrane proteolysis and release of the cytoplasmic stub of the receptor (Pan et al. 1997; Brou et al., 2000). Translocation of the intracellular domain into the nucleus results in the activation of transcription and regulation of developmental processes (Pan et al. 1997; Brou et al., 2000). ADAMs have also been implicated in the generation of APPα. The accumulation of β-amyloid peptide in the brain leads to the development of Alzheimer´s disease (Gandy and Petanceska 2000). β-amyloid peptide is produced by processing of amyloid precursor protein (APP) by β- and γ-secretases, but a soluble form of APPα is produced by the action of α-secretases such as ADAM-9, -10 and -17 which opposes the adverse effects of the β-amyloid peptide (Amour et al., 2000; Slack et al., 2001; Hotoda et al., 2002). Moreover, ADAMs also cleave components of the extracellular matrix as has been shown for ADAM-10 and -15 cleaving collagen type IV *in vitro* (Millichip et al. 1998; Martin et al. 2002).

Apart from the proteolytic activity, ADAMs are involved, through their disintegrin-cysteine domains, in receptor binding and mediate cellular interactions. It is unclear which sequence in these domains is responsible for adhesive activity as only ADAM-15 contains the known integrin-binding sequence RGD (arginine-glycine-aspartic acid). However ADAM-15 has been shown to bind to αvβ3 and α5β1 in an RGD-dependent and independent manner (Nath et al., 1999; Eto et al., 2000). Most of the ADAMs were thought to interact with integrins through an aspartic acid-containing sequence (ECD; glutamic acid-cysteine-aspartic acid) located in the disintegrin loop. Mutation of ECD in ADAM-2 to ECA leads to inhibition of sperm-egg binding (Bigler et al. 2000; Zhu et al. 2000). However, resolution of the crystal structure of vascular-apoptosis-inducing protein-1 (VAP-1), a snake venom homologue of mammalian ADAMs, has revealed that the disintegrin loop, which contains the ECD motif, is masked and inaccessible for protein binding (Takeda et al., 2006). In this study, the high variable region in the cysteine-rich domain was shown to be responsible for substrate interaction. The function of the EGF-like domain is not clear but it is thought that, together with the cysteine-rich domain, it is involved in protein-protein interaction leading to cell fusion (Huovila et al., 1996). This has been shown for ADAM-12 during the fusion of myoblasts cells *in vitro* (Yagami-Hiromasa et al., 1995).

The cytoplasmic tails of the ADAMs contain proline-rich motifs that can bind to SH3 domain containing-proteins (Howard et al. 1999; Poghosyan et al., 2001). Several ADAMs have potential phosphorylation sites for serine-threonine and/or tyrosine kinases. Phosphorylation of the cytoplasmic tail and interaction with cytoplasmic proteins may influence cell signaling, control maturation, sub cellular localization and metalloprotease activity of ADAMs (Izumi et al., 1998; Roghani et al., 1999).

1.2.2 Regulation of ADAM expression and activity

Potential regulatory mechanisms at the transcriptional and post-translational levels have been discussed for the regulation of ADAMs, however lack of knowledge on their promoter regions have limited these studies. For ADAM-17, it was shown that under hypoxia, activation of the specificity protein 1 (Sp1) a transcription factor that binds to the promoter region of ADAM-17 leads to up-regulation of this protein (Szalad et al., 2009). ADAM-8 and -9 are also up-regulated under reduced oxygen conditions (Valkovskaya 2008; Guaiquil et al., 2009). However, the mechanism that governs this regulation, whether it involves Sp1 or another member of this family is

unclear. Sequencing of the proximal promoter regions of *Adam-9* has identified three putative binding sites for transcriptional regulatory elements, namely sites for human muscle-specific Mt, barbiturate-inducible element box and CAS interacting (Cong and Jia 2009). Binding of these proteins to the *Adam-9* promoter and how they affect its expression has not yet been analyzed. ADAMs are also regulated at by extracellular stimuli for example; ADAM-9 expression is down-regulated by IL-1α at transcript and protein level via a JNK mediated mechanism (Zigrino et al., 2005 and A. Schönefuss, doctoral thesis) while ADAM-17 expression is induced by IL-1β and TNF-α (Cesaro et al., 2009; Turner et al., 2010).

Protein trafficking and sub cellular localization also regulate the expression of ADAMs. ADAMs are trafficked through the golgi compartment and need to be transported to the cell surface where their activity is implemented (Mochizuki and Okada 2007). Their cytoplasmic tail regulates the sub cellular localization and catalytic activity of ADAMs through binding to other cytoplasmic proteins (Izumi et al., 1998; Roghani et al., 1999). For example, binding of protein kinase C to ADAM-9 and -17 regulates shedding of HB-EGF when stimulated with phorbol esters (Izumi et al., 1998; Doedens and Black 2000). Intracellular binding of PASCIN3 to the cytoplasmic tail of ADAM-12 regulates shedding of HB-EGF. Therefore, it was suggested that PACSIN3 is involved in the correct transportation of ADAM-12 to the plasma membrane (Mori et al., 2003).

The activity of ADAMs is also regulated by their prodomain which maintains the protein in the latent state (Deuss et al., 2008), or by endogenous inhibitors, e.g. TIMPs with relative specificity. TIMP-1 was shown to inhibit ADAM-10 while TIMP-3 inhibits ADAM-10, -12 and -17. However, not all ADAMs are inhibited by TIMPs, for instance ADAM-8 and -9 are not inhibited by any member of the TIMPs (Amour et al., 2002 Amour et al., 1998 and 2000; Loechel et al., 2000). A number of synthetic inhibitors with a broad inhibitory spectrum towards ADAMs and MMPs have been described, most of these inhibitors function by binding to the catalytic zinc ion. One of the most investigated inhibitors is INCB3619, which inhibits ADAM-8, -9, -10, -17 and -33 and blocks the release of EFGR ligands (Fridman et al., 2007). Other synthetic inhibitors include hydroxamate-based inhibitors CGS 27023 for ADAM-9 (Roghani et al, 1999), GW280264 and GI254023 for ADAM-10 and -17 (Ludwig et al., 2005). Hence, the regulation of ADAMs will depend on their expression profile, stimulus, inhibitor and possibly substrate specificity as it has been suggested that ADAMs

have intrinsic substrate specificity which limits their proteolytic activity (Hattori et al., 2000).

1.3 ADAM-9

1.3.1 ADAM-9 molecular chracteristics and function

Like all other ADAMs, ADAM-9 is characterized by a general conserved domain structure (Weskamp et al., 1996). ADAM-9 is ubiquitously expressed and exists in two forms; membrane-bound and soluble (figure 3). Two soluble variants of the ADAM-9 protein have been described. The first was described by Hotoda et al., (2002) which lacks exon 18 thus resulting in a frame shift and an early stop codon (figure 3; ADAM-9s L). Consequently, it lacks part of the EGF-like domain, the transmembrane domain and the cytoplasmic tail and is released in a soluble form. The second variant is generated by insertion of an extra exon, designated exon 12 that produces an early stop codon resulting in the deletion of part of the cysteine-rich domain, the EGF-like domain, the transmembrane and the cytoplasmic domain (figure 3; ADAM-9s S) (Mazzocca et al., 2005). The first variant was cloned from A-172 human glioblastoma cells and was identified in various tissues such as heart, liver, kidneys and lungs (Hotoda et al., 2002). The second variant has been described in activated hepatic stellate cells (Mazzocca et al., 2005) and in breast cancer tissue and cell lines (Fry and Toker 2010).
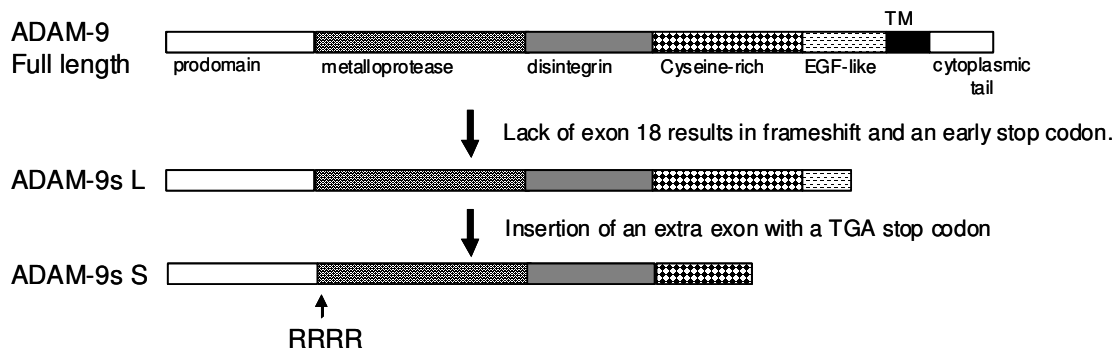
Figure 3. Schematic representation of membrane-bound and soluble forms of ADAM-9. The two soluble variants of ADAM-9 are shown. The furin cleavage site (RRRR) is indicated by the arrow.

ADAM-9 is activated intracellularly in the golgi apparatus by removal of the prodomain by a pro-protein convertase such as furin (Roghani et al., 1999), thus it is exposed on the cell surface or released in the extracellular environment as active

enzyme. Proteolytic activity of ADAM-9 has been shown towards molecules with important roles in growth and angiogenesis such as EGF, FGFR2iiib (Hotoda et al., 2002; Izumi et al. 1998; Peduto et al. 2005), VCAM-1 and EphB4 (Guaiquil et al., 2009). However, ADAM-9 can also directly cleave ECM proteins such as laminin 111 (Mazzocca et al., 2005) and fibronectin (Schwettman and Tschesche 2001). More recently, ADAM-9 was involved in the shedding of ADAM-10, a mechanism that may regulate ADAM-10 levels on the cell membrane (Parkin and Harris 2009).

Apart from its role as a sheddase, ADAM-9 can mediate binding to integrin receptors. Interaction of ADAM-9 has been shown with $\alpha6\beta1$ integrin on fibrosarcoma cells where it enhances cell migration on laminin-coated plates (Nath et al., 2000). Using recombinant disintegrin-cysteine rich domain of ADAM-9, ADAM-9 was shown to interact with $\alpha3\beta1$ integrins on the surface of keratinocytes (Zigrino et al., 2007). Further, on fibroblasts interaction of the disintegrin-cysteine rich domain of ADAM-9 with $\beta1$ integrins led to increased secretion of proteolytic enzymes (Zigrino et al., 2011). Interestingly, the adhesion of these cells to ADAM-9 was shown to be independent of the ECD motif, which is in agreement with lack of exposure of this sequence (Takeda et al., 2006; see section 1.2.1). Soluble ADAM-9 has also been shown to promote colon carcinoma cell invasion *in vitro* by binding to $\alpha2\beta1$ and $\alpha6\beta4$ integrins (Mazzocca et al., 2005). More recently, the same group has demonstrated that when express as membrane-bound or secreted as soluble form, ADAM-9 may differentially modulate migration of breast cancer cells (Fry and Toker 2010).

The cytoplasmic tail of ADAM-9 can bind to endophilin and SH3PX1 (Howard et al., 1999). Given the potential role of endophilin and SH3PX1 in vesicle sorting (Wang et al., 2008), this interaction may play a role in regulating maturation and sub cellular localization of ADAM-9. Using yeast two-hybrid analysis, MAD2β was identified as a cytoplasmic binding partner for ADAM-9. MAD2β shows 23 % similarity to MAD2, which is a component of the spindle assembly checkpoint (Nelson et al., 1999). Perhaps these interactions with MAD2β are involved in coordinating ADAM-9 function with the cell cycle. In addition, ADAM-9 cytoplasmic tail can also bind to PKCdelta and regulates phorbol ester induced shedding of heparin-binding EGF and amyloid precursor protein (Izumi et al., 1998; Roghani et al., 1999). The different characterized functions of ADAM-9 are summarized in figure 4 below.
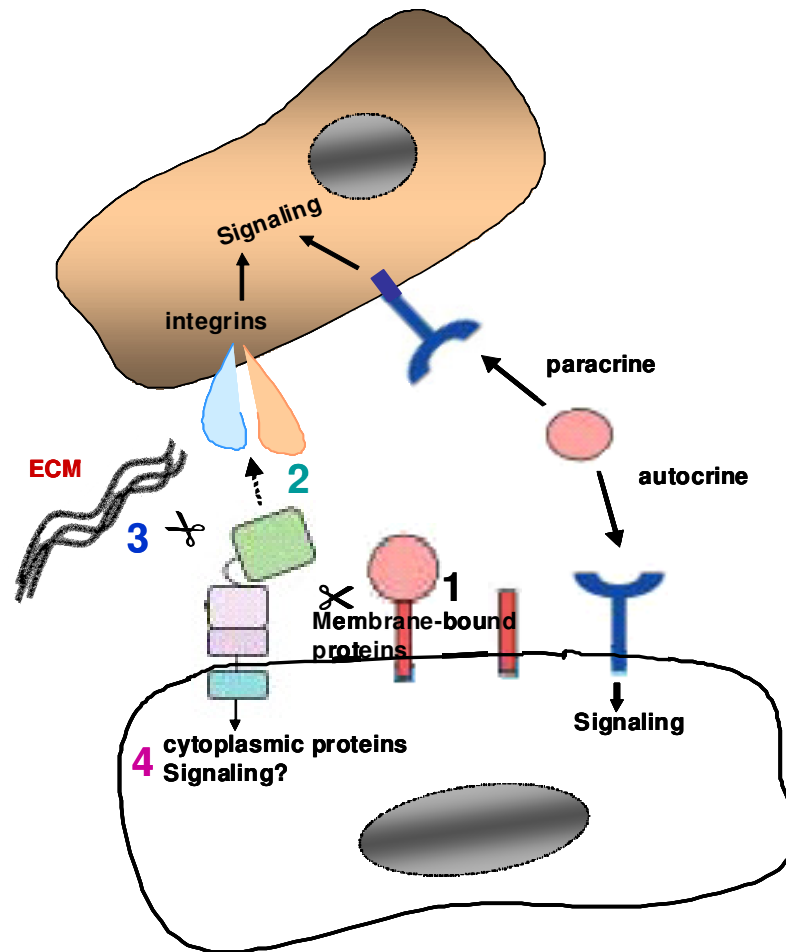
Figure 4. Overview of ADAM-9 functions. 1, ectodomain shedding of membrane-bound growth factors/cytokines and their receptors lead to release of soluble factors which can act in an autocrine or paracrine manner. 2, interaction with integrins can influence adhesion/migration and signaling. 3, processing of the ECM may affect signaling through integrins and cell migration. 4, localization and activity of ADAM-9 can be influenced by its cytoplasmic tail.

As to the control of *Adam-9* transcriptional activity, it has been suggested that a single nucleotide substitution at -1314 influences the transcriptional activity of ADAM-9 with a gain/loss binding of three putative transcriptional regulatory elements. These include the human muscle-specific Mt, the barbiturate-inducible element box and CAS interacting (Cong and Jia 2009). Estrogen is possibly an activator of *Adam-9* promoter activity as the transcriptional activity of *Adam-9* is increased in human neuroblastoma (SH-SY5Y) and human prostate adenocarcinoma (LNCaP) cell lines after treatment with estrogen (Cong and Jia 2009). Estrogen functions as a transcription factor by binding to the estrogen response element (ERE), altogether eight possible ERE sites have been found in the Adam-9 promoter region (Gruber et al., 2004; Cong and Jia 2009).

1.3.2 ADAM-9 in cancer

ADAM-9 is up-regulated in various human cancers such as renal, prostate, breast cancer and melanoma (O´Shea et al., 2003; Peduto et al., 2005; Zigrino et al., 2005; Fritzsche et al. 2008). ADAM-9 is thought to participate in the escape of hepatocellular carcinoma (HCC) cells from NK cell-mediated immunosurveillance by shedding major histocompatibility complex (MHC) class I–related chain A (MICA), a ligand for NKG2D receptor (Kogha et al., 2010). Treatment of HCC cells with Sorafenib, a multikinase inhibitor (Keating and Santoro 2009), reduces MICA shedding by down-regulating ADAM-9 (Kogha et al., 2010). In a mouse model for prostate cancer, ADAM-9 was shown to be highly expressed in well-differentiated carcinomas but not in advanced poorly-differentiated tumors (Peduto et al. 2005). Ablation of ADAM-9 in W^{10} animals, which spontaneously develop prostate tumors, resulted in the development of only well-differentiated tumors as compared to wild type mice, which develop poorly-differentiated tumors suggesting that ADAM-9 is involved in the progression of prostate tumors to advanced grades (Peduto et al., 2005). Using cell-based assays, the authors identified altered FGF and EFG signaling because of reduced FGFR2iiib and EGFR cleavage, as possible molecular mechanism for the observed effect. However, no *in vivo* evidence was provided on the alteration of these two signaling pathways. Soluble ADAM-9 has been found in increased amounts in the peritumoral stroma of liver metastases (Mazzocca et al., 2005). Interestingly, the soluble and membrane-bound forms of ADAM-9 have opposing roles in the migration of breast cancer cells. The soluble form enhances cell migration in a protease-dependent manner, while the membrane-bound form inhibits cell migration by altering integrin-mediated signaling (Fry and Toker 2010). *In vitro* primary keratinocytes lacking ADAM-9 show enhanced migration, this is reflected *in vivo* during wound healing (Mauch et al., 2010). Accelerated wound re-epithelialization is observed in *Adam-9$^{-/-}$* animals because of altered shedding of collagen type XVII (Mauch et al., 2010). Shed collagen type XVII has been described as to have inhibitory effects on cell migration (Franzke et al., 2002).

In human melanoma, ADAM-9 is highly expressed at the tumor-stroma border where it is localized in both tumor and stromal cells (Zigrino et al., 2005). ADAM-9 expression in melanoma cells was confirmed *in vitro.* However, no correlation was observed between Adam-9 transcript levels and the invasive capacity of the cells (Zigrino et al., 2005). One functional activity of ADAM-9 in melanoma cells, which

might be important in progression of melanoma, is the mediation of heterotypic cell interaction between dermal fibroblasts and melanoma cells (Zigrino et al., 2011). Despite these observations, the exact role of ADAM-9 in melanoma growth has not been determined.

1.4 Animal models for malignant melanoma

1.4.1 Mouse models

The increase incidence of melanoma has led to the need for better understanding of the molecular mechanisms involved in the commencement and progression of melanoma. Relevant animal models for addressing experimental questions would benefit melanoma research. The studies of melanoma *in vivo* have employed mouse xenograft models and genetically modified animals with spontaneous development of melanoma. In the xenograph model, melanoma cells propagated *in vitro* are grafted under the mouse skin and allowed to grow (Overwijk and Restifo 2001). Although melanoma does not spontaneously develop in these models, it is efficient in evaluating the contribution of specific host proteins in tumor progression. Tumor development is followed in a short period of 10 to 14 days, tumor cells with different genetic abnormalities or manipulations can be used (Richmond and Su 2008).

Mouse melanoma models, which spontaneously develop melanoma, have been generated to epitomize the histopathology of human melanoma. These models have the advantage that distinct genetic alterations leading to the development of melanoma in humans can be reproduced (Refaeli et al., 2009). Important differences in melanoma development between human and mouse is the localization of the melanocytes. In humans, the melanocytes are located in the basal layer of the epidermis while in mouse they are confined to the hair follicle in the dermis (Herlyn et al., 2000); hence, the histopathologies are not exactly the same (Ha et al., 2005). Tormo et al., (2006), have described an interesting murine melanoma model HGF/CDK4R24C/R24C. This mice over-express hepatocyte growth factor/scatter factor (HGF) and carries a knock-in gene of the mutated cyclin-dependent kinase 4 (CDK4), a mutation which renders CDK4 insensitive to inhibition by p16/INK4a. This mutation has been observed in hereditary and sporadic human melanoma (Chin 2003). The over-expression of HGF leads to continuous signaling through its receptor tyrosine kinase c-Met and subsequent activation of the ras signal transduction pathway, which promotes melanomagenesis (Otsuka et al., 1998). These mice

develop melanoma spontaneously or upon carcinogen treatment in the epidermo-dermal junction of the skin. Importantly, these tumors are invasive and metastatic (Tormo et al., 2006). Another mouse model of melanoma is the Tg(Grm1)EPv(E) mice, that over-express the metabotropic glutamate receptor 1 (mGrm1) in melanocytes under control of dopachrome tautomerase promoter (Pollock et al., 2003). This mouse strain develops melanoma at about 6 months of age with major location in the tail (Pollock et al., 2003). Ectopic expression of mGrm1 transforms melanocytes and causes malignant melanoma *in vivo* (Oritz et al., 2007). The Tg(Grm1)EPv(E) model may recapitulate human uveal melanoma as activation of this pathway has been observed in human uveal melanoma (Van Raamsdonk et al., 2009). The Tyr::CreER; BRAF^{CA}; Pten$^{lox/lox}$ mouse melanoma model (Dankort et al., 2009) initiates the substitution of glutamic acid with valine at position 600, a mutation observed in human melanoma leading to constitutive ERK signaling (Davies et al., 2002). All mice develop melanoma with metastasis to lymph nodes and lungs (Dankort et al., 2009).

1.4.2 Medaka model

Non-mammalian animals like fish also develop melanoma. Fish animal models are increasingly being use to study melanoma (Craig et al., 2008). Fish models for melanoma were first established in Xiphophorus, followed by transgenic melanoma models in zebrafish and medaka (Patton et al., 2011). The medaka melanoma model was generated by over-expression of the oncogene, Xiphophorus medaka receptor kinase (Xmrk) an orthologue of the mammalian epidermal growth factor receptor gene set under the control of the pigment cell-specific promoter, microphthalmia-associated transcription factor (mitf) (Schartl et al., 2009; Meierjohann et al., 2004). Fish homozygous for Xmrk all develop melanoma between 2 to 6 weeks of age, which are highly invasive and metastatic (Schartl et al., 2009). Uveal melanoma and tumor formation in the red and yellow pigment cells called xanthophoroma and erythrophoroma respectively have been described (Schartl et al., 2009). This model has many similarities with human melanoma for one thing, Xrmk receptor induces signaling pathways, which mediate proliferation, resistance to apoptosis and initiation of dedifferentiation, events that are similar to those found downstream of mammalian Egfr (Meierjohan and Schartl 2006). Xmrk induces the Ras-Raf-MAPK signaling pathway, which mediates cell proliferation and differentiation. PI3-K can also bind to

the c-terminal of Xmrk leading to activation of Akt and induction of anti-apoptotic signaling. Signal transducer and activator of transcription (STAT5) is also activated promoting anti-apoptosis by increasing the expression of Bcl-x. These two pathways are well described in human melanoma (Satyamoorthy et al., 2003).

Apart from these indicated similarities, no data on the expression and putative role of molecules such as proteolytic enzymes in this model. Whether tumoral and peritumoral proteolysis plays a role for disease progression in this model, as shown for human and murine melanoma, needs to be investigated. Technical advantages of this model is among others, their easy breeding and large number of offsprings produced, thus offering a model with screening possibilities for pharmacological analysis of potential inhibitors for therapeutic use.

1.5 Aims of the thesis

After formation of a primary tumor within the epidermal layer, melanoma cells progress into the tissue and metastasize to distant organs. Invasion into the dermal compartment and distant organs requires among others, cancer cell adhesion to/and degradation of the ECM. In addition to several proteolytic enzymes, ADAM-9 was found expressed by tumor and stromal cells in malignant melanoma. This protein can exert dual functions. On one hand, it is proteolytically active, and on the other hand, it functions as a cell adhesion receptor making it a molecule with pivotal roles in melanoma development and metastasis. The main aim of this study was to investigate at a molecular level how ADAM-9 produced by the host affects growth and metastasis of malignant melanoma. To achieve this well established *in vivo* melanoma cell grafting model was used to analyze melanoma growth in mice lacking ADAM-9 in the host. Tumor progression was monitored as a function of time and all processes important for tumor progression such as inflammation, tumor-induced neoangiogenesis and proliferation were analyzed in detail to investigate whether ablation of ADAM-9 had an impact on these processes. In addition, the protein modifications in the peritumoral environment in tumors from WT or *Adam-9$^{-/-}$* animals were further investigated *in vivo* by proteomics. *In vitro* co-culture systems using fibroblasts isolated from WT and *Adam-9$^{-/-}$* animals and murine melanoma cells was employed to analyze at a molecular level how the expression of ADAM-9 stromal fibroblasts affected melanoma-fibroblasts cellular cross-talk at the tumor-stroma

border. A direct role for ADAM-9 in ECM processing was addressed using biochemical approach with recombinant ADAM-9, active/inactive.

2 Materials and methods

2.1 Materials

2.1.1 Chemicals

All chemicals were purchased in analytical grade from Roth (Karlsruhe), Sigma-Aldrich (München), Merck (Darmstadt), GIBCO (Karlsruhe) and Perbio (Lausanne/Switzerland). Molecular weight markers for proteins, PageRuler™Plus Prestained Protein ladder and PageRulerTM Unstained Protein ladder were from Fermentas (St. Leon-Roth). DNA molecular weight markers, 100 bp DNA ladder and 1 kb DNA ladder as well as restriction enzymes were from NEB (Frankfurt/Main). Human recombinant TIMP-1 and fibronectin were from Calbiochem (Darmstadt) and R&D systems (Wiesbaden) respectively. Mouse recombinant TNF-α was from Miltenyi (Bergisch Gladbach). Rat tail recombinant collagen type I was from Cell Systems (Remagen, Germany).

2.1.2 Cell culture material

Plastic ware for cell culture was purchased from Greiner (Nürtingen), TPP (Trasadingen/Switzerland) and Becton Dickinson (Heidelberg). Cell culture media were from Invitrogen (Karlsruhe), Biochrom (Berlin) and PAA (Cölbe). Supplements (Penicillin/Streptomycin) were from Biochrom and FCS from PAA. Zeocin and geneticin (G418) antibiotics were purchased from Invitrogen and PAA respectively. Collagenase was from Cell Systems (Troisdorf) and mitomycin C was from Sigma-Aldrich.

2.1.3 Bacteria, vectors and plasmids

For transformation of plasmids, Escherichia coli DH5α (Invitrogen) was used. The genotype is: F- Φ80lacZΔM15 Δ(lacZYA-argF)U169 recA1 endA1 hsdR17(rk-, mk+) phoA supE44 thi-1 gyrA96 relA1 λ-. The linearized vector pCR 2.1, used for subcloning, and the eukaryotic expression vector pcDNA4/TO/myc-His were purchased from Invitrogen.

2.1.4 Antibodies

Antibodies	Company	Application	Dilution
Goat anti-ADAM-9	R&D systems	WB	1:1000
Rat anti-ADAM-9	R&D systems	IF	1:100
Rabbit anti-ADAM-10	Abcam, Cambridge, UK	IF	
Rabbit anti-ADAM-17	Biodesign, Asbach	WB	1;1000
Rabbit anti-MMP-13	Santa Cruz, Heidelberg	IF	1:50
Rabbit anti-MMP-14	Pineda, Berlin	IF	1:100
Goat anti-TIMP-1	R&D systems	WB/IF/ Neutralization	1:1000/1:100 1:2000
Hamster anti-TNF-α (clone TN3-19)	eBioscience Frankfurt	Neutralization	1:2000
Rabbit anti-TNFRI	Abcam	WB	1:10000
Rat anti-Ki67 (clone Tec 3)	Dako, Hamburg	IF/IHC	1:1000/1:50
Rabbit anti-Cleaved caspase-3	Cell signaling, Frankfurt	IHC	1:200
Rat anti-CD45 (clone IBL-3/16)	AbD Serotec Düsseldorf	IF	1:200
Mouse anti-decorin (clone 115402)	R&D systems Wiesbaden	WB/IF	1:1000/1:100
Rat anti-F4/80	AbD Serotec	IF	1:100
Rat anti-Neutrophil	AbD Serotec	IF	1:100
Mouse anti-decorin	R&D systems	WB/IF	1:1000/1:100
Rabbit anti-collagen 14	Gift from Prof. M. Koch, University of Cologne	WB/IF	1:1000/1:100
Rabbit anti-collagen type I	Quartett, Berlin	WB	1:1000/1:50
Rabbit anti-fibronectin	Sigma Aldrich	WB/IF	1:1000/1:100
Rat anti-CD31 (clone MEC 13.3)	AbD Serotec	IF	1:1000
Rabbit-anti-mouse HRP	Dako	WB	1:2000
Rabbit anti-goat HRP	Dako	WB	1:2000
Rabbit anti-rat biotinylated	Dako	IHC	1:300
Donkey anti-goat-Alexa 594-conjugated	Invitrogen,	IF	1:1000
Rabbit anti-rat-Alexa 488-conjugated	Invitrogen,	IF	1:1000
Goat anti-rabbit-Alexa 594-conjugated and 488-conjugated	Invitrogen,	IF	1:1000

2.1.5 Buffers

PBS:	136 mM NaCl; 2.6 mM KCl; 10nM Na_2HPO_4; 1.5 mM KH_2 PO_4; pH 7.4
TBE:	90 mM Tris; 20 mM Na2EDTA; 90 mM boric acid; pH 8
PBST:	PBS + Tween 20 0.5 % (v/v) TBE
DNA lysis buffer:	100 mM Tris/HCl pH 8.5; 5 mM EDTA pH 8.0; 0.2% SDS; 200 mM NaCl
Running buffer:	250 mM Tris base, 0.2 M Glycin, 1 % SDS; pH 8.3
Anode I buffer:	Tris 0.3 M; 20 % Methanol
Anode II buffer:	Tris 25 mM; 20 % Methanol
Cathode buffer:	6- Aminohexan acid 40 mM; 20 % Methanol
Laemmli reducing buffer:	60 mM Tris-HCl pH 6.8; 2 % SDS; 0.1 % Bromphenol blue; 25 % Glycerol; 14.4 mM 2-Mercaptoethanol
Equilibration buffer:	50 mM NaH_2PO_4; 20 mM Tris HCl; 100 mM NaCl; pH 8
Gradient buffer A:	10 mM imidazole; 50 mM NaH_2PO_4; 20 mM Tris HCl; 100 mM NaCl; pH 8
Elution buffer:	250 mM imidazole; 50 mM NaH_2PO_4; 20 mM Tris HCl; 100 mM NaCl; pH 8
Substrate buffer:	50 mm Tris-HCl, 5 mm $CaCl_2$, pH 8.0
Citrate buffer:	2 mM citric acid; 2 mM sodium citrate; pH 6
Cell lysis buffer:	PBS + 20 mM NH4OH; 0.5 % Triton X-100
RIPA buffer:	150 mM NaCl, 0.5 % DOC; 2 % SDS; 1 % NP40; 50 mM Tris; 1 % protease inhibitor cocktail; pH 7.4

2.2 Methods

2.2.1 Cell biology

2.2.1.1 Cells and cell culture

COS-7 kidney fibroblasts from African Green Monkey, SV40 transformed were from ATCC (Gluzman 1981). B16F0, mouse melanoma cells were a kind gift from Prof. C. Blobel, Cornell University, New York (Fidler 1973), and B16F1 were from ATCC (Fidler 1975). All cells were cultured in Dulbecco's modified Eagle's medium (DMEM) supplemented with 10 % FCS, 100 U/ml penicillin, 100 µg/ml streptomycin. B16F1-GFP, B16F1 cells stably expressing GFP (Zigrino et al., 2009) were cultured in DMEM supplemented with 10 % fetal calf serum (FCS), 100 U/ml penicillin, and 100

μg/ml streptomycin and 800 μg/ml G418. The human melanoma cell lines Skmel28 (Carey et al., 1976), WM164/4 (Herlyn et al., 1990), BLM (Van Muijen et al., 1991), A375 (Giard et al., 1973) and 530 (Van Muijen et al., 1991) were cultured in RPMI 1640 medium containing 10 % FCS, 1 % non-essential amino acids, 2 % L-Glutamine, 100 U/ml penicillin, 100 μg/ml streptomycin. Glioma Gli36 cells (Kashima et al., 1995) and malignant transformed HaCaT II-4(rt) cells (SCC) (Boukamp et al., 1990) were cultured in DMEM supplemented with 10 % FCS, 100 U/ml penicillin and 100 μg/ml streptomycin. Basal cell carcinoma cells (BCC) (Yen et al., 1996) were cultured in DMEM-HAM´S F12 supplemented with 10 % FCS, 100 U/ml penicillin, 100 μg/ml streptomycin, 0.1 % adenin, 0.01% hydrocortisone, 0.001 % cholera toxin, 1 % EFG and 1% insulin. All cells were cultured at 37 ℃ with 5 % CO2 and a humidity of 95 %.

2.2.1.2 Isolation of primary fibroblasts

Primary murine dermal fibroblasts were isolated from the back skin of newborn mice. Briefly, newborn mice were euthanized by decapitation, cooled on ice for 1 hour and disinfected in betaisodona iodine for 1 minute, rinsed briefly in PBS and then for 1 minute in 70 % ethanol and finally rinsed in PBS. The skin was incubated overnight with 0.2 % trypsin at 4 ℃. The epidermis was separated from the dermis, which was diced finely before incubating with 400 U/ml collagenase (Worthington) for 2–3 hours at 37 ℃ with gentle agitation. Tissue debris was removed by centrifugation at 1200 rpm. Cell pellet was resuspended in DMEM containing 400 U/ml collagenase and isolated fibroblasts were cultured in DMEM containing 10 % FCS, 2 mM glutamine and 100 U/ml penicillin, 100 μg/ml streptomycin. The fibroblasts were used between passages 2 and 4 for experiments.

2.2.1.3 Preparation of fibroblast conditioned media, cell monolayer and matrix

For the preparation of conditioned medium, fibroblasts were seeded at a density of 5 x 10^4 cells/cm^2 in culture plates and cultured overnight at 37 ℃. Cells were washed twice with PBS and incubated with serum free DMEM for 24 hours. The medium was collected and spun down for 5 minutes at 1200 rpm to eliminate cellular debris. Supernatants were used immediately for cell-stimulation experiments or stored at -20 ℃ for additional analysis.

For the preparation of fibroblast monolayer layer, fibroblasts were seeded at a density of 5 x 10^4 cells/cm^2 and cultured for 3 days. Cells were washed with PBS and fibroblast layers were treated with 40 µg/ml mitomycin-C, for 2 hours at 37 ℃ to inhibit cell growth. For the preparation of fibroblast-deposited matrix the cells were lysed with cell extraction buffer and the cellular debris were removed with a pipette (Beacham et al., 2007). The matrix was washed gently with PBS; the integrity of the matrix was confirmed by staining with 0.25 % Coomassie Brilliant blue (G250, Sigma), 2.5 g Coomassie Brilliant Blue dissolved in methanol 45 %, acetic acid 10 % and H$_2$O, for 10 minutes at room temperature, washed with PBS and visualized with light microscope and recorded with DISKUS 4.50.1638 software.

2.2.1.4 Bromodeoxyuridine (BrdU) incorporation assay

To analyze cell proliferation, B16F1 cells were seeded at a density of 1 x 10^4 cells/cm^2 in a 96-well plate for 24 hours. Cells were washed twice with PBS before treating with or without recombinant TIMP-1 (0.5 µg/ml) in serum-free media, or with serum free fibroblasts conditioned medium (2.2.1.3). Cell proliferation was measured using a BrdU Proliferation assay (Roche, Mannheim) according to the manufacturer's instructions. Briefly, cells were labeled with BrdU (10 µM final concentration per well) for 2 hours at 37 ℃ and fixed with 200 µl of "FixDenat" solution for 30 minutes at room temperature. After removing the "FixDenat" solution, 100 µl of anti-Bromodeoxyuridine-peroxidase conjugated antibody working solution was added for 90 minutes at room temperature. Plates were washed three times with PBS and incubated with substrate solution. The developing reaction was stopped with 25 µl of 1 M H$_2$SO$_4$ after sufficient color development. Colorimetric detection was analyzed at 450 nm using Victor^{3TM} 1420 Multilabel counter (Perkin Elmer, Wellesley, MA, USA). Measurement of empty wells with substrate solution was used as blank. All experiments were performed in triplicate and repeated three times.

2.2.1.5 Apoptosis assay

B16F1 cells were seeded in 6-well plates at a density of 1 x 10^4 cells/cm² and cultured overnight. Culture medium was removed and cells were washed twice with PBS before treating with or without fibroblasts conditioned medium pre-incubated with recombinant TNF-α (100 ng/ml), or hamster anti-TNF-α antibody (2 µg/ml), or goat anti-TIMP-1 antibody (2 µg/ml), or Embrel (5 µg/ml) or IgG control (2 µg/ml)

before used in cell culture. Cells were incubated overnight and apoptosis was quantified by cell death detection ELISA (Roche) according to the manufacturer's manual. Briefly, cells were lysed for 30 minutes at room temperature and clarified by centrifuging at 200 x g for 10 minutes. 20 µl of sample was incubated with a mixture of anti-histone-biotin and anti-DNA-peroxidase-conjugated antibody in streptavidin-coated plates for 2 hours at room temperature with shaking (300 rpm). Unbound components were removed by washing. Peroxidase activity retained on the plate was determined photometrically with substrate solution at a wavelength of 405 nm (reference wavelength 490 nm) using Victor3^{TM} 1420 Multilabel counter (Perkin Elmer). Measurement of empty wells with substrate solution was used as blank. All experiments were performed in triplicate and repeated three times.

2.2.2 Protein analysis

2.2.2.1 Preparation of lysates

Cell lysates were prepared after washing the cells with PBS, by scraping cells directly in RIPA buffer containing general protease inhibitors (Sigma Aldrich) and incubating overnight at 4 °C. Lysates were centrifuged at 12.000 rpm for 15 minutes. The clarified supernatants were transferred to new tubes and protein concentration was determined using a commercial protein assay (BCA^{TM} Protein assay, Pierce) according to the manufacturer's instructions. Protein concentration was determined by using freshly prepared BSA standard curve ranging from 0.1 µg/µl to 10 µg/µl, showing extinction at 578 nm for defined protein concentrations. Tumor lysates were prepared from 6 cryo-tumor sections, each 50 µm thick, which were homogenized in Mixer Mill 300 (Retsch, Hann) at 30 Hz for 1.5 minutes in 1 % SDS/PBS containing general protease inhibitors. The homogenate was centrifuged at 12000 rpm for 15 minutes at 4 °C. The clarified supernatant was transferred to a new tube and protein was quantified as described above.

Protein precipitation was performed using trichloroacetic acid (TCA). For this purpose, 50 µg of protein sample was mixed with 1 % Triton-X 100 and 55 % TCA in a 1:2 ratio and incubated on ice for 10 minutes, then centrifuged at 10000 rpm for 10 minutes at 4 °C. Precipitated proteins were washed with ice-cold acetone and dried at 37 °C for 1 minute. Proteins were solubilized in Laemmli buffer, heated at 95 °C for 5 minutes, spun and resolved by SDS-PAGE.

2.2.2.2 SDS-PAGE and immunodetection

Equal amount of proteins were separated by SDS-PAGE under reducing conditions on a 10 % or 15 % polyacrylamide gel, according to the molecular weight of the protein to be analyzed, and transferred onto a Hybond-C nitrocellulose membrane (GE Healthcare, München) in a semidry transfer system (Sigma-Aldrich, Deisenhof). The transfer efficiency was assessed by staining the membrane with Ponceau Red staining (0.1 % Ponceau S (w/v) in 5 % acetic acid (v/v); Sigma-Aldrich). The membrane was blocked with 5 % milk powder in PBST for 1 hour, and incubated overnight at 4 ℃ with the diluted primary antibody (see section 2.1.4). Membranes were washed three times with 0.5 % PBST for 10 minutes and incubated with horseradish peroxidase-labeled secondary antibody for 1 hour at room temperature. After extensive washing, bound secondary antibodies were detected by ECL$^{®}$ system (Thermo Scientific, Asbach) and the membranes exposed to X-ray films (Thermo Fisher, Karlsruhe).

Alternatively, after separation by SDS-PAGE, proteins were stained with Coomassie Blue by incubating the gels in 0.25 % Coomassie Brilliant blue (G250, Sigma), 2.5 g Coomassie Brilliant Blue dissolved in methanol 45 %, acetic acid 10 % and H_2O, for 30 minutes at room temperature, followed by destaining with 7 % acetic acid, 10 % ethanol overnight at room temperature. After extensive washing in water, gels were incubated for 2 hours in 30 % Methanol, 5 % Glycerin diluted in water and dried between cellophane foils (Roth) according to the manufacturer's manual.

2.2.2.3 Zymographic analysis

Cell culture conditioned media was prepared as described in 2.2.1.3 and fractionated by SDS-PAGE containing 1 mg/ml bovine gelatin (Sigma). After electrophoresis, the gels were washed in 2.5 % Triton X-100 for 30 minutes to remove the SDS and incubated overnight in substrate buffer at 37 ℃. The gels were stained with 0.25 % coomassie brilliant blue (G250) dissolved in methanol 45 %, acetic acid 10 % and H_2O and the bands corresponding to gelatinase activities appeared white against the pale blue background.

2.2.2.4 Mouse cytokine antibody array

Cytokine antibody array analysis (Raybio$^{®}$ Mouse Cytokine Antibody Array, Hölzel Diagnostika Cologne) was performed using conditioned medium prepared from

fibroblasts or using tumor lysates prepared as described in section 2.2.2.1 but using Raybio® lysis buffer, according to the manufacturer's manual. Briefly, membranes were blocked for 30 minutes at room temperature with blocking buffer then incubated overnight at 4 °C with 1 ml fibroblasts conditioned media or 250 µg tumor lysate diluted in blocking buffer. After five washes, the membranes were incubated with biotin-conjugated anti-cytokine diluted 1:200 with blocking buffer overnight at 4 °C. Bound antibodies were detected with horseradish peroxidase-conjugated streptavidin secondary antibody. Proteins were visualized by chemiluminescence detection system.

2.2.2.5 Murine TNF-alpha ELISA

ELISA analysis of TNF-α content in fibroblasts supernatants and lysates, and tumor lysates was performed using mouse TNF-α ELISA Kit (Hölzel Diagnostika) according to the manufacturers' manual. 2 ml of fibroblasts supernatants were concentrated using Vivaspin with a PES membrane of molecular weight cutoff of 10000 (VivaScience, Hannover). 200 µg of fibroblasts lysates and 50 µg of tumor lysates were used for this analysis. Measurements were performed in triplicates and expressed as pg/ml.

2.2.2.6 Immunohistochemistry and immunofluorescence

The marker Ki67 is largely used as an indicator of cellular proliferation (Urruticoechea et al., 2005). To analyze the expression of Ki67, paraffin embedded tumor sections were deparaffinized and hydrated. After antigen retrieval by boiling in citrate buffer pH 7, at 600 Watts for 5 minutes, endogenous peroxidase activity was blocked with 0.3 % H_2O_2 followed by blocking with Avidin/Biotin blocking kit (SP 2001, Vector laboratories). For cleaved caspase-3, cryosections were fixed in 1 % PFA and permeabilized for 5 minutes in ice-cold acetic acid/ethanol. Sections were incubated with primary antibody (see section 2.1.4) overnight at 4 °C; the secondary antibody was added for 1 hour at room temperature. Bound antibodies were detected with AEC substrate (Dako). The nuclei were stained with hematoxylin.

For immunofluorecence, cryosections sections were fixed in ice-cold acetone for 8 minutes and blocked with 10 % normal goat serum or 10 % BSA for 30 minutes at room temperature. Primary antibody (see table 1) diluted in 1 % blocking solution was added and incubated overnight at 4 °C in a humidified chamber. Sections were

washed three times with PBS + 0.05 % Tween. Bound antibodies were detected by incubating for 1 hour at room temperature with donkey anti-goat-Alexa 594 or goat anti-rat-Alexa 488-conjugated secondary antibodies diluted 1:1000 in PBS + 0.05 % Tween. Nuclei were stained using 4,6-diamidino-2-phenylinodole (DAPI; 1:1000; Roche), mounted with immumount (Thermo Scientific) and stored in the dark at 4 ℃.

2.2.2.7 Tissue histology

Hematoxylin and eosin (HE) staining was performed on 6 μm cryosections by incubating in hematoxylin (Sigma Aldrich) for 3 minutes and washing three times with lukewarm tap water. Slides were destained by dipping shortly in acid alcohol (1 % HCl in 70 % ethanol) and stained with Eosin (Sigma Aldrich) for 8 seconds. After rinsing, sections were mounted using Entelan (Sigma Aldrich) and covered with a glass cover slip. Sections were visualized with Leica Microscope as described in section 2.2.2.8.

2.2.2.8 Image analysis of staining

Fluorescently stained tissue sections were analyzed using Nikon and NIS Element AR 2.30 software. For assessment of fluorescence staining, two pictures each per intratumoral and peritumoral parts of the tumor were taken at 100x magnification. Quantification on each recorded tissue field was performed using ImageJsoftware (http://rsb.info.nih.gov/ij). The mean number of positive staining was calculated from four 100x magnification fields per section.

Light microscopy analysis was performed using a Leica with, DISKUS 4.50.1638 software (Heidelberg). Three pictures were taken per section and used for quantification.

2.2.3 Analysis of nucleic acids

2.2.3.1 RNA isolation

Total RNA was isolated by direct lysis in RNAzol solution (WAK-Chemie Medical, Steinbach). Tissue sections were homogenized using Mixer Mill 300 (Haan) for 1 minute at 30 Hz while cell lysates were collected by scraping and transferred in a 1.5 ml eppendorf tube; DNA was sheared using a 5 ml syringe and 22 G needles three times. After incubating on ice for 5 minutes, RNA was extracted using Chloroform-isoamyl alcohol mix (24:1; v/v) and incubated on ice for 5 minutes, centrifuged at

12.000 rpm at 4 °C for 15 minutes. The upper colorless phase containing the RNA was transferred into a new tube and precipitated by adding 1 volume of 100 % Isopropanol and incubating for 30 minutes on dry ice. After centrifugation at 10.000 rpm for 10 minutes, RNA pellet was washed with 75 % ethanol, air-dried, and resuspended in DEPC-treated water. Integrity of RNA was analyzed by electrophoresis on a 1 % agarose-TBE gel and concentration determined by measuring the optical density at 260 nm (OD_{260} x 40 µg/ µl).

2.2.3.2 Reverse transcriptase and polymerase chain reaction (RT-PCR)

cDNA was generated by reverse transcription of 1 µg RNA using Oligo d(T)16 primers (50 µM; Roche) and MuLV reverse transcriptase (50 U/µl) in the presence of RNase Inhibitors (20 U/µl; Perkin Elmer) to preserve RNA integrity. Reverse transcription was performed using the following conditions: 21 °C 10 minutes; 42 °C 20 minutes; 99 °C 5 minutes. 2 µl of the cDNA was used to amplify specific transcripts by PCR using REDtaq™ ReadyMix™ PCR Reaction Mix (Sigma Aldrich) and 10 µM of forward and reverse primers. PCR reactions were performed within the linear range of amplification: denaturation (94 °C, 1 minute), annealing (see table 1, 1 minute), extension (72 °C, 1 minute), and final extension (72 °C, 1 minute). Primers used for mouse (m) and medaka (mk) PCR, cycle numbers and product size are listed in table 1 below. Amplified cDNA was subjected to electrophoresis separation on a 2 % TBE-agarose gel containing 0.5 mg/ml ethidium bromide. Amplification of S26 was used as control. The PCR products were detected using Eagle eye UV transillumination (Peqlab, Erlangen). The ratios of specific PCR products to S26 were quantified by densitometry using the ImageJsoftware (http://rsb.info.nih.gov/ij).

2.2.3.3 Genomic DNA preparation from mouse tails

Genomic DNA was isolated from 0.5 cm tail by incubating in 500 µl genomic DNA lysis buffer containing 200 µg/ml proteinase K overnight at 55 °C with shaking at 300 rpm. Hairs and undigested tissue were eliminated by centrifuging at 10000 rpm for 10 minutes at room temperature. The supernatant was transferred into a new tube containing 500 µl Phenol-Chloroform-Isoamylalkohol (Roth; ratio 25:24:1) and centrifuged at 12000 rpm for 5 minutes. Genomic DNA was precipitated with 1/20 volume of 3 M sodium acetate and washed twice with 70% ethanol. Pelletted DNA was air dried for 5 minutes and dissolved in 100 µl sterile water at 55 °C for 1 hour. 1

µl of dissolved DNA was used for genotyping by PCR Primers used for genotyping are listed in table 1 above.

Table 1. Primers

Gene	Accession No.	Sequence (5' – 3'; f, forward; r, reverse)	Tm (℃)	No. of cycles	Product size (bp)
mAdam-9	NM_007404	f GTAAGAGATCTGCTTGAACTG r TTGCCTCTCTGCGACTAAG	48	40	130
mAdam -10	NM_007399	f GCAACATCTGGGGACAAACT r TTGCATATCCCTTCCTTTGC	60	35	350
mAdam -17	BC145270	f TTGAGCGATTTTGGGATTTC r CATCCTCTGGTGGTCCAGTT	60	35	341
mCollagen XIV	BC138345	f TGGTGGAGAGCCTGACCCGG r GCATCCCACCTGACGCGCAT	58	35	418
mCollagen type I	NM_007743	f CTCCCAGCCTTCACTCAGAC r GAGCAGCCATCGACTAGGAC	56	30	587
mTimp-1	NM_011593	f CTGGCATCCTCTTGTTGCTA r AGGGATCTCCAGGTCCACAA	60	35	567
mTnfrI	M59378.1	f GGCAGAGGAGCCTAGTTG r CACACCCAGGAACAGTCC	50	30	212
mDecorin	NM_001190451	f TGAGCTTCAACAGCATCACC r AAGTCATTTTGCCCAACTGC	50	30	181
mFibronectin	NM_010233	f TGATCATGCTGCTGGGAC r CTCGGTTGTCCTTCTTGCTC	50	30	197
GFP	L29345	f ACCCCGACCACATGAAGCAGC r CGTTGGGGTCTTTGCTCAGGG	68	38	417
mS26	NM_013765	f AATGTGCAGCCCATTCGCTG r CTTCCGTCCTTACAAAACGGCT	56	30	326
mAdam-9 genotyping	11502	f ACTTGGAACAGACTGTCCA r CGTTCATAGTTCTCAAGAG	54	30	WT 121 KO 1000
NeoPolyA cassatte		f GCTATGACTGGGCACAACAGA r CAAGGTGAGATGACAGGAGAT	55	30	280
mk Adam-9	ENSORLT00000021845	f GTACAACTGAACGTTCGCG r GGATGAGCTGAGCTGAG	50	30	163
mk Adam-10	ENSORLT00000006689	f TGAACCCAAATACATGC r CACAATCCACTCGGCGA	50	30	221
mk Adam-12	ENSORLT00000012319	f TTATATCTCTCGGAGAC r CTTGATCTGAAGGCCTT	50	30	181
mk Adam-15	ENSORLT00000021131	f CCAAGTACATTGAACTGGTG r GTTGAGCGTGTCCGTG	45	30	215
mk Adam-17	ENSORLT00000019188	f TTCGAGCCAATGCCTCC r GGTTCTGTCCGGTCAGAT	50	30	301
mk Mmp-2	AB033754.2	f AAGTGTGGAGCGACGTC r CATCAGCGTTTCCAAAC	55	30	243
mk Mmp-9	AB033755.1	f GAAACAGCCTCGCTGTG r CATGATGTCAGCGGTGC	55	30	220
mk Mmp-13	ENSORLT00000018115	f TCCGAATGTGGGCTTTG r CTCCAATACTCTTCATC	45	30	157
mk Mmp-14	ENSORLT00000009177	f AGAGCCACATCTGAAGC r GGTCAAAGTGAGTGTCT	55	30	238
mk β-actin	ENSORLT00000017152	f TGTCATGGTGGGTATGG r GGTCATCTTCTCCCTGT	50	30	235

2.2.4 Animal experiment

2.2.4.1 Ethics and animal care

Adam-9$^{-/-}$ mice of a 129/SvJ and C57BL/6J mixed genetic background were kindly provided by Prof C. Blobel, Hospital for Special Surgery, New York, USA. Animals were kept in cages covered with air filters under specific pathogen-free conditions. The animal experiments have been approved by the local veterinary authority authorization 50.203.2-K 37a, 20/05 and 87-51.04.2010 A356.
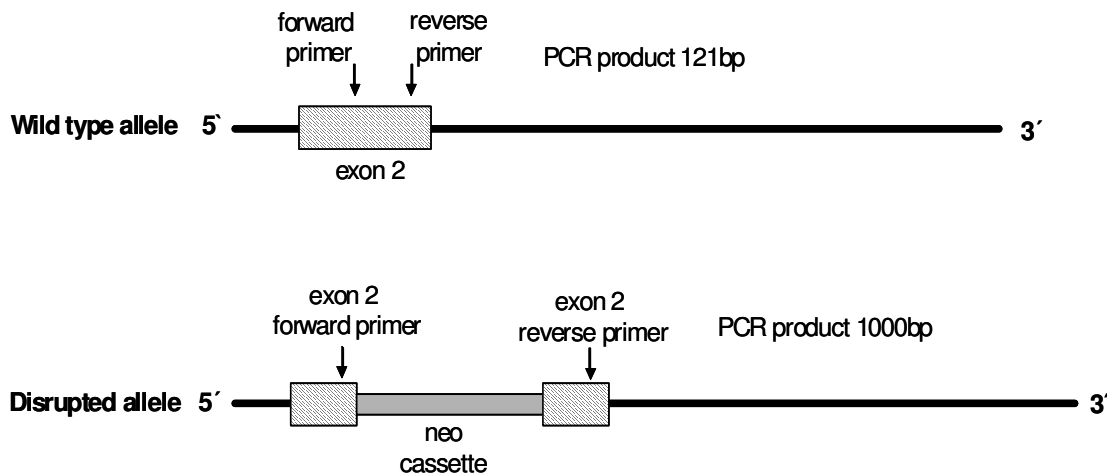

Figure 5. Simplified schematics of targeted mutation of Adam-9. Diagram shows the positioning of the primers for amplifying Adam-9 exon 2. The positioning of the primers allow amplification of a 121 bp fragment in wild type animals and a larger 1000 bp fragment in knockout animals after successful insertion of the neo cassette. The 121 bp fragment is absent in knockout animals.

2.2.4.2 Melanoma grafting

The initial experiments were performed by comparing wild type (WT) and Adam9$^{-/-}$ littermate offsprings of heterozygous Adam9$^{+/-}$ parents. To increase the number of animals for this analysis, Adam9$^{-/-}$ or WT offspring were collected from one pair of heterozygous Adam9$^{+/-}$ parents. The resulting WT or Adam9$^{-/-}$ mice were mated with one another to generate litters of WT or Adam9$^{-/-}$ mice that were closely related, as they were derived from the same heterozygous grandparents. Mice were used at the age of 6-8 weeks. Animals were anesthetized with a single intraperitoneal injection of 0.5 ml 10 % ketamine, 0.25 ml 2 % Xylazine in 4.5 ml 0.9 % NaCl. The fur on the right flank of the body was shaved and bepanthen (Roche) applied to the eyes to maintain eye moisture and protection against irritants. 1 x 10^6 B16F0 or B16F1 cells or 100 µl melanoma explants from HGF/CDK4$^{R24C/R24C}$ mice, were injected intradermally into the flank of the mice, using 1 ml syringes with µl scale and 26G ½

0.45 x 13 mm needles (Neolus). The same volume of cells was plated on culture dishes to check their viability after injection. Tumor size was measured using a precision caliper (Mitutoyo, Neuss) and tumor volume was calculated by multiplying the larger diameter with the smaller diameter and the thickness of the tumor. Animals were sacrificed at day 3, 6, 10 and 13 post-injection or as indicated. Tumors were removed surgically and half the tumor tissue was immediately embedded in optimal-cutting-temperature compound (Tissue-TEK, Vogel, Giessen) and directly frozen, the other half was fixed in formalin overnight at 4 °C and embedded in paraffin. Sections were cut at 8 μm for immunofluorescence and immunohistochemistry (see section 2.2.2.6).

To analyze metastasis formation, to increase blood flow to the tail, mice were placed under a heat lamp and transferred to a holding device to restrains the mouse while allowing access to the tail. 1 x 10^5 B16F1 cells in 0.1 ml PBS were injected into the lateral tail vein. After removing the needle, bleeding was stopped by holding the site with gauze before returning the mice to their cages. Organs (lungs, lymph nodes, kidneys and heart) of the animals were collected after 21 days, washed in PBS and for analysis of metastatic formation. Metastasis was analyzed macroscopically by counting the number of macro-metastases on the surface of the different organs.

2.2.5 Production of recombinant soluble ADAM-9 protein

2.2.5.1 Cloning and site directed mutagenesis

The plasmid containing the short soluble variant of human ADAM-9 was a gift from Dr. A. Toker, Boston University, USA. It was cloned using the BamHI and XhoI restriction site in the pcDNA4/TO/myc-His vector in frame with a C-terminal c-myc and polyhistidine (6x His) tag (figure 6).
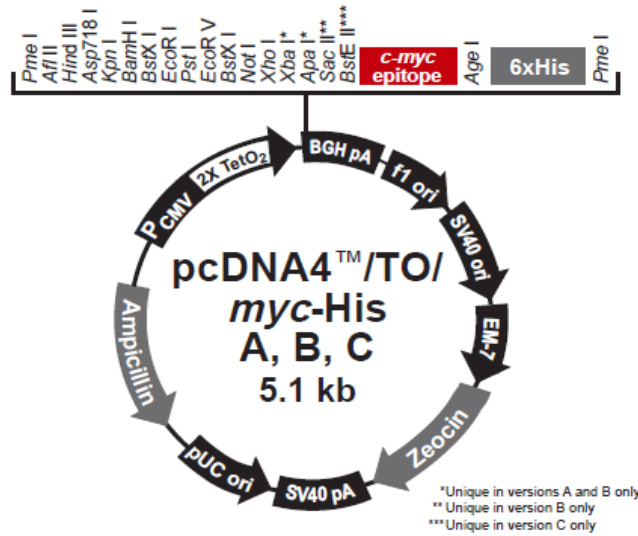
Figure 6. pcDNA4/TO/myc-His expression vector used for eukaryotic expression of recombinant soluble ADAM-9. Adam-9 was inserted in the BamHI and XhoI restriction sites in frame with the c-myc and His tag (edoc.hu-berlin.de/.../HTML/chapter3.htm).

The cDNA encoding the long soluble variant of ADAM-9 (referred to as ADAM-9s L) was amplified from cDNA derived from glioma cell line A-172, where it was first detected (Hotoda et al., 2002), using primers listed in table 2. These primers were designed to contain in the amplified product a HpaI restriction site at the 5´ end and an XhoI restriction site at the 3´ end. The resulting PCR product was inserted into pCR® 2.1 plasmid vector (figure 7) using the TA cloning® kit (Invitrogen) according to the manufacturer's manual.

Figure 7. Features of the pCR® 2.1 vector with Single 3´-thymidine (T) overhangs for TA Cloning (http://igene.invitrogen.com/products/selector/vectors/navs/Cloning%20System/TA).

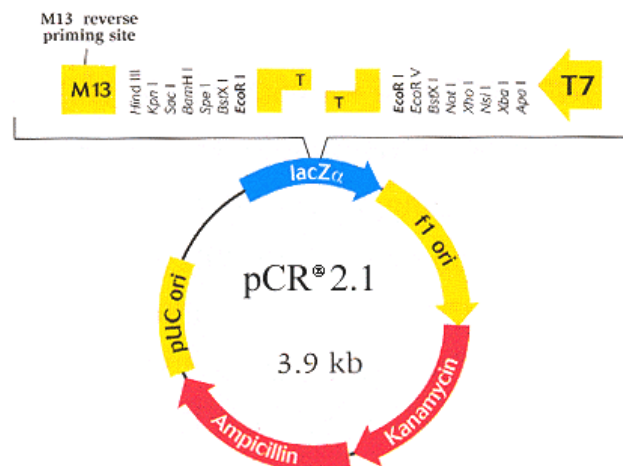Briefly, the PCR product was ran on a 1 % agarose gel and extracted from the gel using Qiagen Gel Extraction® Kit. The eluted DNA fragment was incubated with 5 U/µl Taq-Polymerase (Fermentas) and 10 µM dNTPs (Roche) at 72 °C for 10 minutes to generate 3'-A-overhangs necessary for the TA-cloning. DNA was ligated using 400 U/ml T4 DNA ligase overnight at 14 °C into a linearized pCR® vector with 3´-T-overhangs flanked by EcoRI restriction sites. Plasmid was amplified by transformation into competent DH5α bacteria (Invitrogen) by heat shock and grown in LB-Medium containing 100 µg/ml Ampicillin (PAA) at 37 °C overnight with shaking (125 rpm). Plasmids were purified with Qiagen Mini-prep® Kit. Cloning was verified by digestion with EcoRI and visualization on 1 % TBE-agarose gel. Plasmids containing the long soluble variant of ADAM-9 were cleaved with HpaI and XhoI and directionally cloned into pcDNA4 vector containing the soluble short variant of Adam-9 cleaved with the same enzymes. cDNA identity was further verified by sequencing (performed by the sequencing facility of the Center for Molecular Medicine, University of Cologne).

Table 2. Primers used for cloning of ADAM-9 soluble long and for site directed mutagenesis.

	Tm °C	Primer sequence (5' – 3'; f, forward; r, reverse)
Adam-9 for. HpaI	50	f. 5´<u>GTTAAC</u>TTTAAATAAAGGAGGAAACTGCC 3´
Adam-9 rev. XhoI	50	r. 5´ <u>CTCGAG</u>TTTCCCATGTCCATGACAC 3´
Adam-9 mutagenic	60	f. 5´ CATTGTTGCTCATGCATTGGGTCATAATC 3´
		r. 5´ GATTATGACCCAATGCATGAGCAACAATG 3´

Underlined are the added restriction sites, highlighted in red are the mutagenic base pairs.

The transformer site directed mutagenesis kit (CloneTech laboratories) was used to introduce specific mutations in the zinc binding motif of the metalloprotease domain (amino acid substitution E>A) leading to generation of a proteolytic inactive protein (Rhoghani 1999). The codons for glutamic acid and alanine in the zinc binding motif are indicated below; the amino acid resulting from the point mutation is indicated in red. Underlined and highlighted in red is the base pair change that leads to the conversion of glutamic acid to alanine,

	Zinc binding motif	**H**	**E**	**L**	**G**	**H**
ADAM9	-	**CAT<u>GAA</u>TTGGGTCAT**				
Mut. ADAM9	-	**CAT<u>GCA</u>TTGGGTCAT**				
		H	**A**	**L**	**G**	**H**

Briefly, plasmid DNA was denatured and mutagenic primers were annealed to the DNA template for the synthesis of the mutant DNA strand using T4 DNA polymerase (5 U/µl) at 37 °C for 2 hours. The reaction was stopped by heating at 70 °C for 5 minutes. The parental DNA was linearized by adding 1 µl Nde I and incubating for 1 hour at 37 °C. The mutated strand was amplified by transforming into E.coli DH5α. Primers used are listed in table 2 above. Insertion of the mutation was confirmed by DNA sequencing, performed by the sequencing facility of the Center for Molecular Medicine, University of Cologne.

2.2.5.2 Production and purification of recombinant soluble ADAM-9

COS-7 cell were seeded at a density of 1×10^3 cells per cm². At a confluency of 90 % cells were transfected with 2 µg of pcDNA4/To/myc-His containing either ADAM-9 soluble long or the mutated (E>A) form using Lipofectamine 2000 (Invitrogen, Karlsruhe). Cells were cultured in DMEM for 24 hours after which they were splitted and cultured in the presence 500 µg/ml zeocin (Invitrogen) to select stably transfected clones. Serum-free supernatants collected and clarified by centrifugation at 1200 rpm for 5 minutes. The presence of ADAM-9 in the supernatant was checked by western blot before purified by affinity chromatography. TALON metal affinity resins (Clontech) were added to the supernatant at a ratio of 1:100, incubated overnight at 4 °C to allow binding of the His tagged protein to the resins. Resins were washed twice with gradient buffer A and bound proteins were eluded with 250 mM imidazole overnight at 4 °C. Purified proteins were concentrated using the Vivaspin 10000 MWCO PES (VivaScience) by centrifuging at 1200 rpm until the desired volume was achieved; the sample was recovered from the concentrate pocket with a pipette. Recombinant proteins were stored at 20 °C.

2.2.5.3 *In vitro* enzymatic analysis

Recombinant proteins (0.5 µg/µl) were incubated with active or inactive (E>A mutated) recombinant soluble human ADAM-9 protein (0.05 µg/µl) in substrate buffer pH 8 overnight at 37 °C. The reaction was terminated by boiling with 5 µl Laemmli

reducing loading buffer at 95 °C for 5 minutes and analyzed by western blot (section 2.2.2.2).

2.2.6 Statistical analysis

Results were expressed as mean values with standard deviations (SD) or standard error of mean (SEM) as indicated. Student t-test was used to analyze the statistical differences. All *in vitro* experiments were carried out in triplicates and repeated at least three times. All statistical tests were performed using GraphPad Prism™ software (GraphPad™, Califonia, USA) and a p value < 0.05 was considered as a statistically significant.

3 Results

3.1 ADAM-9 in melanoma

3.1.1 ADAM-9 in human melanoma *in vivo*

ADAM-9 is over-expressed in a number of human cancers including human melanoma where it is expressed at the tumor-stroma border by both tumor and stroma cells (Zigrino et al., 2005). Latest studies have shown that the expression of this protein on the surface of melanoma and stroma cells mediates melanoma-fibroblasts cell-cell interaction (Zigrino et al., 2011) however the molecular activities mediated by these interactions in tumor cells and in host cells, and their functional role in melanoma progression are not yet understood.

3.1.2 Analysis of Adam-9 in murine melanoma grafts

In order to characterize the expression of ADAM-9 *in vivo*, we injected B16F1 melanoma cells intradermally in the flank of wild type (WT) mice of a 129/SvJ and C57BL/6J mixed genetic background. After 13 days, tumors were harvested and the expression and localization of ADAM-9 was analyzed by immunofluorescence. ADAM-9 was detected in tumor cells adjacent to the stroma and in peritumoral stromal cells (figure 8), an expression pattern which is similar to that observed in human melanoma (see section 3.1.1).
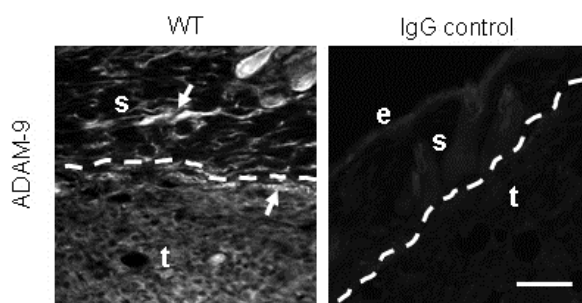

Figure 8. Expression of ADAM-9 in murine melanoma. A, representative image of immunofluorescence detection of ADAM-9 in melanomas from WT mice. The arrow indicates ADAM-9 expression at the tumor-stroma border. Dashed lines denote the tumor-stroma border. IgG control confirms the specificity of the staining. s, stroma; t, tumor; e, epidermis. Scale bar, 200 μm.

3.2 Role of host-derived ADAM-9 in growth of B16F1 melanoma *in vivo*

3.2.1 ADAM-9 expression in melanoma from *Adam-9^{-/-}* in comparison to WT mice

To investigate the role of host-derived ADAM-9 in melanoma progression *in vivo*, we used mice with complete deletion of *Adam-9*. These mice do not show any major phenotype during development and in adulthood (Weskamp et al., 2002). Furthermore, skin formation and differentiation was not altered in the absence of *Adam-9* (Mauch et al., 2010). Disruption of *Adam-9* in these animals was confirmed by genotyping of tail genomic DNA, by amplification of a fragment of the NeoPolyA cassette sequence used to disrupt the Adam-9 gene (Weskamp et al., 2002) and a fragment of the *Adam-9* exon2 (figure 9A). The Adam-9 exaon2 primers were positioned so that a 121bp fragment is amplified in WT animals and a larger 1000bp fragment in knockout animals after successful insertion of the neo cassette. The 121bp fragment is absent from knockout animals (figure 5; section 2.2.4.1).

Transcript and protein expression of ADAM-9 in melanoma from *Adam-9^{-/-}* mice in comparison to those from WT mice was analyzed. Adam-9 transcripts were analyzed by PCR and protein expression by immnunofluorescence. Adam-9 transcript was detected in healthy back skin from WT mice but absent in the skin from *Adam-9^{-/-}* animals, thus confirming host depletion (figure 9B). In melanomas from *Adam-9^{-/-}* animals (induced as described for WT mice, section 3.1.2 above), Adam-9 transcript was detected in reduced amounts compared to melanomas from WT mice. These data were confirmed by quantitative PCR analysis (figure 9B lower panel). In melanoma developed in *Adam-9^{-/-}* mice, ADAM-9 protein was absent the surrounding stroma and expressed, to a lesser extent, in the tumor mass compared to tumors from WT mice.
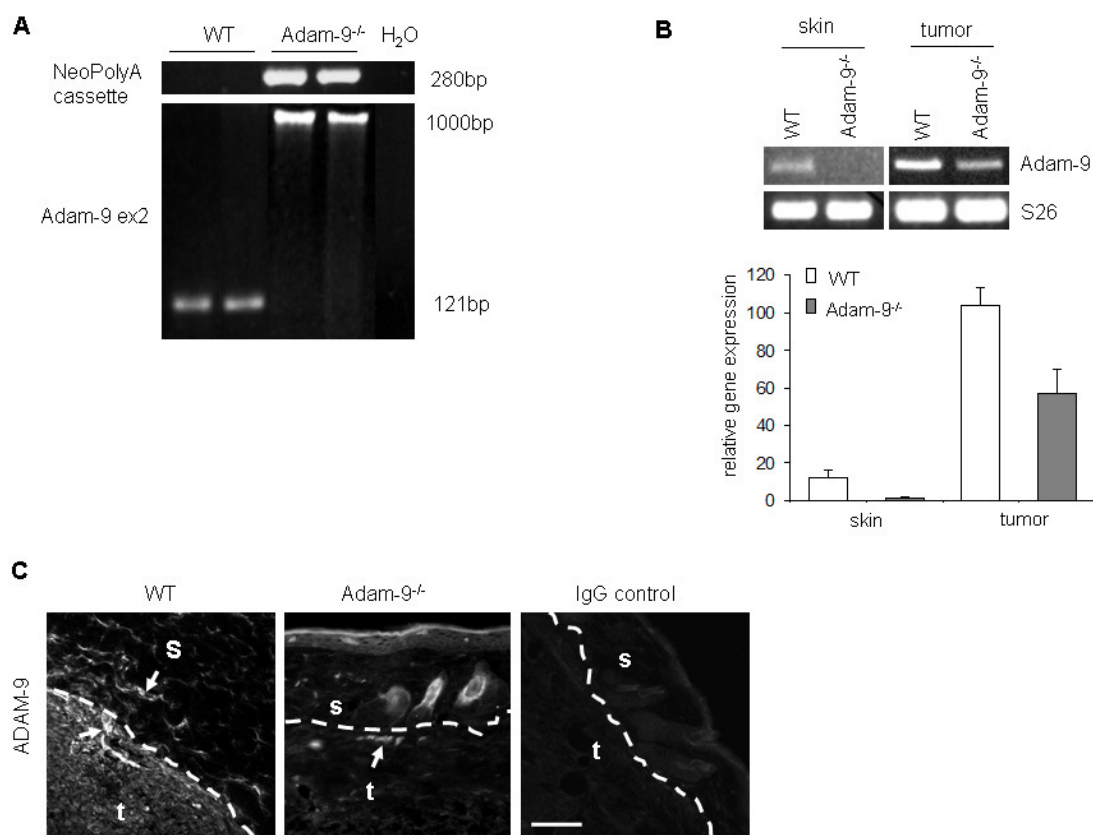
Figure 9. Expression of Adam-9 in *Adam-9*^{-/-} and WT mice. A, genotype of *Adam-9*^{-/-} and WT mice. Lack of Adam-9 is shown by the presence of a band for NeoPolyA cassette and absence of a band for Adam-9 exon2. Water was used as negative control. B, upper panel, Adam-9 transcripts in back skin of mice and melanoma from WT and *Adam-9*^{-/-} mice. S26 ensures equal loading. Lower panel, relative expression levels of Adam-9 transcript as analyzed by quantitative real time PCR. Data are represented as the relative average expression (n=3). ∗∗ p< 0.0028. C, ADAM-9 protein expression in melanoma from *Adam-9*^{-/-} and WT mice. The arrow indicates ADAM-9 expression at the tumor-stroma border. Dashed lines denote the tumor-stroma border. IgG control confirms the specificity of the staining. s, stroma; t, tumor. Scale bar, 200 μm.

3.2.2 B16F1 tumor growth kinetics

Melanoma tumor growth kinetic in mice was determined by grafting B16F1 murine melanoma cells, stably expressing GFP, into the flank of age and sex-matched litters of WT and *Adam-9*^{-/-} animals. Tumor growth was measured with a precision caliper, over a period of 13 days. Tumors developed in WT mice had an average volume of 0.017 cm³ at day 3 and 0.56 cm³ at day 13 (figure 10). In *Adam-9*^{-/-} mice, we observe significantly larger tumors with an average size of 0.036 cm³ at day 3 post injection and 2.1 cm² at day 13, a 3-fold increase in tumor size as compared to WT animals. Furthermore, at day 13 post injection, 10 out of 12 knockout mice had tumors larger than 1 cm³ while only 3 out of 14 WT mice developed tumors larger than 1 cm³.
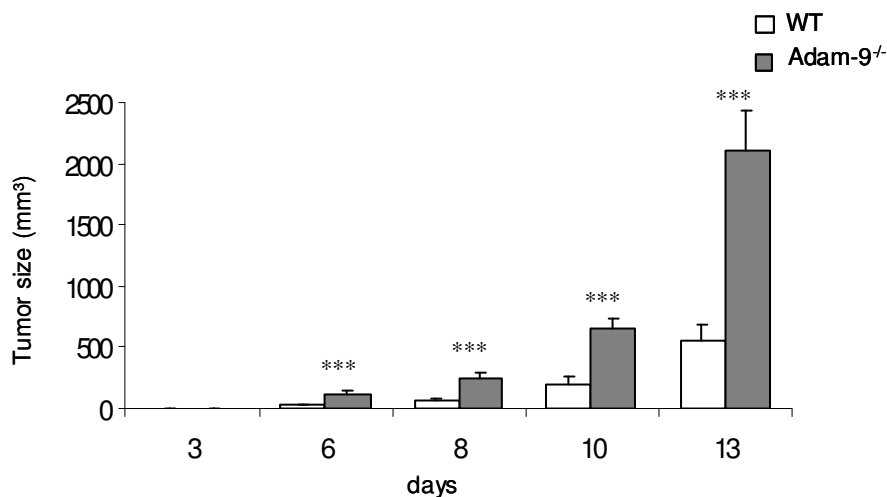
Figure 10. Loss of host-derived ADAM-9 favors B16F1 melanoma growth. B16F1 melanoma growth upon intradermal injection of B16F1 melanoma cells in the flank of *Adam-9*^{-/-} and WT mice. Tumor volume was measured using a precision caliper and average size is presented as mean ± SEM (day 3: WT n=27, *Adam-9*^{-/-} n=26; day 6: WT n=22, *Adam-9*^{-/-} n=20; day 8 and 10: WT n=18, *Adam-9*^{-/-} n=16; day 13 WT n=14, *Adam-9*^{-/-} n=12). ∗∗∗ p< 0.0001.

Gauiquil et al, (2009) reported reduced tumor growth in *Adam-9*^{-/-} mice after subcutaneous injection of B16F0 cells. To exclude the possibility that increased tumor growth observed in *Adam-9*^{-/-} animals was specific to the melanoma cell type, we performed similar experiments using a less aggressive melanoma cell line, the subline B16F0 (Fidler 1975). Moreover, to demonstrate that this finding is also true for primary tumor cells we used explants from spontaneously developed melanomas prepared from HGF/CDK4[R24C/R24C] mice (Tormo et al., 2006). To exclude the possibility that different amounts of Adam-9 produced by these melanoma cells could influence tumor growth, we analyzed Adam-9 expression in these cells by RT-PCR. This analysis showed comparable amounts of Adam-9 transcript in B16F0 and B16F1 cell lines as well as explants from HGF/CDK4[R24C/R24C] mice (figure 11C) thus excluding altered ADAM-9 expression profile as causative for any differences observe in tumor growth.

When grafted intradermally in mice, a similar difference in tumor growth was observed in all the different melanoma cells, with tumors developed in *Adam-9*^{-/-} mice larger than those from WT animals (figure 11A and B). This indicates that the difference in tumor growth between WT and *Adam-9*^{-/-} is not specific to the melanoma cell type used but rather depending on the host.
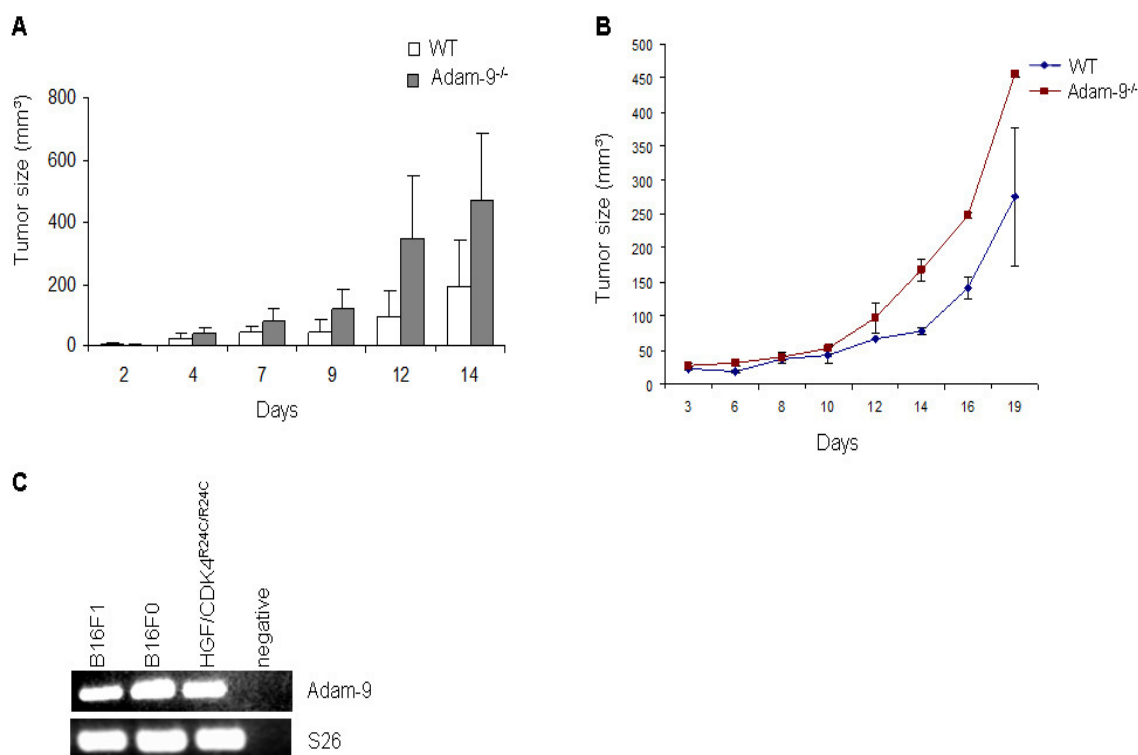
Figure 11. Melanoma development is increased in *Adam-9*$^{-/-}$ mice. B16F0 cells and tumor explants from HGF/CDK4$^{R24C/R24C}$ mice were injected intradermally into the flanks of WT and *Adam-9*$^{-/-}$ mice and tumor volume of (A) B16F0 cells (WT and *Adam-9*$^{-/-}$ n=6) and (B) melanoma explants from HGF/CDK4$^{R24C/R24C}$ mice (WT and *Adam-9*$^{-/-}$ n=5) was measured as a function of time. All values are expressed as mean ± SEM. C, RT-PCR analysis of Adam-9 mRNA expression in cells used in *in vivo* tumor growth experiments.

3.2.3 Melanoma metastasis in *Adam-9*$^{-/-}$ mice

In mice, as in human melanoma development is followed by progressing of tumor cells into the underlying dermis and metastasis to distant organs. Melanoma metastasis to the lungs is often the first site of visceral metastasis (Balch et al., 2003). The regional lymph nodes are the first lymph nodes to encounter fluid draining from the primary tumor and are thought to represent the first site tumor cells will spread to (Nathanson 2003). To investigate whether ablation of ADAM-9 in the stroma leads to altered metastasis formation, B16F1 colonization of lymph nodes and lungs was characterized by amplification of GFP transcripts, expressed by B16F1 cells, using total RNA prepared from these different organs. Although tumors were larger in *Adam-9*$^{-/-}$ as compared to WT mice, the number of lungs and lymph nodes harboring GFP-positive tumor cells was similar in *Adam-9*$^{-/-}$ and WT animals at day 3, 6, and 10. At day 13, there was a 10 % decrease in metastasis to lungs and lymph nodes in *Adam-9*$^{-/-}$ mice compared to WT (figure 12A).
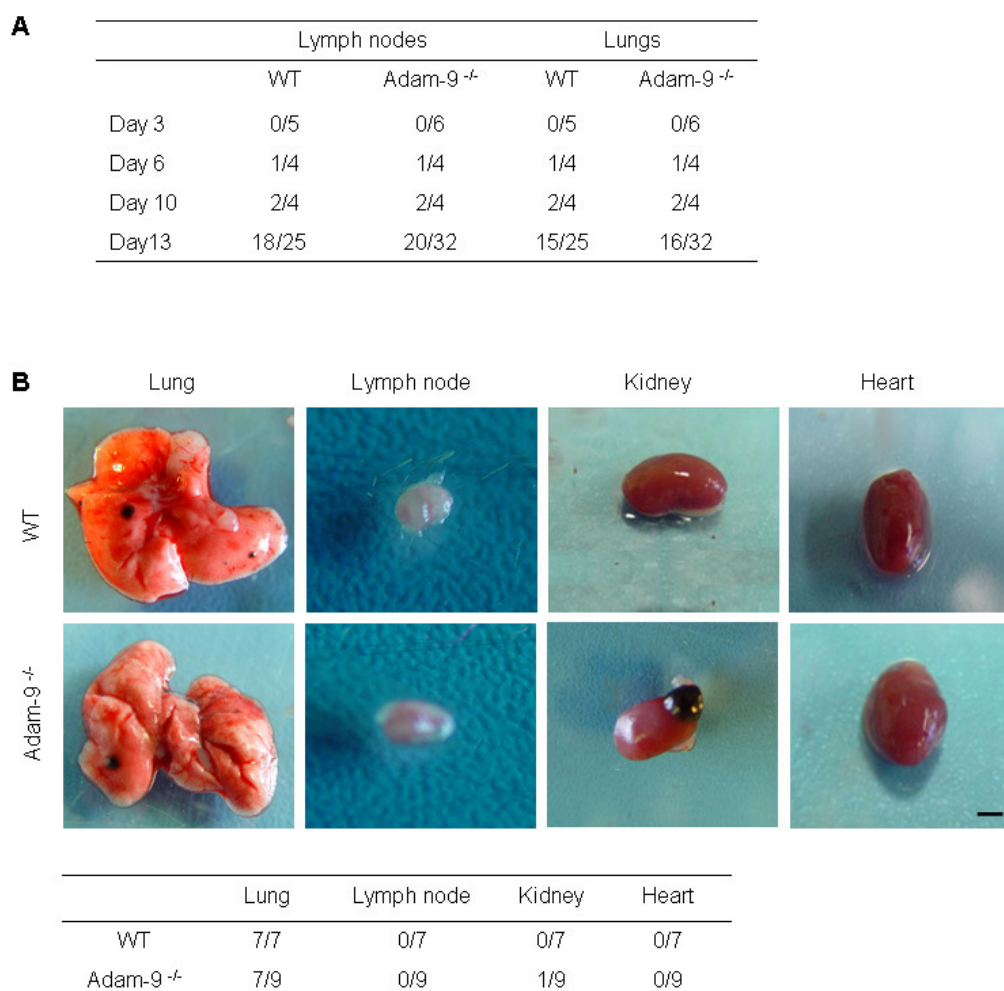
A

	Lymph nodes		Lungs	
	WT	Adam-9 -/-	WT	Adam-9 -/-
Day 3	0/5	0/6	0/5	0/6
Day 6	1/4	1/4	1/4	1/4
Day 10	2/4	2/4	2/4	2/4
Day 13	18/25	20/32	15/25	16/32

B

	Lung	Lymph node	Kidney	Heart
WT	7/7	0/7	0/7	0/7
Adam-9 -/-	7/9	0/9	1/9	0/9

Figure 12. Loss of *Adam-9*$^{-/-}$ does not affect metastasis. A, RT- PCR amplification of the GFP to detect B16F1 melanoma cells in lungs and lymph nodes. Results are expressed as a ratio of the number of positive animals to the total number of animals analyzed. B, upper panel, representative pictures of the analyzed organs. Scale bar 5 mm. Lower panel, analysis of metastasis to different organs after B16F1 injection into the tail vein. Visible metastasis on the surface of organs was identified macroscopically and counted presented as number of positive organs.

In considering the steps required for successful metastasis, extravasation of circulating tumor cells from blood vessels into target organs is a critical process. The metastatic potential of blood-borne tumor cells was evaluated by tail vein injection. B16F1 cells were injected intravenously into 8 weeks old female WT and *Adam-9*$^{-/-}$ mice. After 21 days, the animals were sacrificed and metastases formation in the lymph nodes and visceral organs analyzed visually to assess the number of macro-metastasis. Metastases appeared on the surface of the organs as dark spots (figure 12B), while metastasis to lymph nodes was detected by increased size of the lymph

node as well as the presence of strongly pigmented melanoma cells. There was no difference in the number of macro-metastasis on the surface of lungs from WT and *Adam-9*^{-/-} animals (figure 12B, upper panel). No metastasis was observed in lymph nodes and hearts from WT and *Adam-9*^{-/-} animals. Only one kidney from *Adam-9*^{-/-} and none from WT mice had macro-metastasis. This suggests that while host-derived ADAM-9 may play a role in melanoma growth, but is not involved in modulating metastasis.

3.3   Processes involved in melanoma growth

3.3.1   Vascularization of tumors

Ablation of host-derived Adam-9 favors melanoma development, several events may contribute to this effect, including, angiogenesis, inflammation and stroma activation. Angiogenesis is important to supply nutrients to the tumor and in addition offers a way to metastatic spread (Bergers and Benjamin 2003). ADAM-9 is expressed on endothelial cells and has been shown to influence pathological neovascularization in the retina after oxygen restriction, probably by processing membrane-bound proteins present on endothelial cells (Guaiquil et al., 2009). We investigated whether alterations in angiogenesis contributed to the increase tumor growth in *Adam-9*^{-/-} animals, and analyzed blood vessel density by immunodetection of the endothelial cell marker CD31 (De Young et al., 1993). This analysis was performed using sections from four different animals per group, per time point. ImageJ software analysis was used to quantify the amount of positive CD31 pixel count from four 100x magnification fields per section. We observed increased blood vessel density within the tumor (intratumoral) in *Adam-9*^{-/-} as compared to WT tumors at all three time points (figure 13A and B) but no differences in peritumoral vascularization (figure 13A and B).
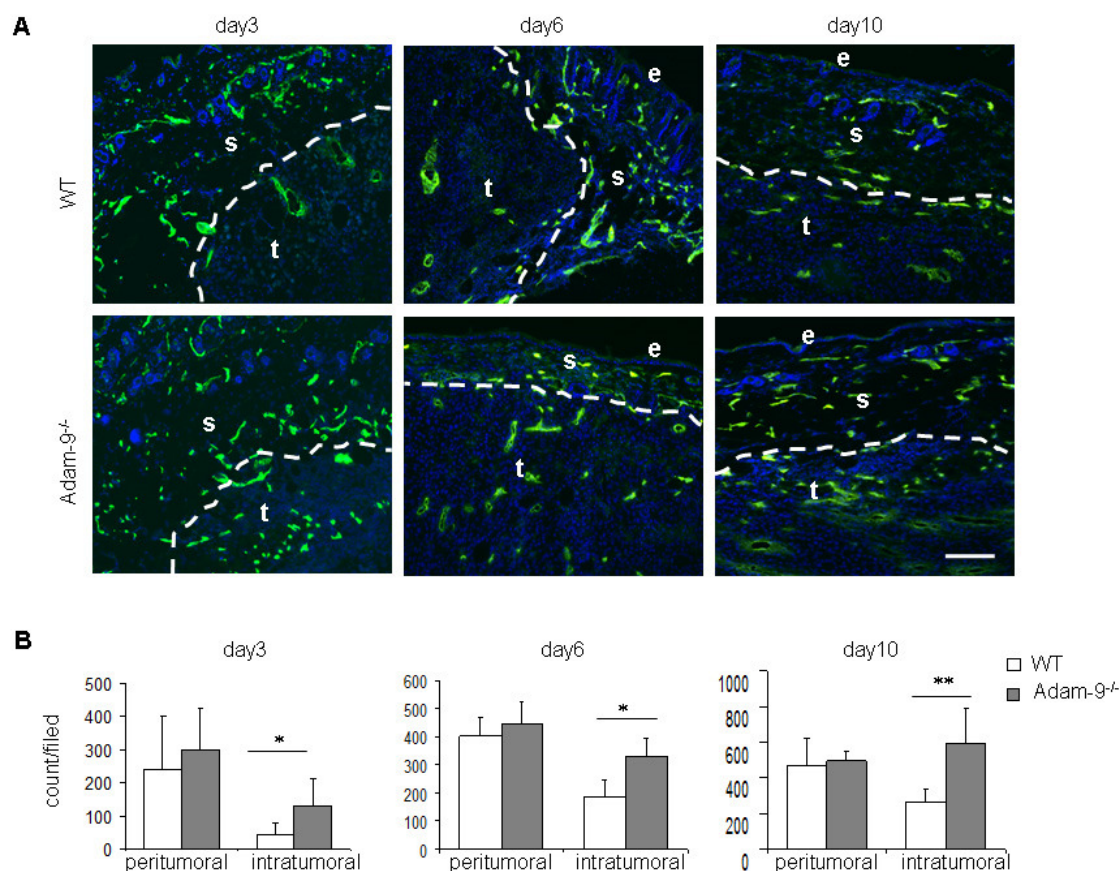
Figure 13. Intratumoral angiogenesis is increased in *Adam-9*^{-/-} mice. A, tumor vascularization was analyzed by staining for CD31 in 3, 6 and 10 days old tumors from WT or *Adam-9*^{-/-} mice. Dashed lines indicate the tumor-stroma border. e, epidermis; s, stroma; t, tumor. Scale bar 100 µm. B, quantification of CD31 staining by densitometry on four 10x fields. Graph shows the average positive staining (count) per 10x field. WT n= 4; *Adam-9*^{-/-} n=4, per time point. Scale bar 100 µm. $*$ p<0.05, $**$p<0.005.

The increased blood vessel density observed in tumors from *Adam-9*^{-/-} mice could be associated to the increased tumor size in these animals and not to the absence of ADAM-9. Hence, we have analyzed blood vessel density in tumors of comparable sizes even though from different time points. We could not observe differences in blood vessel density in the peritumoral and intratumoral area when tumors of similar sizes from WT and *Adam-9*^{-/-} animals were analyzed (figure 14). This indicates that the previously observed difference in blood vessel density (figure 13) was due to the increased tumor size in *Adam-9*^{-/-} *mice* and not to increase neoangiogenesis in the absence of Adam-9.
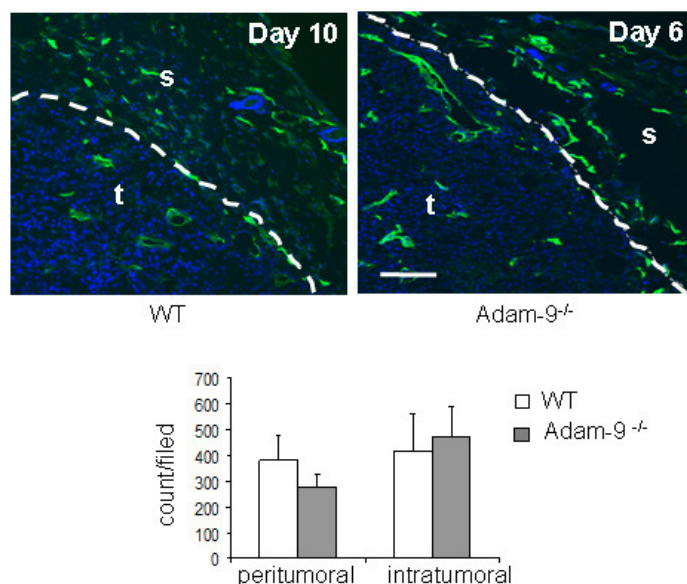
Figure 14. Loss of ADAM-9 does not influence angiogenesis. Quantification of blood vessel density in tumors of similar sizes, but from different time points, from WT and *Adam-9$^{-/-}$* mice. Blood vessel was quantified by densitometry on four 10x fields per section. Graph shows the average blood vessel count per 10x field. WT n= 5, *Adam-9-/-* n= 5. s, stroma; t, tumor. Scale bar 100 µM.

3.3.2 Inflammatory response in tumors

Another event important for tumor development and modulating tumor growth is inflammation (reviewed by Coussens and Werb 2002). Tumor cells produce a variety of cytokines and chemokines, which attract inflammatory cells such as macrophages, lymphocytes and neutrophils, to the tumor site. This infiltrate in turn generates an environment that can promote or suppress tumor growth. Whether altered inflammation contributed to the increased tumor growth we have observed in the absence of ADAM-9 (3.1.2), was determined by analyzing the recruitment of inflammatory cells to the tumor site. This was achieved by immunofluorescent detection of neutrophils, T-/B-cells (CD45) and macrophages (F4/80) (figure 15A). To semi-quantify the number of infiltrated cells, the staining was quantified by densitometry. No difference was observed in the staining intensity of all analyzed cells at day 3 and day 6. At day 10 no difference was observed in the amount of pixel count of neutrophils and B-cells recruited to the tumor site, however, a slight but not significant increase in macrophage infiltration was observed in tumors from *Adam-9$^{-/-}$ mice* (p=0.089, figure 15B). These results suggest that altered inflammation did not contribute to the increase in tumor growth observed in knockout animals.
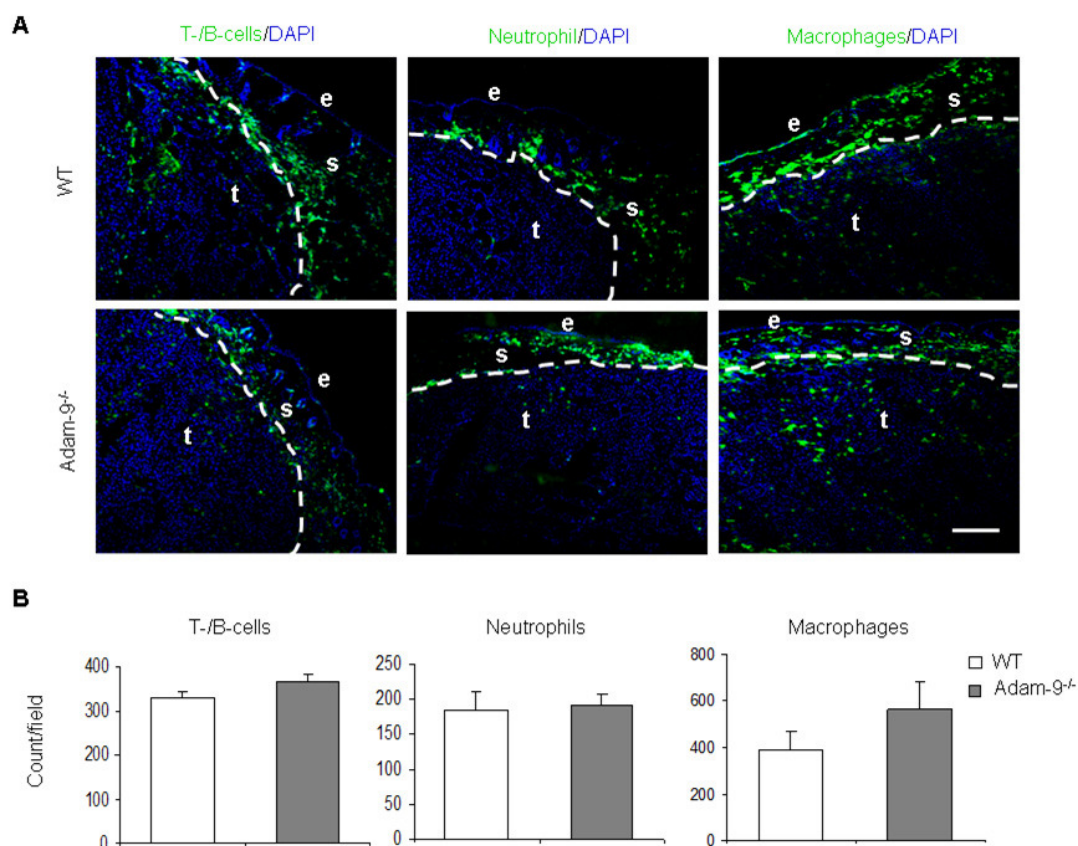
A

B

Figure 15. Inflammatory reaction at the tumor site is not altered. A, analysis of inflammation in tumor sections by staining for T-/B-cells, neutrophil and macrophages (CD68) markers all shown in green. DAPI was used to stain the nuclei. e, epidermis; s, stroma; t, tumor. Scale bar, 100µM. B, quantification of T-/B-cells, neutrophils and macrophages by densitometry of four 10x fields per section. Data represents mean ± SD (*Adam-9*$^{-/-}$ n=10, WT n=9).

3.3.3 Proliferation and apoptosis of B16F1 melanoma cells *in vivo*

Unlimited potential to replicate and resistance to apoptosis are hallmarks of cancer and a balance between these two contributes to tumor development (Hanahan and Weinberg 2000). We studied the proliferation of B16F1 melanoma cells *in vivo* by staining for Ki67, a nuclear proliferation marker (Urruticoechea et al., 2005) by immunohistochemistry in melanoma sections from WT or *Adam-9*$^{-/-}$ animals. Positive cells were counted in three representative fields and expressed as a percentage of the total cells in the same field. Tumor cell proliferation was significantly increased in tumors from *Adam-9*$^{-/-}$ mice (40.3 % positive cells) as compared to those from WT mice (15.8 % positive cells, figure 16A). We have analyzed apoptosis by immunochemical detection of active cleaved caspase-3, a key executor of apoptosis (Lakhani et al., 2006). The number of cleaved caspase-3 positive cells was 2.6 fold lower in tumors from *Adam-9*$^{-/-}$ mice as compared to WT, being 1.2 % in *Adam-9*$^{-/-}$

and 3.2 % in WT mice (figure 16). Altered ratio of Ki67 and active cleaved caspase-3 was also observed in tumors from WT and *Adam-9*^{-/-} animals of similar sizes despite the difference in excision time (figure 16B), demonstrating the differences in proliferation and apoptosis were due to the lack of ADAM-9. These results suggest that increased tumor growth in *Adam-9*^{-/-} animals resulted from altered balance between proliferation and apoptosis.
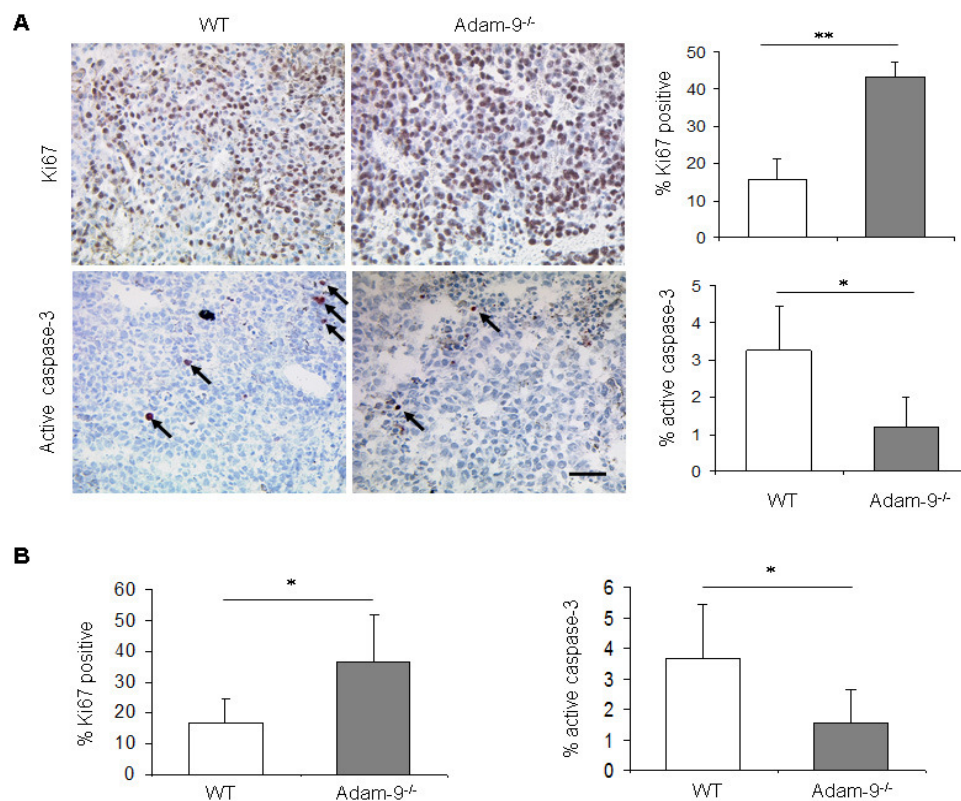

Figure 16. Tumor cell proliferation is increased in *Adam-9*^{-/-} animals while apoptosis is reduced. A, tumor cell proliferation as determined by detection of Ki67. The number of Ki67 positive cells in three 20x fields were counted and expressed as a percentage of the total number of cells. Assessment of tumor cell apoptosis by detection of cleaved caspase-3 followed by quantification as described above. (WT n=6; *Adam-9*^{-/-} n=7). B, analysis of proliferation and apoptosis in tumors of similar sizes as described above. (n=5 per genotype). Values are expressed as mean ± SEM. Scale bar 200 µM. ∗ $p < 0.05$; ∗∗ $p < 0.005$.

3.4 Role of fibroblast-derived Adam-9 on melanoma cell growth

3.4.1 Influence of cellular contacts and matrix synthesis/modification on melanoma cell proliferation

There is increasing evidence that cancer-associated fibroblasts play a role in the progression of cancer by direct cell-cell communication with tumor cells or, indirectly by secreting cytokines and growth factors and matrix components (Orimo et al.,

2001; Mueller and Fusenig 2004). To gain more insights on the molecular mechanisms how the lack of Adam-9 in the host and in particular in stromal fibroblasts can influence B16F1 cell proliferation and apoptosis, we used *in vitro* co-culture systems of B16F1 cells and primary dermal fibroblasts isolated from WT or *Adam-9*^{-/-} newborn mice. First, we ask the question whether in the absence of ADAM-9, cellular contacts between melanoma cells and fibroblasts alter melanoma cell proliferation. For this, we cultured B16F1 cells on a dense monolayer of mitotically inactive fibroblasts (figure 17 upper panel, experimental setup). After 24 hours, B16F1 cell proliferation was measured by BrdU incorporation, to detect cells that were actively replicating their DNA. Mitotic inactivation of fibroblast was performed to ensure that only the proliferation of B16F1 cells are measured and to annul the effect of cytokine/growth factors which are produced during cell proliferation. The absorbance was measured at 450 nm and expressed as a percentage to the positive control (B16F1 cell proliferation in the presence of 10 % FCS). The absorbance of mitotic inactive fibroblast monolayer was also measured to correct for background absorbance. Induction of proliferation was detected in B16F1 cells upon direct culture with fibroblasts monolayers, however, no difference was detected between B16F1 cells cultured on WT or *Adam-9*^{-/-} fibroblasts monolayer (figure 17).
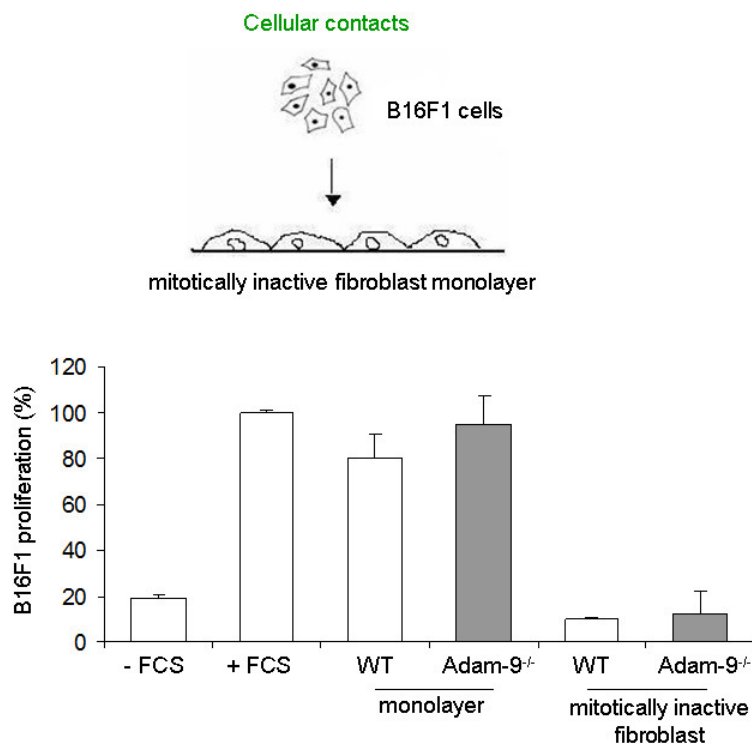
Figure 17. Cell-cell interactions do not influence B16F1 cell proliferation. Assessment of B16F1 cell proliferation by BrdU incorporation after 24 hours incubation on WT or *Adam-9*^{-/-} mitotically inactivated fibroblasts monolayer. The experimental set-up is shown in the upper panel, Cell proliferation was calculated as percentage relative to the 100 % FCS control (+, 10 % FCS; -, serum free control). The background absorbance of the mitotically inactive fibroblast monolayer was also measured. Shown is a representative of three independent experiments. Values are presented as mean ± SD.

Next we wanted to find out whether the extracellular matrix, its proteolytic modification or synthesis, also played a role in the induction of melanoma cell proliferation (Lukashev and Werb 1998) since ADAM-9 has been identified as a matrix modifying enzyme (Schwettmann and Tschesche 2001; Mazzocca et al., 2005). To investigate whether lack of ADAM-9 leads to altered matrix modifications and in turn affect B16F1 cell proliferation, we have plated B16F1 cells on matrices produced by either WT or *Adam-9*^{-/-} fibroblast as described by Beacham et al., (2007) see section 2.2.1.3.
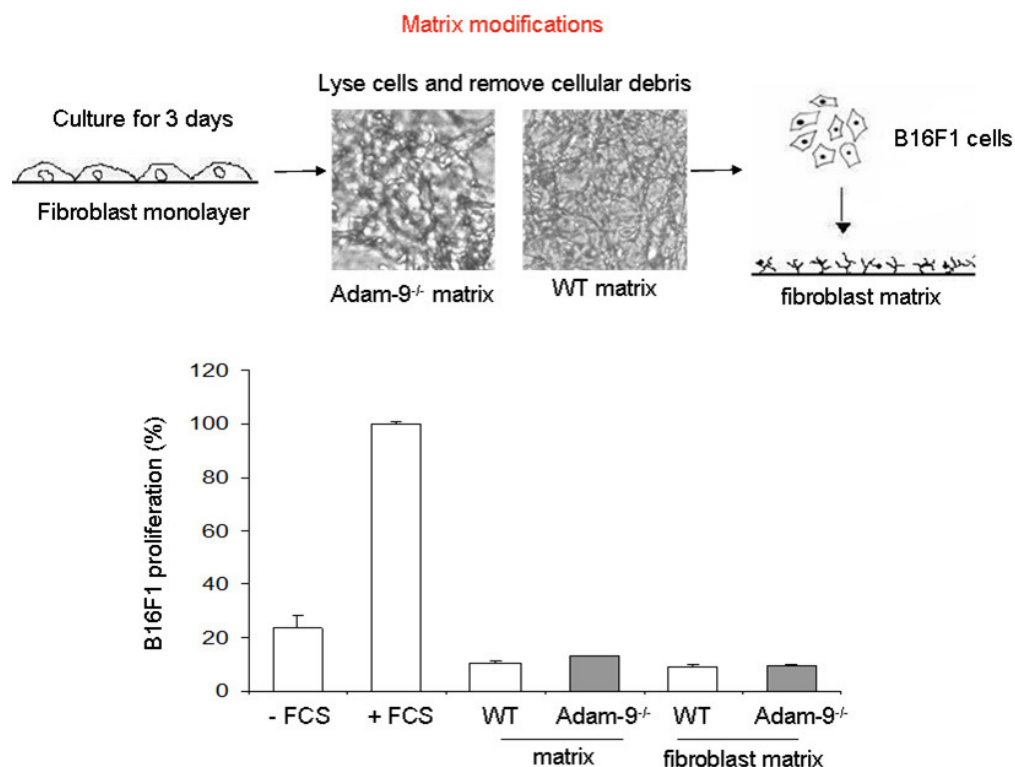
Figure 18. Matrix synthesis/modifications do not influence B16F1 proliferation. Cell proliferation of B16F1 cells after 24 hours incubation on matrix derived from WT or *Adam-9*^{-/-} fibroblast. Experimental set-up and coomassie blue staining of matrix deposited by WT and *Adam-9*^{-/-} fibroblasts is depicted in the upper panel. Lower panel, B16F1 cell proliferation after 24 hours culture on matrix-coated plates in serum-free conditions was assessed by BrdU incorporation. Cell proliferation in the presence of 10% FCS was used as the 100 % reference value (+, 10 % FCS; - serum free). Background absorbance of cell matrix was also measured. A representative of three experiments is shown.

Matrix deposition was confirmed by light microscopy visualization after staining with Coomassie brilliant blue (figure 18, upper panel). Matrix deposited by WT fibroblasts was evenly distributed while matrix deposited by *Adam-9*^{-/-} fibroblasts appeared dense and seemed to consist of larger fibers (figure 18, upper panel). Proliferation of B16F1 cells grown on these matrices in serum-free conditions was assessed by BrdU incorporation; matrix background absorbance was also measured to correct for background absorbance. After 24 hours, B16F1 cells cultured on matrix deposited by WT or *Adam-9*^{-/-} fibroblasts were not stimulated to proliferate (figure 18).

These data indicate that the absence of ADAM-9 in fibroblasts does not result in altered cellular contacts or matrix modification involved in the modulation of B16F1 cell proliferation ADAM-9.

3.4.2 Soluble factors as mediators of melanoma-stoma communication leading to cell proliferation

One of the best described activities of ADAM proteases is their proteolytic cleavage of growth factors and cytokines leading to autocrine or paracrine cell signaling. One important example is the activation of EGF family proteins (Blobel 2005). Thus, ADAMs can play an important role in modulating cellular cross talk by cleaving cell surface proteins. To address whether altered release or synthesis of soluble factors in the absence of ADAM-9 influenced B16F1 cell proliferation, B16F1 cell proliferation was assessed either in indirect co-cultures with fibroblasts. In one case fibroblasts were seeded in transwell culture systems were they were separated from the melanoma cells by a membrane with 0.4 μm pore size permitting permeation of soluble molecules. In another case co-culture was performed by culturing the B16F1 cells in the presence of serum-free conditioned medium (c.m.) prepared from sub confluent WT or *Adam-9*^{-/-} fibroblasts (see scheme in Figure 19). B16F1 cell proliferation was assessed by BrdU incorporation. Cell proliferation was expressed as percentage relative to the proliferation of cells in the presence of 10 % FCS, which was set as the 100 % reference value. B16F1 cells co-cultured with *Adam-9*^{-/-} fibroblasts in transwell chambers grew significantly faster, by approximately 19 %, compared to those co-cultured with WT fibroblasts (figure 19). Similarly, increased B16F1 proliferation was detected when cells were cultured with media conditioned from *Adam-9*^{-/-} as compared to those cultured with media from WT dermal fibroblasts ($p=0.037$; figure 19). These data show that the increased melanoma cell proliferation

was mediated by soluble factors produced by *Adam-9*^{-/-} fibroblasts and indicates that an active cross talk between the two cell types was not necessary.
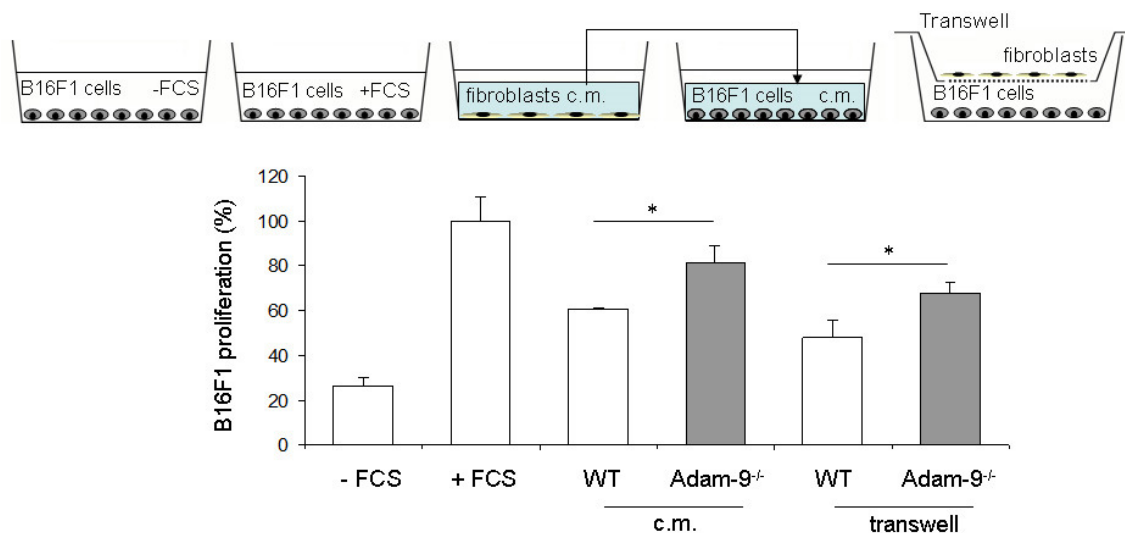

Figure 19. B16F1 cell proliferation is induced by supernatant from *Adam-9*^{-/-} fibroblasts in vitro. Upper panel, schematic presentation of experimental setup. B16F1 cell proliferation by BrdU incorporation after 24 hours incubation in transwell with WT or *Adam-9*^{-/-} fibroblasts or with conditioned media (c.m) from *Adam-9*^{-/-} or WT fibroblasts. The mean absorbance of triplicates was expressed as a percentage to the 100 % reference value (+, 10 % FCS; -, serum free). Mean values are presented and the bar represents the standard deviation. One representative experiment out of three is shown. * $p < 0.05$.

The proliferative potential of conditioned medium from *Adam-9*^{-/-} fibroblast was not limited to B16F1 melanoma cells only. Different cancer cell lines were incubated for 24 hours in serum-free medium (-) as negative control or in 10 % FCS as positive control (+) or in the presence of conditioned media collected from WT or *Adam-9*^{-/-} fibroblasts. Cell proliferation was assessed by BrdU incorporation. As shown in figure 20, conditioned media from *Adam-9*^{-/-} but not WT fibroblasts, could significantly increase the proliferation of the human melanoma cell line A375 or the glioma cell line Gli36. A minor but not significant increase was detected by culturing basal cell carcinoma cell line (BCC) and malignant transformed HaCaT cell line II4RT (SCC) cells with c.m. from *Adam-9*^{-/-} as compared to WT conditioned media (figure 20). This shows that the pro-proliferative effect of conditioned media from *Adam-9*^{-/-} fibroblast was not limited to murine melanoma cells (B16F1) but was also detected with human melanoma and glioma cells, whereas the proliferation of epithelial tumor cells was not affected.
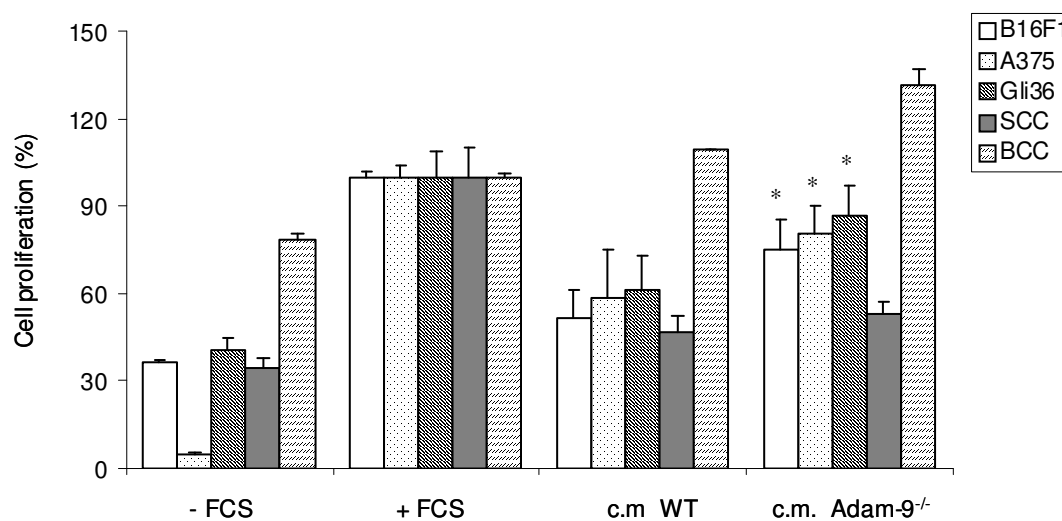
Figure 20. *Adam-9*$^{-/-}$ fibroblasts conditioned medium (c.m.) enhances the proliferation of melanoma cell lines. Cells were cultured in the absence (-) or presence (+) of serum or with WT or *Adam-9*$^{-/-}$ fibroblasts c.m. for 24 hour. Cell proliferation was assessed by BrdU incorporation. Proliferation in the presence of 10 % FCS was set as the 100 % reference value. Values are expressed as mean $\pm$ SD. p-values were calculated for cells cultured with c.m. from *Adam-9*$^{-/-}$ fibroblasts as compared to cells cultured with c.m. from WT fibroblasts. $*$ p<0.05

As shown in 3.3.3, *in vivo*, in parallel to increased proliferation we could also detect reduced apoptosis in the absence of host ADAM-9. To find out whether soluble factors, which mediated increased proliferation, also influence cell apoptosis we analyzed apoptosis of B16F1 cells after treatment with c.m. from WT or *Adam-9*$^{-/-}$ fibroblasts. Stimulation of B16F1 cells with recombinant TNF-α was used as positive control, as it effectively induce apoptosis in B16F1 cells, and set as the 100 % reference value. Apoptosis was measured by ELISA detection of the amount of cytoplasmic oligonucleosomes released into the cytoplasm during apoptosis. The apoptosis of B16F1 cells after culture with *Adam-9*$^{-/-}$ fibroblasts conditioned media was significantly reduced compared to cells treated with WT conditioned media (figure 21). This indicates that the reduction in apoptosis observed in tumors from *Adam-9*$^{-/-}$ mice was also mediated by a soluble factor-derived mechanism.
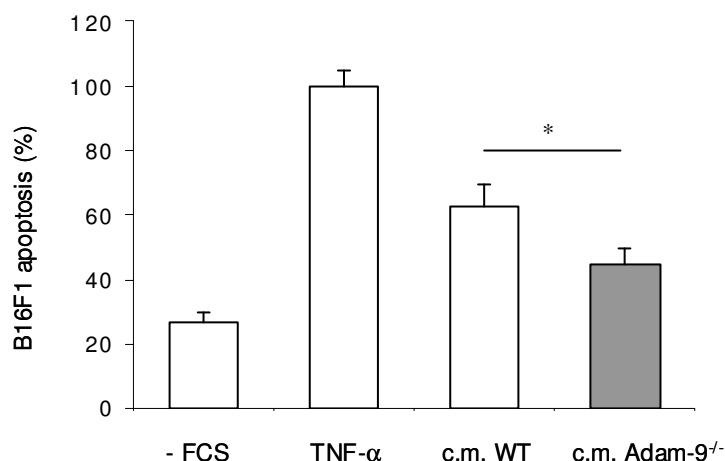
Figure 21. Apoptosis of B16F1 cells. B16F1 cell apoptosis analyzed by ELISA detection of cytoplasmic oligonucleosome and expressed as percentage relative to the 100 % reference value (cell apoptosis in the presence of 100ng/ml TNF-α). The graph is a representative of three independent experiments. Values represent mean ± SD. * p<0.05.

3.5 The role of soluble factors in the regulation of melanoma cell proliferation

3.5.1 Identification of soluble factors in *Adam-9*^{-/-} fibroblasts

To gain insight on factors, which were altered in *Adam-9*^{-/-} fibroblasts and in turn could modulate B16F1 melanoma cell proliferation and apoptosis, we analyzed growth factor/cytokine levels in fibroblasts supernatants by RayBio® mouse cytokine antibody array. This antibody-based array can simultaneously detect 62 different mouse cytokines and growth factors. This analysis was also performed with tumor lysates from day 3 tumors, the time point at which tumor size starts to differ between WT and *Adam-9*^{-/-} mice. The densities of the different cytokines dots were quantified by densitometry using imageJ software, the background intensity (blank) was subtracted, and the data was normalized to the biotin-conjugated IgG positive internal control. The *Adam-9*^{-/-} to WT expression ratio was calculated and we set a minimum a fold change of two as baseline above which expression was considered significant. Several factors were identified which were up-regulated in lysates from tumors developed in the *Adam-9*^{-/-} animals as compared to WT, however we have only considered those factors which were equally altered in both, tumor lysates and fibroblasts supernatants (figure 22). This indicated which factors *in vivo* might be derived mainly from differential secretion by stromal fibroblasts than other cell types around the tumors. Factors up-regulated in *Adam-9*^{-/-} fibroblast supernatants as compared to WT, were amongst others, TIMP-1 (6.72 fold), TNF-α (5.58 fold), sTNFRI (3.66 fold) and sTNFRII (3.53 fold). These proteins were also up-regulated in

tumor lysates from *Adam-9*^{-/-} compared to WT mice; TIMP-1 (7.92 fold), TNF-α (3.17 fold), sTNFRI (31.99 fold) and sTNFRII (17.05 fold). Presented in figure 22 are the relative expression levels of the soluble factors analyzed and their fold difference in *Adam-9*^{-/-} as compared to WT fibroblast supernatants or tumor lysates. There is a small group of factors differentially expressed in *Adam-9*^{-/-} fibroblasts or tumor lysates that are known to play an important role in tumor cell proliferation and apoptosis.

	Tumor lysate			Fibroblast supernatant		
	Adam-9-/-	WT	ratio Adam-9-/- vs. WT	Adam-9-/-	WT	ratio Adam-9-/- vs. WT
IL-6	34.68	19.33	1.79	6.50	2.05	3.17
IL-1a	105.78	108.81	0.97	15.35	7.59	2.02
MIP-2	101.66	62.51	1.63	31.47	12.30	2.56
GM-CSF	46.30	35.08	1.32	2.53	3.44	0.73
TIMP-1	19.35	2.88	6.72	28.59	3.61	7.91
BLC	49.71	41.37	1.20	2.56	3.61	0.71
SDF-1α	52.12	31.88	1.63	27.00	12.64	2.14
TNF-α	26.21	4.70	5.58	4.19	1.32	3.18
sTNFRI	56.65	15.48	3.66	52.78	1.65	31.93
sTNFRII	39.46	11.19	3.53	16.03	0.94	17.05

Figure 22. Differential expression of soluble factors. Relative expression levels of cytokines/growth factors as quantified by densitometry, values are expressed as arbitrary units/ biotin-conjugated IgG positive control. Presented are some differentially expressed proteins detected in both fibroblast supernatants and tumor lysates in *Adam-9*^{-/-} as compared to WT.

3.5.2 TIMP-1 expression in fibroblasts and melanoma cells

Tissue inhibitor of metalloproteinases-1 (TIMP-1), among others, was identified from RayBio analysis as being up-regulated in *Adam-9*^{-/-} fibroblasts supernatants and tumor lysates as compared to WT controls (3.3.1). To confirm the results obtained from the RayBio array, TIMP-1 protein expression was analyzed in the supernatants of five different WT and *Adam-9*^{-/-} fibroblast preparations by immunoblot analysis. The volume of supernatant used was normalized to the protein content in fibroblast lysate (50 μg). TIMP-1 was highly up-regulated in all *Adam-9*^{-/-} fibroblast supernatants as compared to WT, two representatives are shown for each genotype in Figure 23A.

Regulation of TIMP-1 expression may occur at transcript and protein levels (Richard et al., 1993; Aicher et al., 2003). Semi-quantitative analysis of TIMP-1 transcripts in all five different fibroblast preparations, displayed a significant increase in *Adam-9*^{-/-} as compared to WT fibroblasts (figure 23B). Thus, the increased secretion of TIMP-1 derives from *de novo* synthesis. *In vivo*, by immunofluorescence analysis of

melanoma tumor sections, TIMP-1 was detected mainly in the stoma and in a few tumor cells and tumor penetrating stromal cells at the tumor periphery. TIMP-1 expression was increased in peritumoral areas of melanomas developed in *Adam-9*^{-/-} animals with strong positivity detected in many fibroblast-like cells, whereas little expression was observed in the peritumoral stoma of melanomas developed in WT littermates (figure 23C).
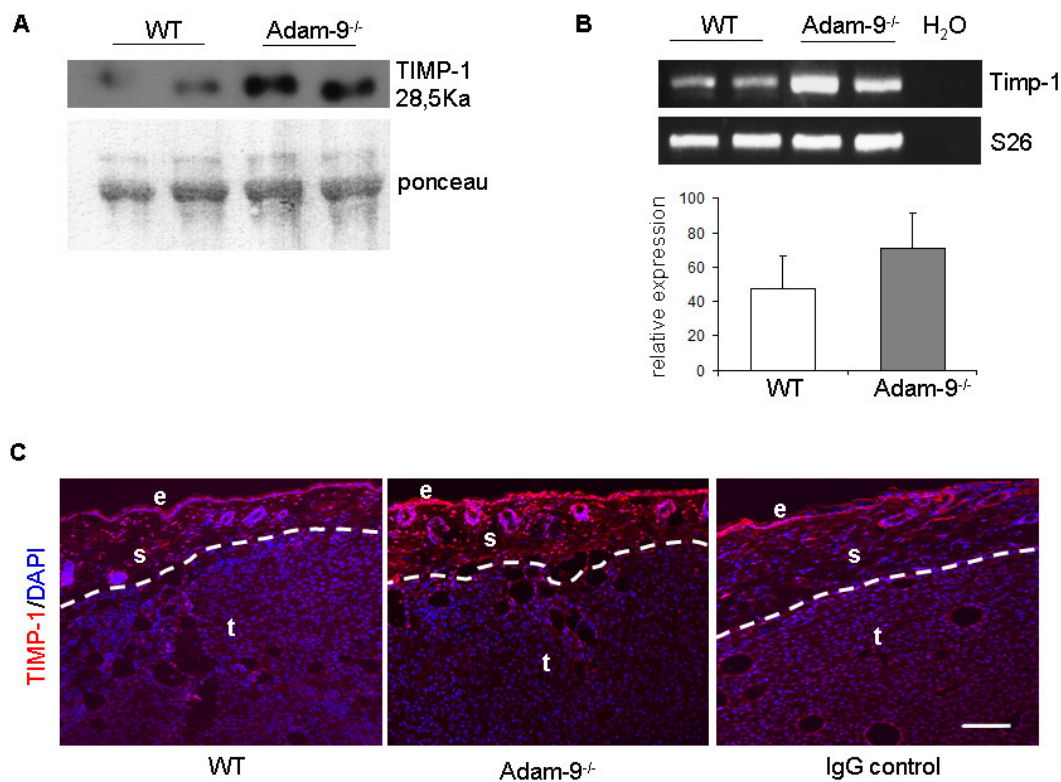

Figure 23. TIMP-1 expression is increased in the absence of ADAM-9. A, analysis of TIMP-1 expression in supernatants from *Adam-9*^{-/-} and WT dermal fibroblasts by western blot. Shown is a representative of n=5 per genotype. Ponceau staining ensures equal loading of gels. B, amplification of Timp-1 transcript by RT-PCR on cDNA synthesized from RNA isolated from fibroblasts. Shown is a representative per group n=8. RT-PCR was quantified by densitometry, and shown as mean expression relative to S26 ± SD. C, detection of TIMP-1 (red) in acetone fixed tumor sections from WT or *Adam-9*^{-/-} mice. DAPI was used to stain the nuclei. IgG control confirms the specificity of the staining. Dashed lines indicate tumor-stoma border. s, stoma; t, tumor. Scale bar 200 µM.

3.5.3 Effect of TIMP-1 on melanoma cell proliferation

TIMP-1 is generally known as the natural inhibitor of several matrix metalloproteases however, it may also function as a growth and/or survival factor in a MMP-independent manner (Moller Sorensen et al., 2008; Ricca et al., 2009). To assess the growth stimulating effect of TIMP-1 on B16F1 melanoma cells, we analyzed B16F1

cell proliferation in the presence of exogenous TIMP-1. Cell proliferation was expressed as percentage relative to cell proliferation in the presence of 10 % serum (+). Cells cultured in the presence of 0.5 µg/ml recombinant TIMP-1 grew 4 times faster than cell grown in serum-free medium (-) (figure 24) and their growth was comparable to that observed in the presence of 10 % serum. Serum also contains, among other cell proliferating factors, also TIMP-1 ranging from 0.1 to 0.46 µg/ml depending on the distributor (Hayakawa et al., 1992). Showing that TIMP-1 is used as a growth factor in serum.
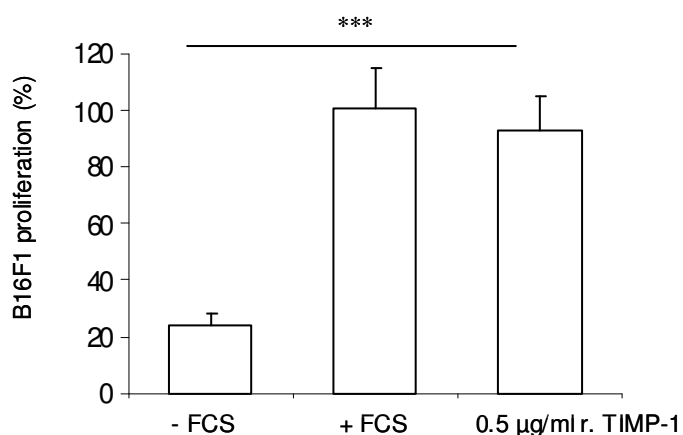
Figure 24. Exogenous TIMP-1 enhances B16F1 cell proliferation. B16F1 cell proliferation in the presence of recombinant TIMP-1 (r. TIMP-1) was assessed by BrdU incorporation compared to serum-free control. (+, 10 % serum positive, -, serum-free). The graph is a representative of three experiments. Values are expressed as mean ± SD. ∗∗ p<0.0008.

To investigate whether TIMP-1 exerts a growth stimulating effect in human melanoma cells (as shown in figure 24), we cultured different melanoma cell lines with two concentrations of recombinant TIMP-1 (0.5 and 1 µg/ml) for 24 hours and assessed cell proliferation. As control, cells were cultured in serum-free medium or medium containing 10 % FCS (100 %). The proliferation of all cell types was significantly increased when cells were cultured in medium containing recombinant TIMP-1, except the cell line A375 that showed only a modest increase in cell proliferation (figure 25). This indicates that TIMP-1 can act as a growth-stimulating factor for both murine and human melanoma cells.

Figure 25. TIMP-1 dependent proliferation of human melanoma cell lines. Cells were cultured in the absence or presence of 0.5 µg/ml or 1 µg/ml recombinant TIMP-1 for 24 hour. Cell prolifera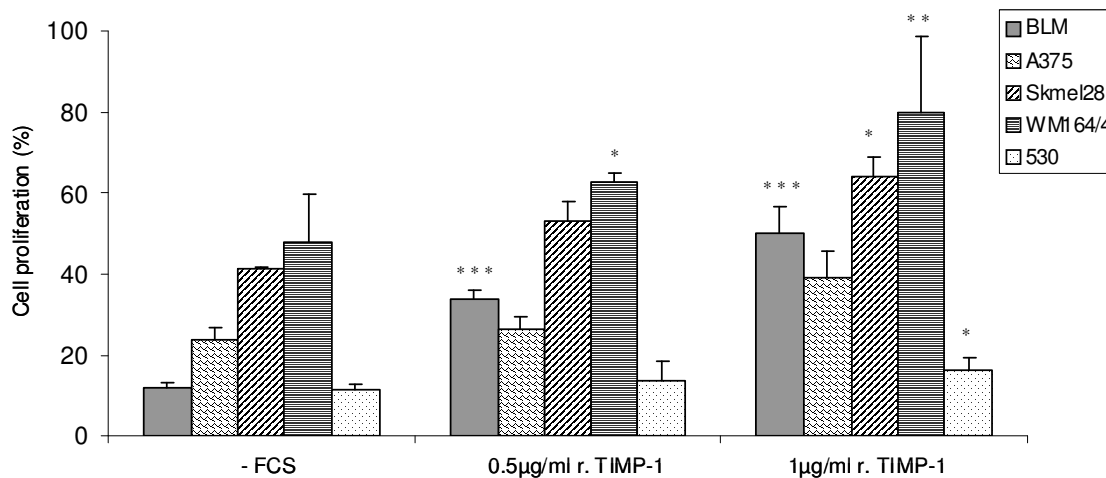tion was assessed by BrdU incorporation. Proliferation in the presence of 10 % FCS was set as the 100 % reference value. The graph is a representative of three experiments showing mean ± SD. p-values were calculated for TIMP-1 treated cells compared to serum-free controls * p<0.05, ** p<0.0065, *** p<0.0002.

To prove that the enhanced amount of TIMP-1 in *Adam-9*^{-/-} fibroblast supernatants is responsible for the increase in B16F1 cell proliferation we neutralized TIMP-1 using specific antibody prior to melanoma cell stimulation with *Adam-9*^{-/-} fibroblasts supernatant. As control, mouse IgG was used at the same concentration as the TIMP-1 antibody. Neutralization of TIMP-1 in fibroblasts media resulted in a significant reduction in B16F1 cell proliferation by approximately 30 % reaching levels comparable to those detected when B16F1 were cultured in the presence of WT fibroblast conditioned medium (figure 26A). TIMP-1 has also been shown to mediate survival of erythroid UT-7 (Lambert et al., 2003) and human breast epithelial cells (Li et al., 1999). We therefore investigated whether TIMP-1 apart from proliferation, may also influence B16F1 cell-survival. Neutralization of TIMP-1 did not affect B16F1 cell apoptosis, as no differences in cytoplasmic oligonucleosome was detected in cells cultured in the presence of *Adam-9*^{-/-} fibroblasts conditioned media with or without TIMP-1 neutralization (figure 26B). The IgG control had no effect on B16F1 cell proliferation and apoptosis (figure 26A and B). These results indicated that the increased TIMP-1 in *Adam-9*^{-/-} fibroblasts conditioned medium contributes to the enhanced B16F1 cell proliferation *in vitro* but does not affect apoptosis.

A

B
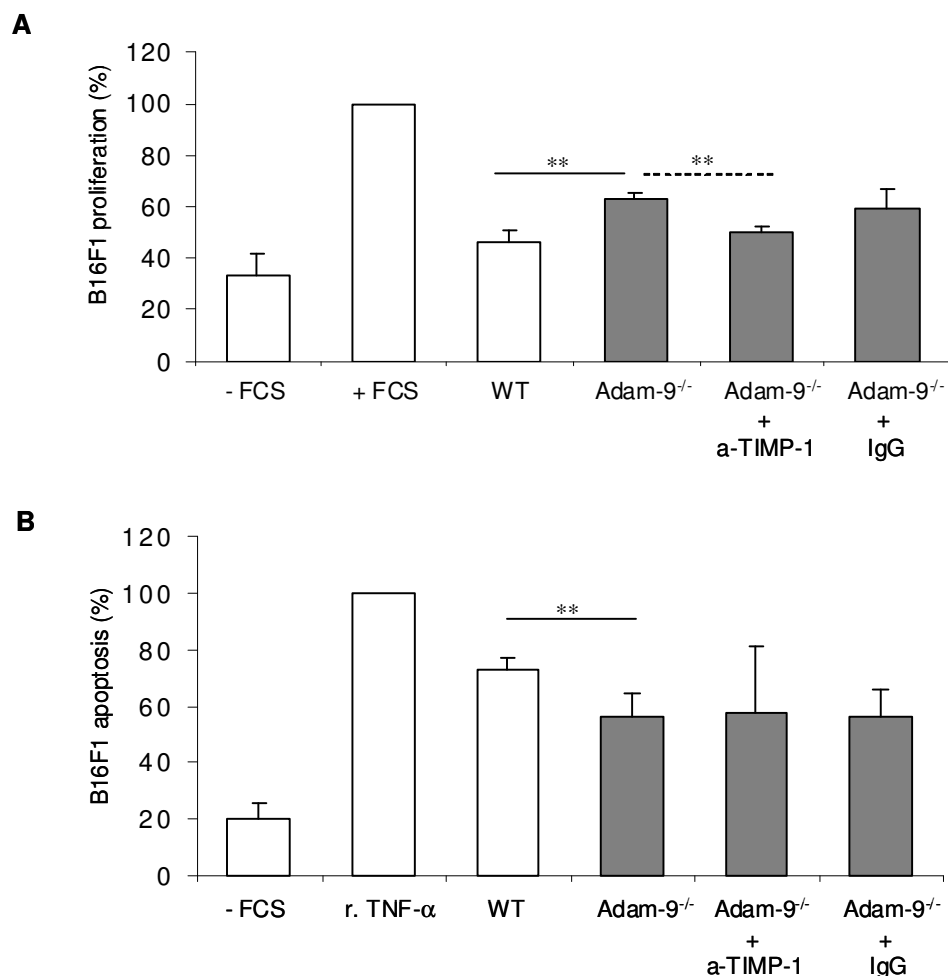
Figure 26. Neutralization of TIMP-1 reduces B16F1 cell proliferation but does not affect apoptosis. A, analysis of B16F1 cell proliferation in the presence of fibroblast conditioned medium (c.m.) with or without anti-TIMP-1 antibody (a-TIMP-1; 2 µg/ml) or control IgG (2 µg/ml). Cell proliferation in the presence of 10 % serum (+) was used as positive control. B, apoptosis of B16F1 cells after neutralization of TIMP-1 in *Adam-9*$^{-/-}$ fibroblasts (c.m.) with an anti-TIMP-1 antibody (2 µg/ml). Mouse IgG (2 µg/ml) was used to show specificity. Cell apoptosis in the presence of recombinant TNF-α (TNF-α; 100 ng/ml) was used as the 100 % reference value. Each graph is a representative of three independent experiments. Values represent mean ± SD. ∗ $p<0.05$, ∗∗ $p<0.005$.

3.5.4 Expression of TNF-α and TNFRI

TNF is one of the most potent inducer of apoptosis. Its function is mediated by binding and activation of TNFRI death domain, which initiate the apoptotic cascade (Rath and Aggarwal 1999). TNF-α and TNFRI exist as transmembrane proteins, which undergo ectodomain shedding by the activity of ADAM proteases, releasing soluble forms (Garton et al., 2006). An additional soluble form has been described for TNFRI; the exosome associated 55 kDa (Hawari et al., 2003).

RayBio mouse cytokine analysis identified TNF-α and its soluble receptors (TNFRI and II) as up-regulated in supernatants from *Adam-9*^{-/-} fibroblasts and in tumor lysates from *Adam-9*^{-/-} compared to WT mice (figure 22). To investigate whether alterations in the TNF/TNFR axis mediate reduced apoptosis detected in melanoma grown in *Adam-9*^{-/-} mice, we first confirmed the results obtained from the RayBio array. The TNF-α protein levels were analyzed by ELISA in WT and *Adam-9*^{-/-} fibroblast lysates and supernatants. The concentrations of TNF-α in cell lysates and supernatants were increased in *Adam-9*^{-/-} as compared to WT fibroblasts. Similarly, also in tumor lysates of melanomas induced in *Adam-9*^{-/-} mice TNF-α concentration was 3-fold higher than in those from WT animals (figure 27A).

TNFRI protein expression was analyzed by western blot in fibroblast supernatants and cell lysates. This analysis revealed that apart from the exosome associated 55 kDa soluble protein of TNFRI, the 28 kDa shed soluble form was detected in *Adam-9*^{-/-} but not in WT fibroblast supernatants (Figure 27B). This increased shed TNFRI in *Adam-9*^{-/-} fibroblast supernatants was accompanied by a concomitant decrease of the membrane bound form detected in lysates from *Adam-9*^{-/-} as compared to WT fibroblasts (figure 27B). TNFRI transcript analysis showed no differences between WT and knock out fibroblasts (figure 27C).

A

	TNF-α (pg/mL)		
	Fibroblast supernatant	Fibroblast lysate	Tumor lysate
WT	34.8 ± 5.9	20.2 ± 12.9	142.3 ± 18.3
Adam-9^{-/-}	46.6 ± 6.7	55.2 ± 38.3	449.3 ± 66.6

B

C
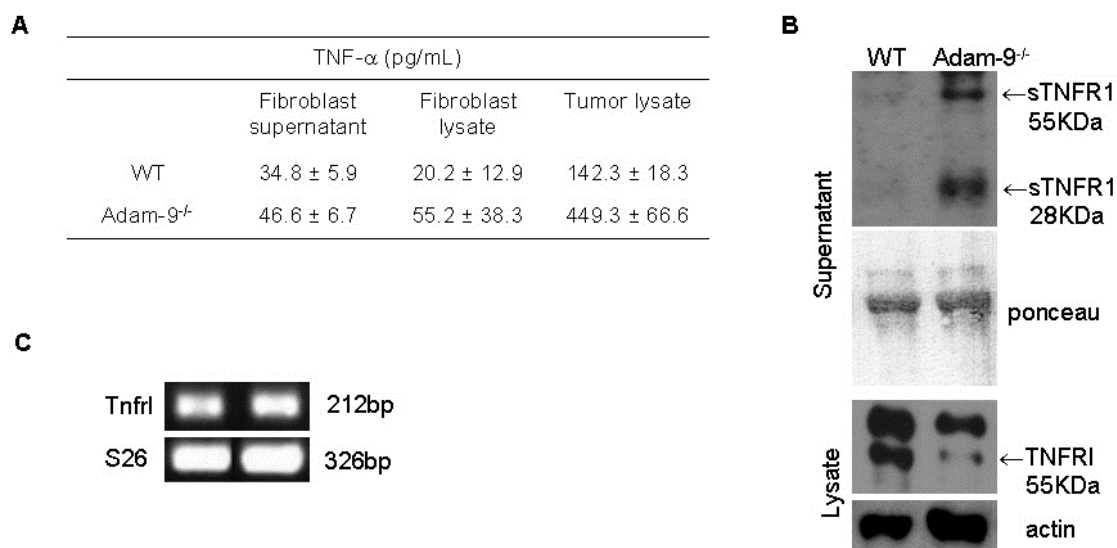
Figure 27. TNF-α and sTNFRI expression is increased in *Adam-9*^{-/-} fibroblasts. A, ELISA detection of soluble and membrane bound TNF-α in fibroblast culture supernatants and cellular lysate and, in melanoma tissue lysate obtained from WT or *Adam-9*^{-/-} mice (n=4 per genotype). Values are presented as mean ± SD. B, representative images of TNFRI protein and transcripts in *Adam-9*^{-/-} and WT fibroblast by western blot (n=4 per genotype) and RT-PCR (n=8 per genotype). Ponceau staining was used to control equal loading of supernatants while actin was used as loading control for protein lysates. S26 was used as control of cDNA loading.

3.5.5 Modulation of apoptosis induced by TNF-α and TNFRI

As described above, the majority of TNF-α´s biological activity is mediated through binding to TNFRI (Chen and Goeddel 2002) and can be inhibited by the proteolytic release of the receptor, which functions as a decoy receptor (Garton et al., 2006). We hypothesize that increased sTNFRI in the supernatant from *Adam-9*^{-/-} fibroblasts neutralize TNF-α, leading to reduced cellular apoptosis. To prove this theory, B16F1 cells were cultured first with c.m. from *Adam-9*^{-/-} fibroblasts supplemented with 100 ng/ml recombinant murine TNF-α, a concentration that would not only saturate the soluble TNFRI but also be available for binding to membrane-bound receptor. Under these conditions, B16F1 cells underwent apoptosis to levels similar to that of cells stimulated with supernatants from WT fibroblasts (figure 28). On the other hand, neutralization of TNF-α in WT fibroblast supernatant with neutralizing TNF-α antibody or Enbrel (also known as Etanercept), a recombinant fusion protein which functions as a decoy receptor, prior to B16F1 cell stimulation, significantly reduced B16F1 apoptosis by 25 % and 35 % respectively. Pre-incubating WT fibroblast supernatant with IgG control did not affect B16F1 apoptosis (figure 28).
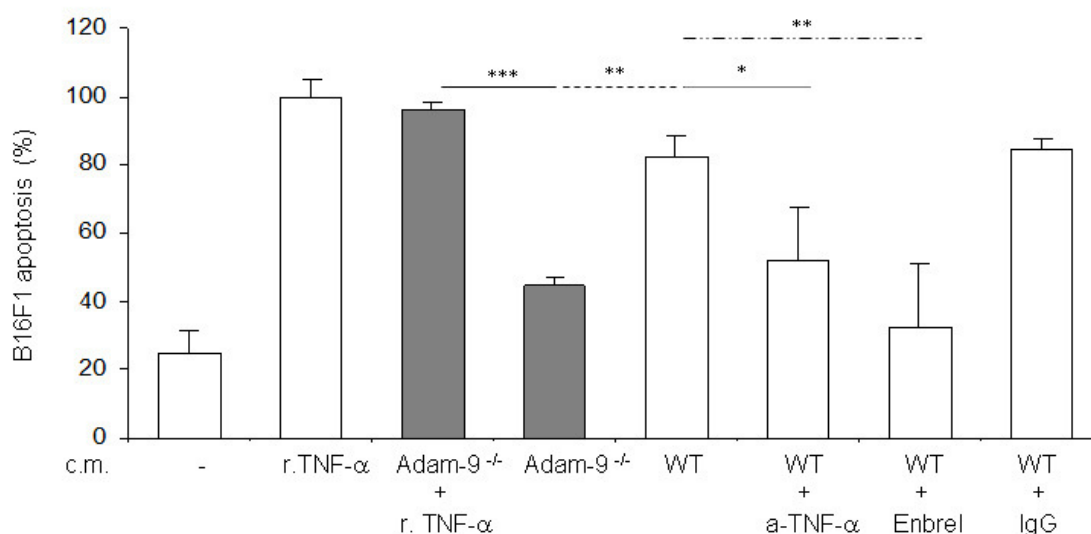
Figure 28. Neutralization of TNF-α reduced B16F1 apoptosis. Apoptosis was measured in B16F1 cells by ELISA detection of cytoplasmic oligonucleotides. B16F1 cells were cultured with supernatants from fibroblasts pre-incubated with or without recombinant TNF-α (r. TNF-α, 100 ng/ml), anti-TNF-α antibody (a-TNF-α, 2 µg/ml), Enbrel (5 µg/ml) or IgG control (2 µg/ml). B16F1 cell apoptosis in the presence of recombinant TNF-α was used as 100 % reference value. Data represents mean ± SD. ∗ $p<0.0353$, ∗∗ $p<0.0065$, ∗∗∗ $p<0.0009$.

The proteolytic release of the soluble TNFRI was shown to be mediated primarily by ADAM-10 and -17 (Zheng et al., 2004). Expression of Adam-10 and -17 transcripts in

Adam-9^{-/-} fibroblasts was indeed higher than in WT cells as detected by RT-PCR analysis (figure 29A). Quantification of the amplified transcripts by densitometry and normalization to S26 control showed that Adam-10 and -17 were significantly up-regulated in *Adam-9*^{-/-} as compared to WT fibroblasts (figure 29A, right panel). At the protein level, total protein of ADAM-10 and -17 proteins were up-regulated in *Adam-9*^{-/-} fibroblasts as compared to WT, however a tiny band corresponding to active ADAM-10 was observed only in WT fibroblasts while more active ADAM-17 was observed in *Adam-9*^{-/-} cells (figure 29B). The second ADAM-17 band in *Adam-9*^{-/-} fibroblasts is likely an unspecific band.
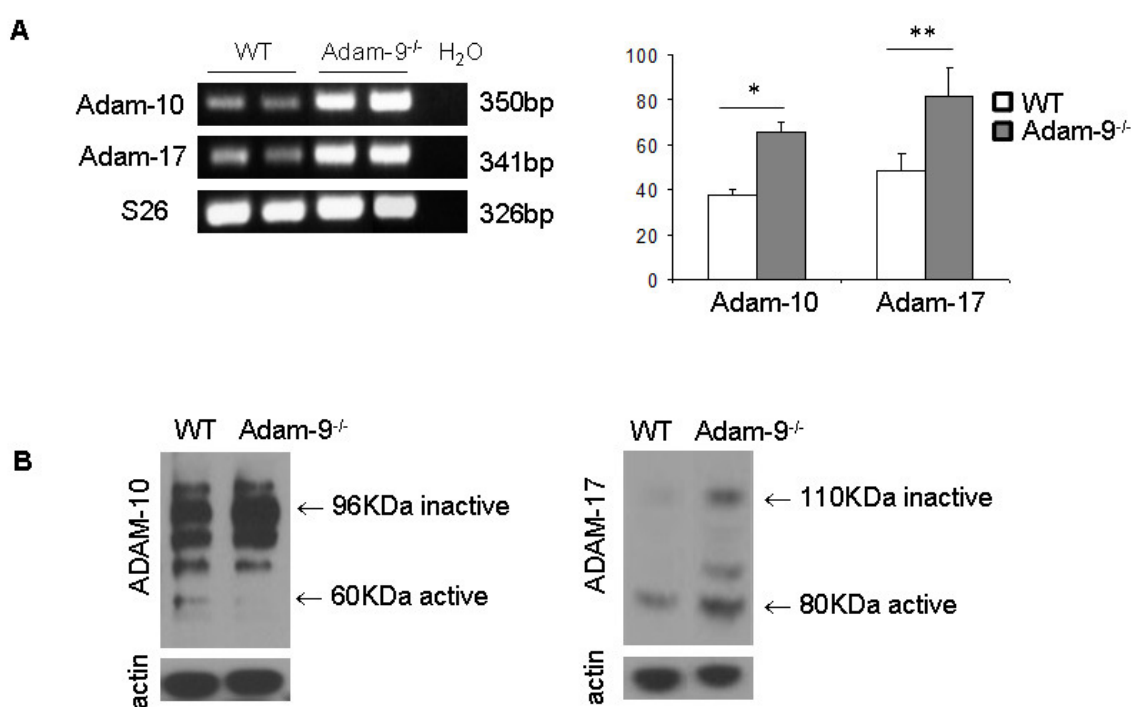
Figure 29. Adam-10 and -17 are up-regulated in the absence of Adam-9. A, analysis of Adam-9, -10 and -17 transcripts in *Adam-9*^{-/-} and WT fibroblasts by RT-PCR (n=5). S26 was used as internal control and H_2O as negative control. RT-PCR was quantified by densitometry, normalized to S26 control and expressed as the mean ± SD. Shown is a representative PCR for each genotype. ∗ $p < 0.05$. ∗∗ $p < 0.005$. B, ADAM-10 and -17 protein expression in fibroblasts. Actin serves as loading control. Shown is a representative of n=4 for each genotype.

ADAM-10 but not ADAM-17 is inhibited by TIMP-1, which is up-regulated in *Adam-9*^{-/-} fibroblasts (Amour et al., 2000). We therefore hypothesize that increased shedding of TNFRI is the result of increased ADAM-17 synthesis. To inhibit the shedding of TNFRI by ADAM-17, *Adam-9*^{-/-} fibroblasts were incubated overnight with a hydroxamate-based inhibitor, TNF-α Protease Inhibitor-0 (TAPI-0) whose target

includes ADAM-17, MMP-1 (not expressed in mouse, Balbin et al., 2000) and MMP-2 (Roghani et al., 1999). As control, fibroblasts were incubated with DMSO, which was used as solvent for the inhibitor. The generation of soluble TNFRI was analyzed by western blot. Treatment with TAPI-0 effectively reduced shedding of TNFRI in *Adam-9$^{-/-}$* fibroblasts as less shed TNFRI was detected in supernatant of fibroblasts treated with TAPI-0 (figure 30). In addition to the decreased shed form of TNFR1 we also detected reduced exosome associated receptor. In parallel, the membrane-bound form of TNFRI was increased in lysates from fibroblasts treated with TAPI-0 as compared to control (figure 30). Stimulation of B16F1 cells with supernatants from TAPI-0 treated fibroblasts resulted to a 20 % increase in apoptosis as compared to control (figure 30). Taken together, these results support the hypothesis that reduced B16F1 cell apoptosis results from neutralization of TNF-α by soluble TNFRI, which is increased in *Adam-9$^{-/-}$* fibroblast supernatants.
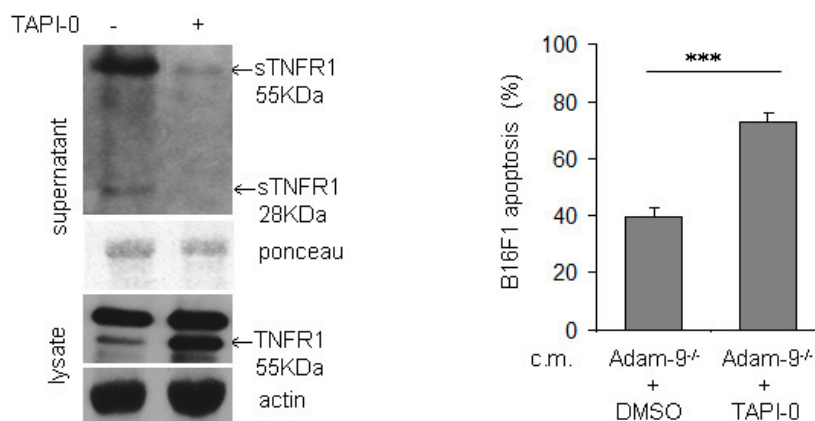
Figure 30. Inhibition of TNFRI shedding reduced B16F1 apoptosis. Left, western blot analysis of TNFRI in *Adam-9$^{-/-}$* fibroblasts with or without TAPI-0 (10 µM) treatment. Ponceau and actin were used as loading control for supernatant and lysates respectively. Right, analysis of B16F1 cell apoptosis after culturing with supernatant from *Adam-9$^{-/-}$* fibroblasts treated with or without TAPI-0. B16F1 cell apoptosis induced with recombinant TNF-α was used as 100% reference value. Data represents mean ± SD. ∗∗∗ p<0.0009.

3.5.6 Differential fibroblast gene expression in the absence of Adam-9

To identify possible factors that could give insight as to how Adam-9 may alter protein expression in fibroblasts, RNA isolated from WT and *Adam-9$^{-/-}$* fibroblasts were analyzed by RNA array. This analysis was performed in cooperation with Prof. Jay Fox of the University of Virginia, USA. The data was analyzed with Ingenuity Systems IPA. Identification of statistically significant changes was performed by t-test. Of the genes analyzed, 64 were up-regulated while 116 genes were down-regulated in *Adam-9$^{-/-}$*

fibroblasts compared to WT fibroblasts. We have considered as significant only genes regulated with p-values less than 0.05 or a fold change of at least 2 (positive values, up-regulated; negative values, down-regulated). The identified genes included those involved in transcriptional regulation, cell proliferation, melanoma progression, and synthesis of extracellular matrix protein. The differentially regulated genes are presented in table 3 below.

Table 3. Differential fibroblasts gene expression after Adam-9 knockout

Functional annotation	Regulated genes	Fold change Adam-9-/- vs. WT
Transcription factors	Klf14 (Sp6)	2.6
	Runx3	3.4
	E2f7	7.1
	Tcfec	-3.7
	Atf4	-2.8
	Tcf15	-2.6
Melanoma progression	Kif23	5.3
	Slc1a3	7.5
	IGFBP4	-2.9
	Cdkn2a	-2.8
Proliferation of cell lines	Dlk1	8.3
	Cdca8	3.7
	Cdkn2a	-2.8
ECM	Col1a1	2.0
	Col14a1	7.8
	Fn1	-3.7

Among the genes differentially regulated in fibroblast the absence of ADAM-9, were genes involved in proliferation, strongly increased for instance was Delta like 1 homolog (drosophila) (Dlk1). Interestingly, Dll-1 (Delta-like 1, in mammals) has been shown to be a substrate for ADAM-9 when ADAM-12 is absent (Dyczynska et al., 2007) and its cleavage, as shown for the notch receptor, may lead to modulation of intracellular signaling (Qi et al., 1999). Transcription factors were also differentially regulated like trans-activating protein (Sp6 or Klfl4) and E2F transcription factor (E2f7) which were both up-regulated in the absence of Adam-9. We have also detected genes involved in the regulation of cell cycle like cyclin dependent kinase

inhibitor 2A (Cdkn2a) which was down-regulated, and cell division cycle associated 8 (Cdca8) that was up-regulated in the absence of *Adam-9*. Genes involved in the synthesis of extracellular matrix components for example fibronectin (Fn1) and collagen type XIV (Col14a1) were also differentially expressed. The differential expression of transcription factors and membrane receptors among others which could offer the molecular link between ADAM-9 and regulation of intracellular signaling could not be evaluated within the time-frame of this thesis and remain to be validated.

3.6 ADAM-9 and its role in the modification of the peritumoral matrix

3.6.1 Extracellular matrix protein expression at the tumor-stoma border

The tumor microenvironment consist of the extracellular matrix (ECM) and stromal cells (Mueller and Fusenig 2004). ADAM-9 has been shown to cleave extracellular matrix proteins including fibronectin (Fn1) and laminin 111 (Schwettmann and Tschesche 2000; Mazzocca et al., 2005). To analyze how ablation of ADAM-9 *in vivo* influences matrix composition around the tumors we performed proteomic analysis of the tumor-stoma border of day 3 tumors from WT and *Adam-9*$^{-/-}$ animals. This analysis was done in cooperation with Prof. Jay Fox at the University of Virginia. The black dotted lines in figure 31 indicate the tumor-stoma border area that was microdissected and analyzed by mass spectrometry. We have identified differentially expressed proteins belonging to different molecular functional groups amongst others binding, catalytic activity and enzyme regulator activity.
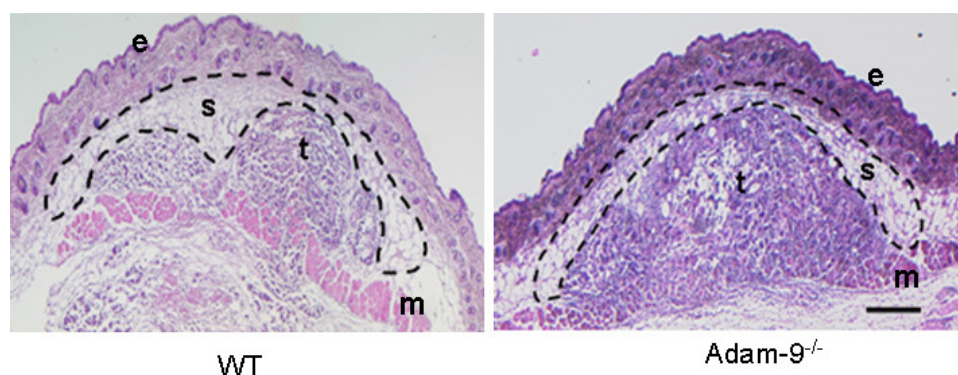

Figure 31. Analysis of ECM proteins at the tumor-stoma border in melanoma from WT and *Adam-9*$^{-/-}$ mice.,Black dotted lines indicate the areas that was extracted and analyzed by mass spectrometry, WT n=2; *Adam-9*$^{-/-}$ n=2).   t, tumor; s, stoma; e, epidermis; m, subcutaneous muscle. Scale bar 50 µM.

The relative expression of the proteins analyzed were used to calculate the fold change of proteins in *Adam-9*^{-/-} as compared to WT. 496 proteins analyzed were similarly expressed in both genotypes. Only 53 proteins were altered at the tumor-stoma border of tumors from *Adam-9*^{-/-} animals compared to WT controls. Proteins with a fold change of at least two were considered relevant (positive values, up-regulated; negative value, down-regulated). The fold changes of differentially expressed proteins are presented in table 4 below, where positive values indicate up-regulation and negative values indicate down-regulation at the tumor-stoma border in tumors from *Adam-9*^{-/-} mice as compared to those from WT controls.

Table 4. Differential expression of proteins at the tumor-stoma border.

ECM proteins	MW	Fold change Adam-9-/- vs. WT tumor
Isoform 1 of Collagen alpha-1(I) chain	138 kDa	2,00
Collagen alpha-2(I) chain	130 kDa	2,00
Collagen alpha-1(III) chain	139 kDa	-2,00
Collagen alpha-2(V) chain	145 kDa	2,00
Collagen alpha-1(V) chain	184 kDa	2,00
Isoform 1 of Collagen alpha-1(XIV) chain	193 kDa	-4,00
Fibronectin	272 kDa	-4,00
Decorin	40 kDa	2,00
Enzymes		
Fatty acid synthase	272 kDa	-8,16
Long-chain-fatty-acid--CoA ligase 1	78 kDa	-2,67
triosephosphate isomerase 1	32 kDa	4,39
Pyruvate kinase isozymes R/L	62 kDa	2,20
Dolichyl-diphosphooligosaccharide--protein glycosyltransferase subunit 2	69 kDa	2,20
trypsin 4	26 kDa	-2,73
Mast cell protease 4	27 kDa	-2,72
Peroxiredoxin-1	22 kDa	2,20
Peroxiredoxin-4	31 kDa	2,20

Of the differentially expressed ECM proteins, decorin, collagen type I and V were up-regulated in *Adam-9*^{-/-} animals. Fibronectin, collagen type III and XIV were down-regulated at the tumor-stoma border of melanomas developed in *Adam-9*^{-/-} animals compared to WT animals. Enzymes involved in the fatty acid metabolism such as

fatty acid synthase and Long-chain-fatty-acid-CoA ligase 1 were down-regulated in tumor-stoma border of tumors from *Adam-9$^{-/-}$*. Enzymes involved in glycolysis such as triosephosphate isomerase 1 and pyruvate kinase isozymes R/L, and enzyme involved in protein gylcosylation, dolichyl-diphosphoooligosaccharide-protein glycosyltransferase subunit 2, were up-regulated. The antioxidant enzymes Peroxiredoxin-1 and 4 were up-regulated regulated in tumor-stoma border of tumors from *Adam-9$^{-/-}$*. Surprisingly no matrix remodeling enzymes were detected; reasons for this could be the extraction and analysis procedure that do not enables analysis of low expressed proteins (personal communication with Prof J.W. Fox).

The differential expression decorin and collagen XIV, which are important in collagen fibrillogenesis (Lozza 1998; Ansorge et al., 2009), collagen type I, which has a predominantly structural role in tissue (Kadler et al., 2007) and fibronectin which mediates a variety of cellular interactions with the ECM (Ansorge et al., 2009) were further analyzed by immunofluorescence. Collagen type I was analyzed by picrosirius red staining. Increased intensity of staining for decorin was observed at the tumor-stoma border in tumors from *Adam-9$^{-/-}$*, whereas fibronectin expression was not altered at the tumor-stoma border however, increased positivity was detected in the periphery of the tumor (figure 32A). No obvious differences were detected in the expression of collagen XIV at the tumor-stoma border in tumors from both animals (figure 32A). Collagen type I bundles visible by polarized light visualization of picrosirius red stained tissue (figure 32B right panel), were moderately increased at the tumor-stoma border in melanomas from *Adam-9$^{-/-}$* animals as compared to those from in WT animals (figure 32B). Thus, increased expression of collagen type I and decorin could be confirmed, whereas reduction in fibronectin and collagen XIV at the tumor-stoma border, as suggested by the proteomic analysis, could not be confirmed by this analysis.
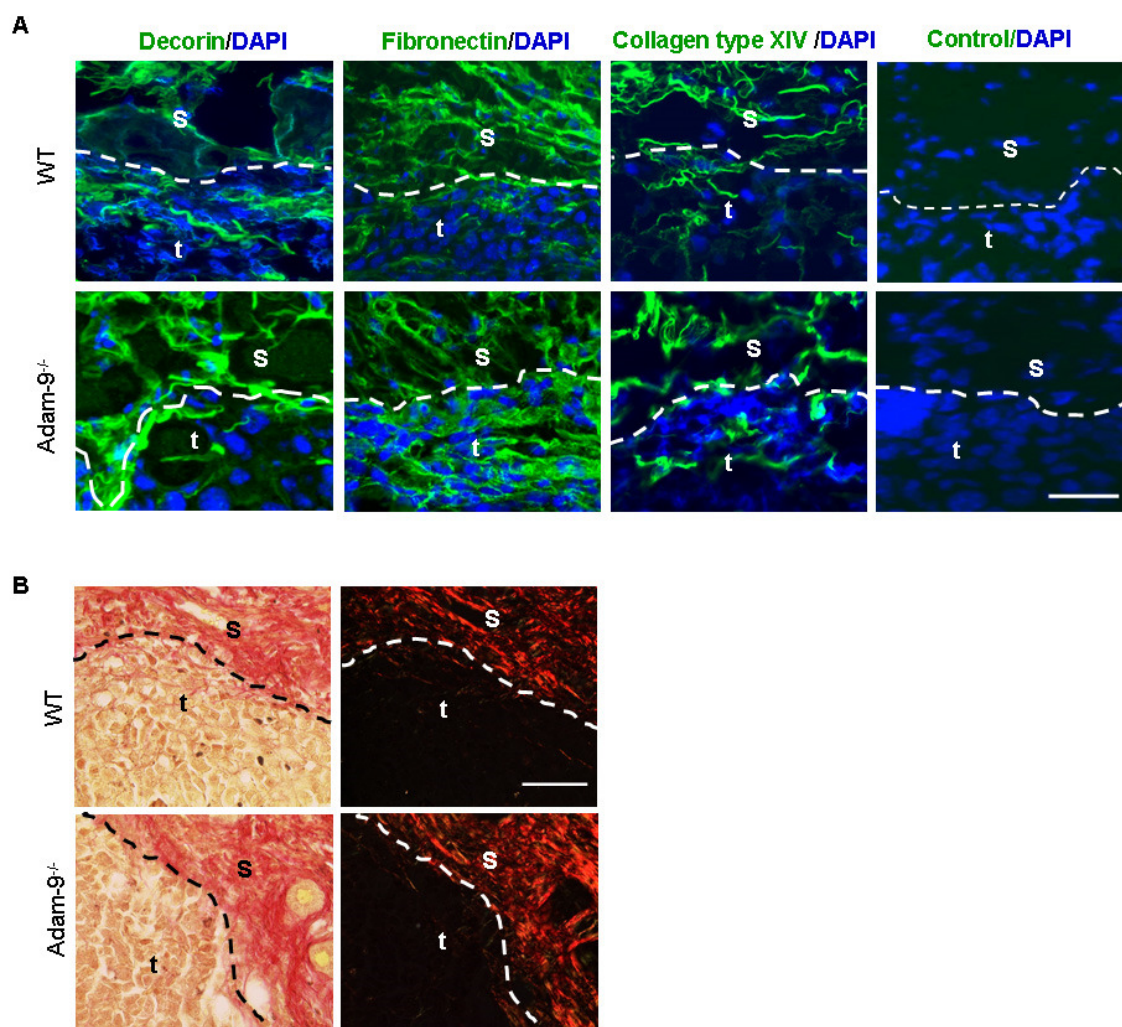
A

Decorin/DAPI   Fibronectin/DAPI   Collagen type XIV /DAPI   Control/DAPI

WT

Adam-9$^{-/-}$

B

WT

Adam-9$^{-/-}$

Figure 32. Expression of ECM proteins in melanoma from WT and *Adam-9*$^{-/-}$ mice. A, analysis of decorin, fibronectin and collagen type XIV (green), nuclei (blue) by immunofluorescence. For negative control, sections were incubated in 1 % blocking buffer without primary antibody. B, analysis of collagen type I by immunohistochemistry using picrosirius red with bright field pictures on the left (collagen type I, red; nuclei, brown-grey) and polarized light assessment on the right (collagen type I, red). Shown are representative images (WT n= 5; *Adam-9*$^{-/-}$ n=5). t, tumor, s, stoma. Scale bar 400µM.

3.6.2 Expression of ECM proteins by fibroblasts

We have detected in the tumor-stoma border of melanomas from *Adam-9*$^{-/-}$ and WT mice differential expression of matrix proteins. In the tumor microenvironment, fibroblasts are largely responsible for the synthesis of ECM components (Rodemann and Muller 1991). To find out whether the altered expression of ECM proteins *in vivo* was due to altered secretion by fibroblasts in the absence of ADAM-9, we have examined the synthesis of the differentially expressed ECM proteins by *Adam-9*$^{-/-}$ and WT fibroblast *in vitro*. By immunoblotting we detected slightly increased amounts of decorin in *Adam-9*$^{-/-}$ fibroblasts lysates. A low molecular weight form of decorin of

about 30 KDa, known to be a cleaved form (Monfort et al., 2006), was detected in increased amounts in *Adam-9⁻ᐟ⁻* compared to WT fibroblasts supernatant (Sp.) (figure 33). Fibronectin and collagen type XIV were detected in both lysates and supernatants from WT and *Adam-9⁻ᐟ⁻* fibroblasts in comparable amounts (figure 33). Collagen type I was increased in *Adam-9⁻ᐟ⁻* as compared to WT fibroblast lysates and supernatants. A low molecular weight fragment of about 70 KDa was detected in WT as well as *Adam-9⁻ᐟ⁻* fibroblast supernatants. However, the amount of this fragment was reduced in *Adam-9⁻ᐟ⁻* fibroblasts compared to WT (figure 33).
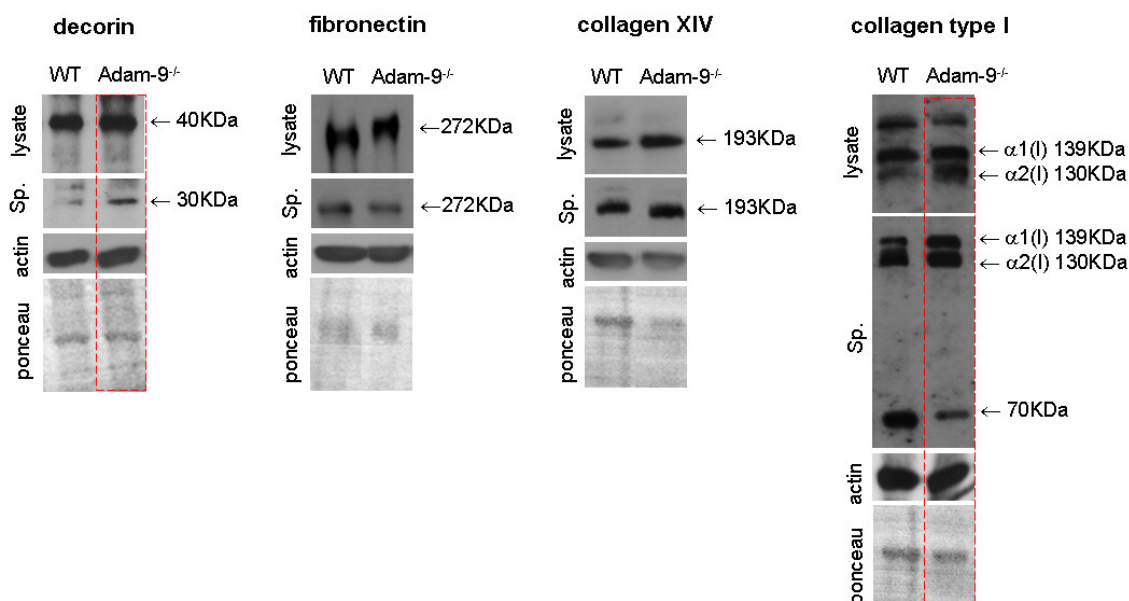

Figure 33. ECM protein expression by fibroblasts supernatant and lysate. Synthesis of ECM proteins by dermal fibroblasts as analyzed by western blot. Ponceau was used to control loading and transfer efficiency of fibroblast supernatants while actin was used as loading control for protein lysates. Images are representatives of WT n=5, *Adam-9⁻ᐟ⁻* n=5.

Tumor cells can influence the composition of the tumor stoma by producing cytokines that regulate the activity of fibroblasts, including the secretion of ECM components (De Wever and Mareel 2003). To mimic the *in vivo* situation of how tumor cells influence the secretion of ECM proteins by fibroblasts, WT and *Adam-9⁻ᐟ⁻* fibroblasts were cultured with conditioned media from B16F1 melanoma cells. Analysis of protein expression by western blot showed a minimal increase in decorin expression by *Adam-9⁻ᐟ⁻* as compared to WT fibroblast lysates and supernatants (Sp.) (figure 34). While the expression of fibronectin and collagen type XIV were not altered by treatment with B16F1 conditioned media, a prominent increased in collagen type I was detected in *Adam-9⁻ᐟ⁻* as compared to WT fibroblasts lysates and supernatants (figure 33 and 34). The low molecular weight fragment of collagen type I of about 70

KDa (previously described in figure 33) was also detected in reduced amounts in *Adam-9⁻/⁻* as compared to WT fibroblast supernatants (figure 34). This indicates that the increased collagen type I, observed in the tumor-stoma border of tumors from *Adam-9⁻/⁻* animals (figure 32) may derive from fibroblast. Decorin, fibronectin, collagen XIV and collagen type I were not detected in the B16F1 supernatant used in treating the fibroblasts.
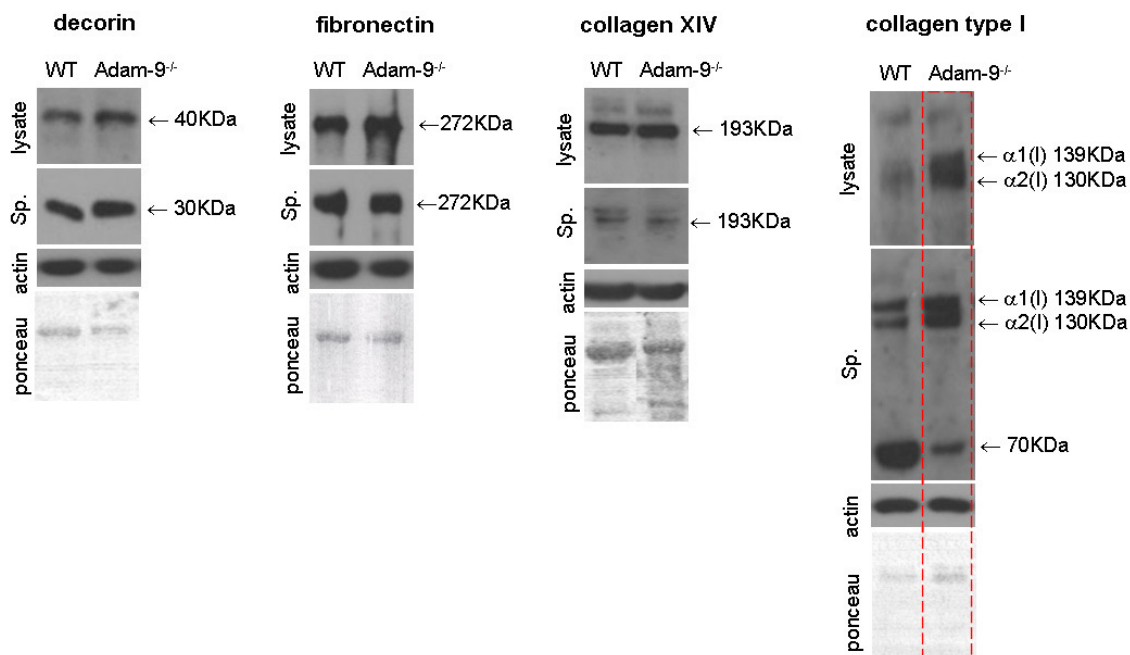
Figure 34. Influence of B16F1 on ECM protein secretion by fibroblasts. Expression of ECM proteins, decorin, fibronectin, collagen XIV and collagen type I by fibroblasts in the presence of supernatant from B16F1 cells using western blot analysis. Ponceau and actin were used as loading control for supernatant and lysate respectively. Shown are representatives of WT n=5, *Adam-9⁻/⁻* n=5.

To find out whether the minor difference in expression of decorin and the more prominent difference in collagen type I in *Adam-9⁻/⁻* fibroblast were because of increased *de novo* synthesis, we analyzed the transcript expression of these proteins in WT and *Adam-9⁻/⁻* fibroblasts using semi-quantitative RT-PCR. The expression of decorin was significantly increased in *Adam-9⁻/⁻* fibroblast with a p-value of 0.014, this difference was less prominent upon culturing fibroblasts with B16F1 melanoma conditioned medium. Collagen type I transcript was similar in WT and *Adam-9⁻/⁻* fibroblasts in monoculture or when cultured with B16F1 conditioned medium (figure 35).

Figure 35. Differential expression of ECM proteins in WT and *Adam-9*^{-/-} fibroblasts. The expression of ECM proteins by fibroblasts with or without treatment with B16F1 conditioned medium (+B16F1 c.m.) was analyzed by RT-PCR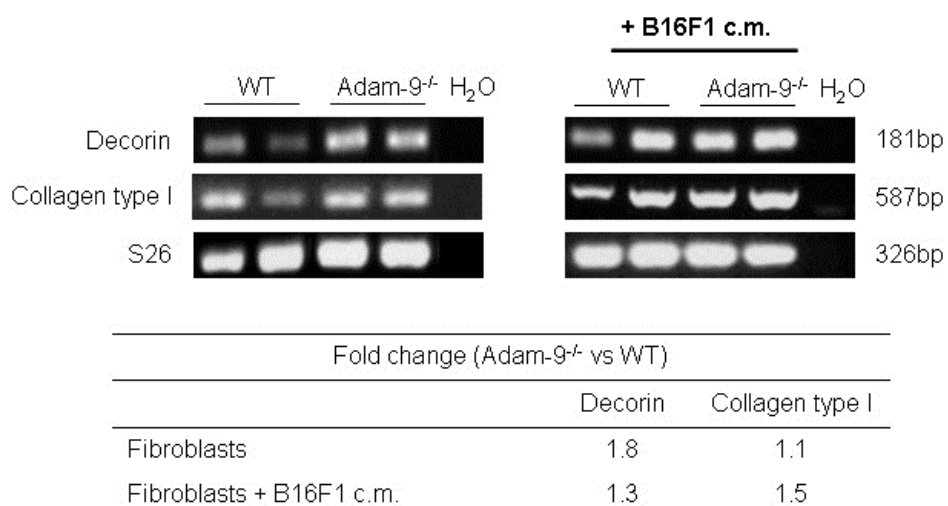 and quantified by densitometry and normalized to S26 loading control and the fold change of transcript expression in *Adam-9*^{-/-} versus WT fibroblasts was calculated. Water was used as negative control. Fibroblast; WT n=5, *Adam-9*^{-/-} n=5, fibroblasts treated with B16F1 c.m. WT n=2, *Adam-9*^{-/-} n=2.

From these data, we conclude that the increased decorin protein, but not collagen type I, in fibroblasts from *Adam-9*^{-/-} mice is a result of increase *de novo* synthesis. Collagen type I synthesis has been extensively studied and shown to be is regulated at multiple levels including mRNA synthesis and stability, protein synthesis and degradation (Bishop and Laurent 1995; Lindquist et al., 2000). As we did not observe any difference in collagen type I mRNA levels between *Adam-9*^{-/-} and WT fibroblasts we speculate that the difference in collagen type I protein resulted from altered post-translational events, for example, accumulation in *Adam-9*^{-/-} fibroblast due to altered proteolysis in the absence of ADAM-9 protein.

3.7   Cleavage of ECM proteins by ADAM-9

3.7.1   Production of recombinant soluble ADAM-9

Accumulation of collagen type I in *Adam-9*^{-/-} fibroblasts supernatants which we have shown above (Figure 33 and 34), did not result from enhanced transcriptional activity (figure 35), but from post-translational events. ADAM-9 is an ECM degrading enzyme, shown to degrade fibronectin and laminin 111 (Schwettmann and Tschesche 2001), however both decorin and collagen type I have not been tested as possible substrates for ADAM-9. To find out whether ADAM-9 was involved in the cleavage of decorin and collagen type I, we produced recombinant soluble ADAM-9

proteins tagged with 6xHis and c-myc. Nucleotide sequence coding for ADAM-9 soluble long (Adam-9s L) was amplified from cDNA derived from glioma cells. Proteolytic inactive form of this protein was produced by mutating the catalytic glutamic acid in the zinc binding motif to alanine by site-directed mutagenesis (see material and method section 2.2.5.1).
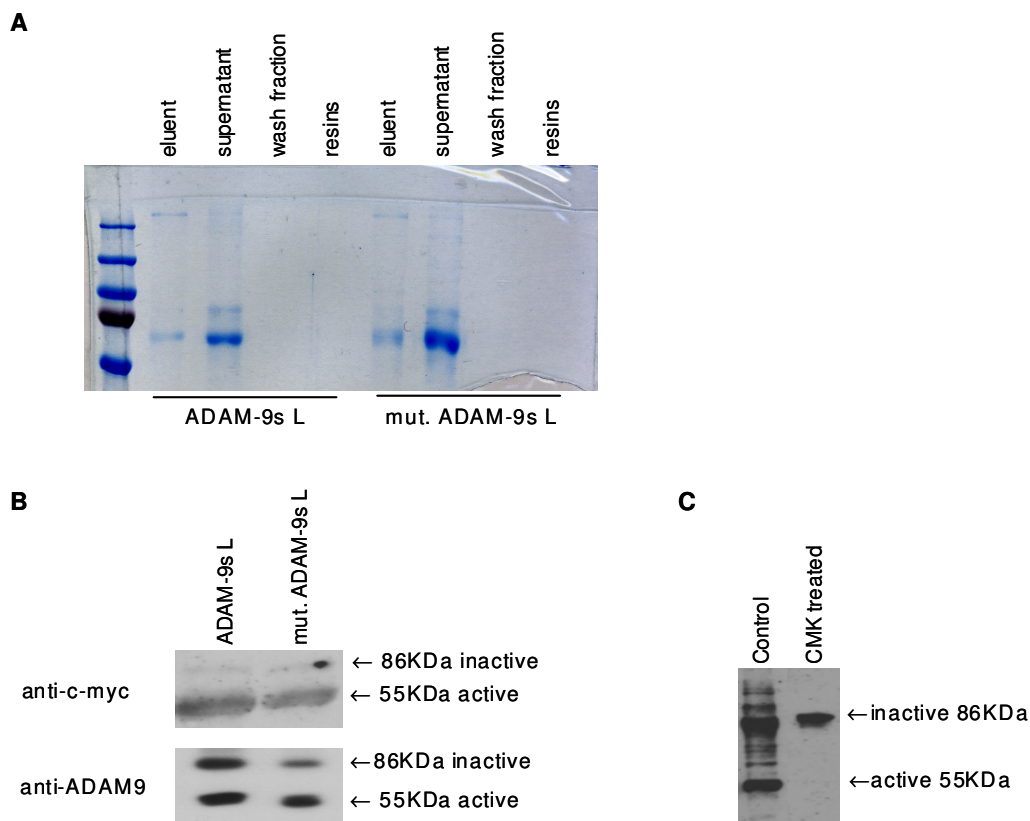
Figure 36. Purification of recombinant soluble ADAM-9. A, purification of ADAM-9 by metal affinity chromatography. B, detection of purified ADAM-9 in eluent by western blot using anti-c-myc and anti-ADAM-9 antibodies. C, detection of soluble ADAM-9 in supernatant from COS-7 cells transfected with soluble ADAM-9 plasmid, with or without treatment with CMK. S; ADAM-9 soluble long, ADAM-9s L; mut., mutated form.

The soluble Adam-9s L constructs were expressed in COS7 cells. Supernatants from transfected cells were collected and purified by size exclusion chromatography (figure 36A). Purified proteins were detected by western blot using anti-c-myc and anti-ADAM-9 antibodies. With both antibodies, we could detect a 86 KDa band corresponding to the inactive unprocessed form of ADAM-9 still containing the pro-domain (figure 36B) and a 55 KDa band corresponding to the active processed form of ADAM-9 lacking the pro-domian. ADAM-9 is activated by removal of the pro-domain by a furin-type pro-protein convertase in the secretory pathway (Roghani et al., 1999). To confirm that the 55 KDa band was the active processed form, we

treated transfected COS7 cells with a dec-RVKR-cmk furin inhibitor (Roghani et al., 1999). After treating cells with furin inhibitor, ADAM-9 was detected only as a 86 KDa inactive unprocessed form (figure 36C), indicating that the 55 KDa band was the furin-activated form of ADAM-9.

3.7.2 Degradation of proteins by ADAM-9

The proteolytic activity of soluble ADAM-9s L was tested by gelatin zymography as previously shown (Schwettmann and Tschesche 2001), where ADAM-9 was detected as a gelatinolytic band of about 55 KDa (figure 37). A slight band was detected for the proteolytic inactive recombinant protein (mut. ADAM-9s L) indicating that the mutation did not lead to 100 % efficient blockage of proteolytic activity. To find out whether ADAM-9 has proteolytic activity towards decorin and collagen type I proteins, we have incubated them with either the proteolytic active or inactive recombinant ADAM-9s L in substrate buffer at 37°C overnight. Degradation of these proteins was analyzed by immunoblotting. Several bands of different sizes were generated when fibronectin was incubated with ADAM-9s L (figure 37). While no cleavage products were detected after incubation either with the mutated proteolytic inactive form of ADAM-9s L or with the substrate buffer alone, confirming the proteolytic activity of the recombinant ADAM-9s L and the previous results obtained by Schwettmann and Tscheche (2001). In case of decorin only the intact 40 KDa band was observed after incubation with soluble ADAM-9s L or mutated ADAM-9s L. A band of about 70 KDa was detected when collagen type I was incubated with ADAM-9s L and was absent when incubated with mutated ADAM-9s L or with substrate buffer alone (figure 37). The identity of this collagen fragment was confirmed by peptide mass fingerprint at the proteomic facility of the Center for Molecular Medicine, University of Cologne.

These data indicate that ADAM-9 is not involved in the degradation of collagen type I since we could not detect differences in the total amount of the protein, but it may release a smaller fragment whose functional activity needs to be further investigated.
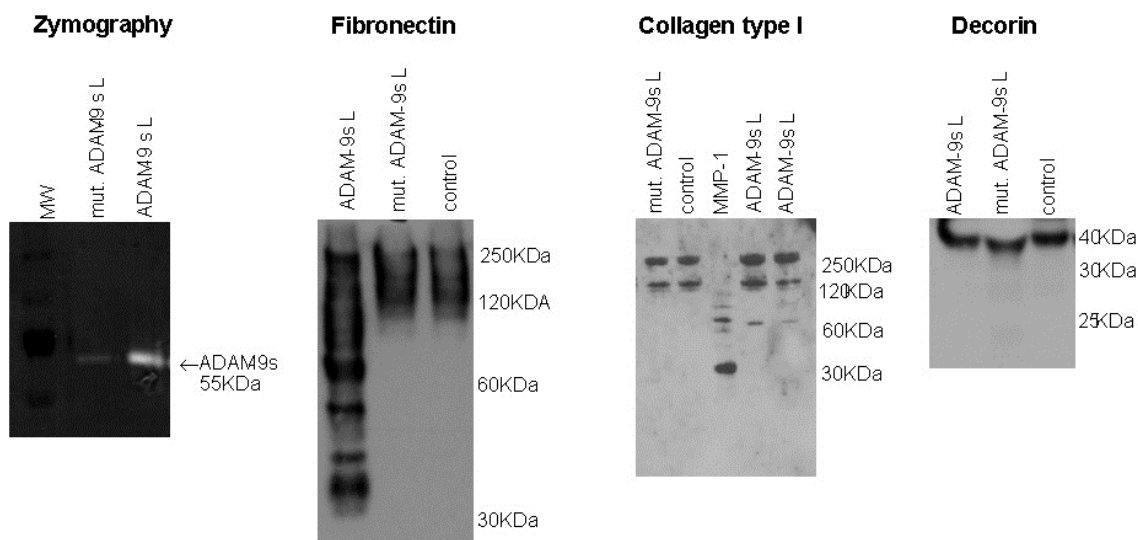
Figure 37. ADAM-9 is involved in the degradation of ECM proteins. Analysis of the proteolytic activity of ADAM-9 soluble long (ADAM-9s L) by gelatin gel zymography under non-reducing conditions. Degradation of fibronectin, collagen type I and decorin by recombinant ADAM-9s L. 500 ng of each ECM protein was incubated with 1 µg/ml recombinant active ADAM-9s L or mutated inactive ADAM-9 soluble long (mut. ADAM-9s L). Proteolysis of recombinant proteins was analyzed by western blot. Recombinant proteins incubated in substrate buffer without the recombinant ADAM-9 was used as control.

Another known substrate for ADAM-9 is the transmembrane collagen type XVII (Franzke 2002). In a previous study, we were able to demonstrate a role for ADAM-9 in cutaneous wound healing. We have observed accelerated reepitheliazation in A*dam-9*^{−/−} animals, because of increased migration of keratinocytes due to decreased shedding of collagen type XVII (Mauch et al. 2010). *In vitro,* primary keratinocytes lacking ADAM-9 also showed increased in migration. Expression of soluble active ADAM-9 constructs in *Adam-9*^{−/−} mouse keratinocytes resulted in collagen type XVII shedding and rescued the migration phenotype observed (Mauch et al. 2010). Shedding of collagen type XVII was not observed when cells were transfected with catalytically inactivated ADAM-9 (Figure 38).

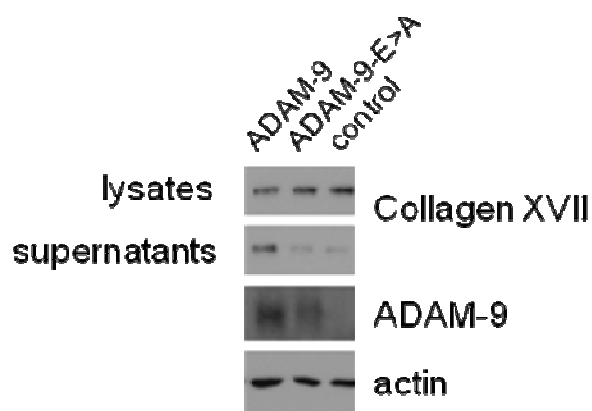

Figure 38. Collagen type XVII is shedd by ADAM-9. Collagen type XVII shedding was restored by transient transfection of murine *Adam-9*^{−/−} keratinocytes with the active but not inactivated (E>A) human ADAM-9. Actin was used as loading control.

3.7.3 Significance of collagen type I accumulation for melanoma progression

We have shown that collagen type I is increased in *Adam-9*^{-/-} fibroblast and at the tumor-stoma border of melanomas induced in *Adam-9*^{-/-} mice (figure 32, 33 and 34). The functional significance of collagen type I accumulation at the tumor-stoma border for melanoma progression was established by assessing the proliferation of B16F1 melanoma cells in the presence of different concentrations of collagen type I. Proliferation of B16F1 cells in the presence of increasing collagen type I concentration in culture was biphasic. Proliferation increased reaching a maximum when cells were cultured with 10 µg/ml collagen type I but decreased with further increase in collagen type I concentration (figure 39B). Thus, it is possible that the modest increase in collagen bundles at the tumor-stoma border in *Adam-9*^{-/-} mice also contributed, in addition to TIMP-1 (3.5.4) to increase tumor cells proliferation, which we have found enhanced in these animals (3.3.3). This hypothesis is further corroborated by the detection of an increased number of actively proliferating (Ki67 positive) tumor cells at the tumor periphery close to this ECM-rich matrix *in vivo* in *Adam-9*^{-/-} as compared to WT mice (Figure 39A).
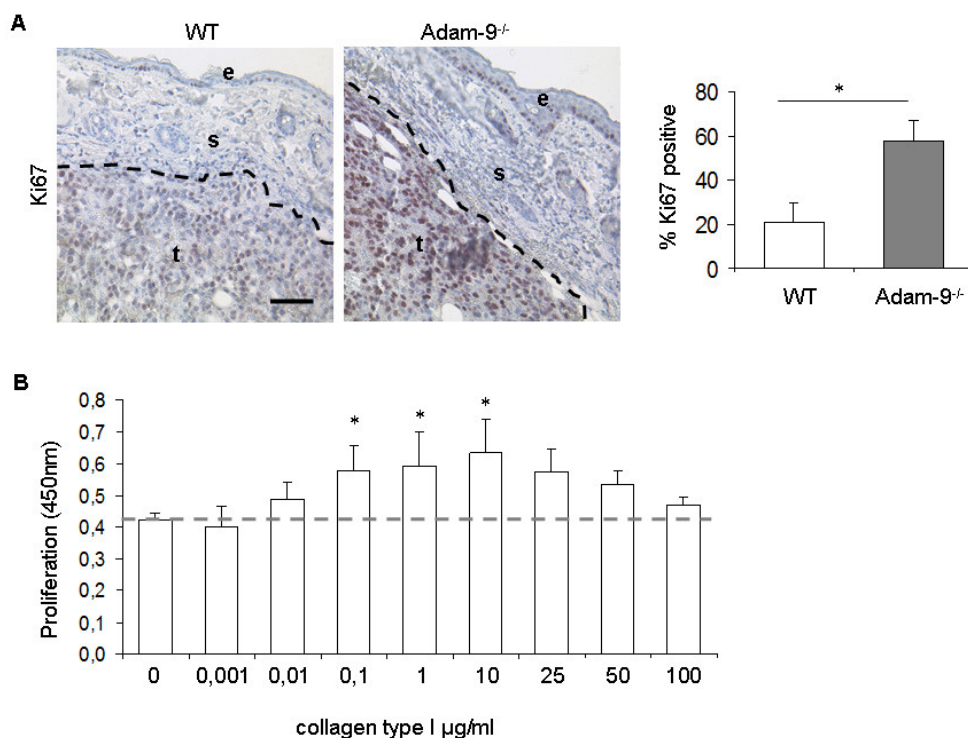
Figure 39. Significance of collagen type I accumulation for B16F1 proliferation. A, tumor cell proliferation at the tumor periphery was assessed by detection of Ki67 nuclear protein. t, tumor; s, stoma; e, epidermis. Scale bar 200 µm. B, proliferation of B16F1 melanoma cells in the presence of collagen type I. The graph represents mean ± SD. p-values were calculated for cell proliferation in the presence of collagen type I compared to serum-free control. ∗ $p < 0.05$.

3.8 ADAMs and MMPs in melanoma models

The medaka spontaneous melanoma model offers another possibility for *in vivo* study of melanoma progression. We have analyzed the expression of *Adams* and *Mmps* in a spontaneous melanoma model generated in medaka (Meierjohann et al., 2004). Our cooperation partner Svenja Meierjohann and Mannfred Schartl of Department of Physiological Chemistry I, University of Wurzburg, provided the tissue samples used in this study. We analyzed the mRNA expression of Adams and Mmps in RNA isolated from healthy skin, melanoma and yellow exophytic erythrophoreoma by RT-PCR (figure 40). Very low expression of all analyzed proteases, apart from Mmp-9, was detected in normal skin. A strong up-regulation of Adam-9, -10, and Mmp-13 and -14 were observed in melanoma and yellow exophytic erythrophoreoma as compared to healthy skin. Mmp-2 was only slightly up-regulated in melanoma but strongly up-regulated in yellow exophytic erythrophoreoma. Mmp-9 was strongly and equally expressed in healthy skin, melanoma and yellow exophytic erythrophoreoma, whereas Adam-12 was not detected in any tissue sample. In skin and melanoma, Adam-15 was similarly expressed and up-regulated in yellow exophytic erythrophoreoma. Adam-17 was detected in skin but absent in melanoma and yellow exophytic erythrophoreoma. Representative images of the RT-PCR analysis are shown in figure 40 below.
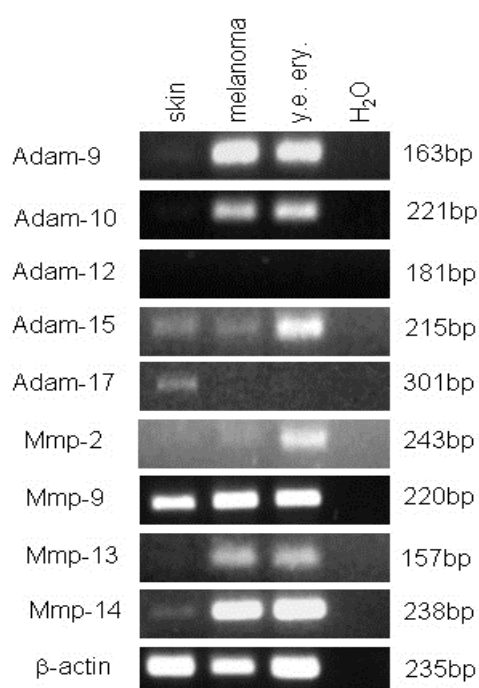

Figure 40. Expression of Adams and Mmps in medaka melanoma model. RT-PCR analysis of Adams and Mmps in medaka skin, melanoma and yellow exophytic erythrophoroma (y.e. ery.). Representative images showing transcript expression of Adams and Mmps (n=3; two sets of tissue). β-actin was used as control for mRNA integrity and equal loading.

The RT-PCR was quantified by densitometry and expression level of specific genes was normalized to β-actin to obtain the relative expression values. The expression ratio of each gene in melanoma and yellow exophytic erythrophoroma as compared to skin was calculated and presented in table 5 below. The expression of genes with ratios greater than 3 were set as "high" , ratios between 1 and 2 as "medium", ratios less than 1 were considered "low", while ratios greater than 2.5 but less that 3 were considered "medium/high". Adam-9, -10, Mmp-13 and -14 showed high expression in melanoma or yellow exophytic erythrophoroma as compared to skin. Adam-15 and Mmp-2 showed moderate expression in melanoma and yellow exophytic erythrophoroma as compared to skin. Mmp-9 showed medium/high expression while Adam-17 showed low expression in melanoma and yellow exophytic erythrophoroma as compared to skin.

Table 5. Relative expression of Adams and Mmps in medaka melanoma model.

Gene	Ratio melanoma/skin	Expression	Ratio yellow exophytic erythrophoroma/skin	Expression
ADAM-9	6.88	high	6.02	high
ADAM-10	6.10	high	5.41	high
ADAM-12	n.d	n.d	n.d	n.d
ADAM-15	1.31	-	1.80	medium
ADAM-17	0.16	low	0.16	low
MMP-2	1.61	medium	1.95	medium
MMP-9	2.68	Medium-high	2.59	Medium-high
MMP-13	4.19	high	3.78	high
MMP-14	4.49	high	3.77	high

Low < 1; moderate 1-2; medium high >2.5; high > 3, - no difference, n.d, not detected

Commercially available antibodies against medaka ADAMs and MMPs are rare. There however exist antibodies against ADAMs and MMPs antibodies, which were originally raised against human, or mouse and cross-react with the fish protein. e first analyzed the homology between human, murine and medaka ADAMs and MMPs and set up staining protocols using antibodies against mouse or human ADAMs and MMPs which have good cross reaction. Shown in table 6 below are the homologies between the different ADAMs and MMPs (complete protein) analyzed in the medaka melanoma model. The analysis was performed with Pairwise Alignment tool software; EMBOSS Needle, provided by The *European Bioinformatics Institute* (*EBI*).

Table 6. ADAMs and MMPs protein homology

	% homology		
	Human-mouse	**human-medaka**	**mouse-medaka**
ADAM-9	83	59	53
ADAM-10	93	75	76
ADAM-12	84	74	64
ADAM-15	40	47	41
ADAM-17	92	56	55
MMP-2	96	72	73
MMP-9	72	57	54
MMP-13	86	59	58
MMP-14	97	64	64

To analyze the protein expression and localization of the genes in melanoma and yellow exophytic erythrophoroma as compared to skin was analyzed we have established immunoflourescence staining protocols testing several available antibodies. H&E staining was used to show an overview of the structures of the tissues (figure 41A). ADAM-9 was detected in the epidermis but not in the muscle of the healthy medaka skin (from fish trunk). In the invasive melanoma ADAM-9 staining was up-regulated and was predominantly expressed in the surrounding tumor stoma, little ADAM-9 was observed the exophytic erythrophoroma. In normal skin, ADAM-10 was expressed in the epidermis and around the muscle fibers, and in both invasive melanoma and exophytic erythrophoroma; it was expressed in the tumor cells but showed very little stoma expression (figure 41B). MMP-13 was not detected in normal skin, melanoma nor in erythrophproma. MMP-14 was detected around the muscle fibers in the trunk. In invasive melanoma MMP-14 was localized in both tumor and stoma cells. In exophytic erythrophoroma, MMP-14 expression seems to be limited to the hyperplastic epidermis (figure 41B).
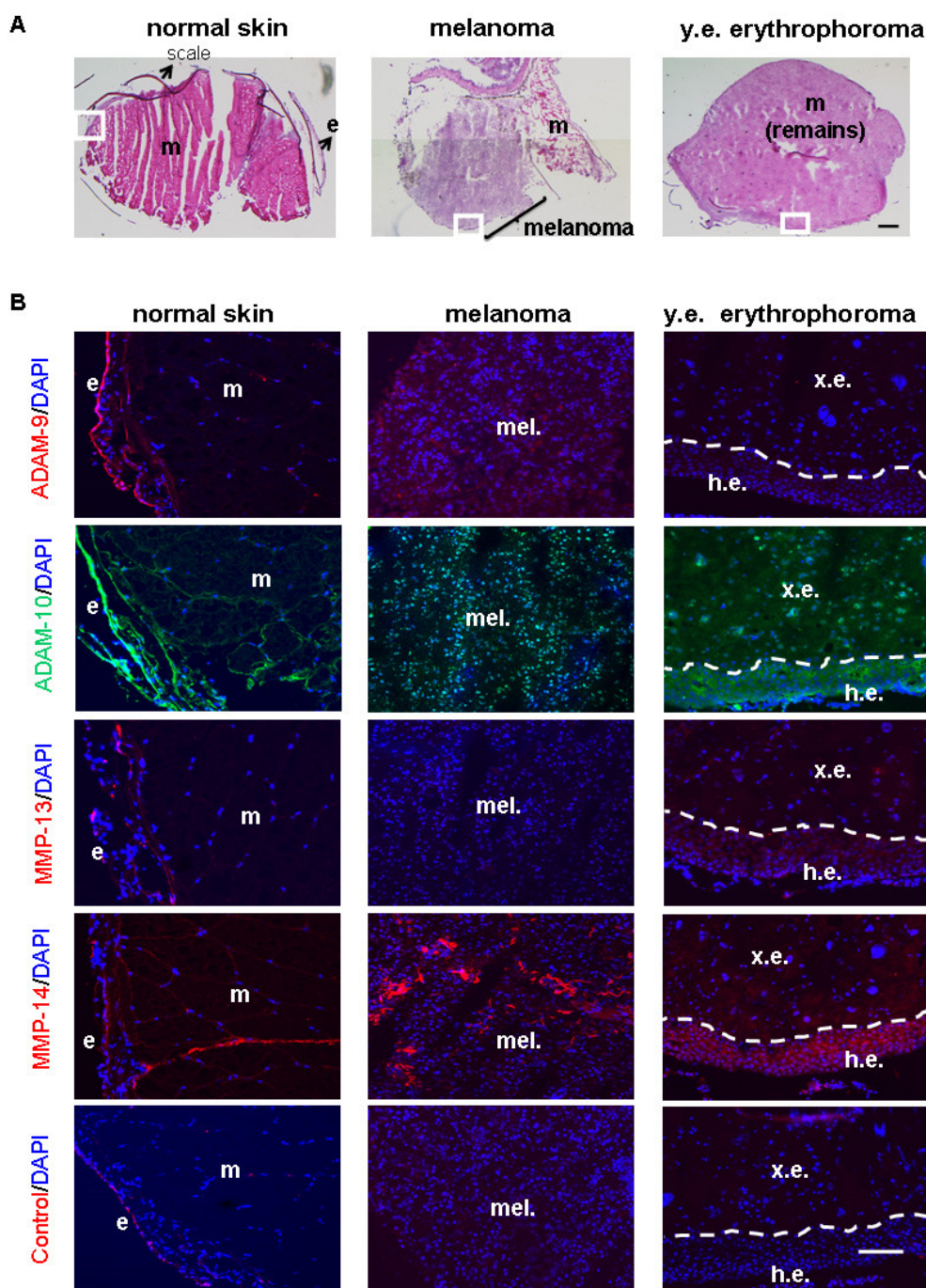
Figure 41 Expression of ADAMs and MMPs in medaka melanoma. A, H&E staining of, left, healthy trunk, middle, melanoma, right, yellow exophytic erythrophoroma (y.e. erythrophoroma). White squares indicate the areas shown in the immunofluorescence staining. Scale bar 25 µm. B, detection of ADAMs and MMPs in normal skin, melanoma and y.e. erythrophoroma. DAPI was used to stain the nuclei (blue). As negative control, sections were incubated without primary antibody. e, epidermis; m, muscle; h.e., hyperplastic epidermis, x.e., erythrophoroma; mel, melanoma. Scale bar 200 µm.

4 Discussion

Melanoma is the most aggressive type of skin tumor and can only be cured when diagnosed early and removed surgically before it metastasizes (MavKie et al., 2009). In melanoma progression, different proteolytic enzyme systems play important roles in degrading basement membranes, dermal matrices components, shedding adhesion molecules, and releasing growth factors and receptors (Airola et al., 1999; Duffy et al., 2011). ADAMs are a family of proteases which function in proteolysis and mediate cellular interaction (Mochizuki and Okada 2007). Several ADAMs are over-expressed in cancers including melanoma (Mochizuki and Okada 2007). In this context, studies using cell lines and animal models have shown that ADAMs influence proliferation and invasion *in vitro* and tumor formation *in vivo.* For example; down-regulation of ADAM-17 in breast cancer cells using siRNA decreases tumor cell proliferation (Zheng et al., 2009) whereas knockout of ADAM-15 leads to reduced growth of heterotopically injected tumor cells in mice (Horiuchi et al., 2003). Recent investigation of our laboratory shows that ablation of ADAM-15 results in significantly reduced lung metastasis of melanoma (Schönefuss et al. 2012). In recent report, ADAM-9 was identified as a high-priority therapeutic target for human breast cancer (Chin et al., 2006). ADAM-9 is up-regulated in various human cancers such as renal, prostate, breast cancer and melanoma (O´Shea et al., 2003; Peduto et al., 2005; Zigrino et al., 2005; Fritzsche et al. 2008).

ADAM-9 is ubiquitously expressed and is not essential during development, as mice lacking ADAM-9 are viable, fertile and do not have any major developmental defects (Weskamp et al., 2002). However, cone-rod dystrophy and retinal degeneration were detected in older *Adam-9$^{-/-}$* mice (Parry et al., 2009). Using *Adam-9$^{-/-}$* animals, we could show that upon skin injury ADAM-9 is involved in shedding of collagen XVII (figure 39) thereby modulating keratinocytes migration during re-epithelialization (Mauch et al., 2010).

In a mouse model for prostate cancer, ADAM-9 was shown to play a causal role in the progression of tumor from well-differentiated to poorly-differentiated tumors; this was attributed to the ability of ADAM-9 to cleave EGF and FGFR2iiib (Peduto et al., 2005). The adhesive function of ADAM-9 may play a role in mediating cell-cell interactions (Zigrino et al., 2011). Although the expression of ADAM-9 in melanoma has been analyzed its exact function in melanoma progression, whether it mediates cellular interactions between melanoma cells and stromal cells or whether it acts as a

proteolytic enzyme releasing cellular receptors or bound growth factors is yet unclear.

4.1 Regulation of tumor development by ADAM-9

In murine melanoma, we could detect ADAM-9 with a similar expression pattern as that observed in human melanoma namely, ADAM-9 was expressed at the tumor-stoma border in both tumor and stromal cells (figure 8). In these areas, both direct and indirect cell-cell communication are ongoing to either counteract tumor development or support it by generating a permissive peritumoral environment. *In vitro*, ADAM-9 can mediate interaction of melanoma cells with stromal fibroblasts, and the absence of ADAM-9 expression on fibroblasts negatively influences the invasive capacity of melanoma cells (Zigrino et al., 2011). This indicates that the expression of ADAM-9 by the host may play a role in melanoma progression. When we grafted ADAM-9 expressing B16F1 cells into the flank of WT and *Adam-9*$^{-/-}$ mice we detected significantly larger tumors in the *Adam-9*$^{-/-}$ as compared to WT mice. Contrary to our results Guaiquil et al., 2009 reported reduced melanoma growth in *Adam-9*$^{-/-}$ mice compared to WT upon injection of B16F0 cells. However, when we grafted B16F0 cells or primary melanoma cells derived from the Hgf/Cdk4^{R24C} mice, which spontaneously develop melanoma (Tormo et al., 2006), *Adam-9*$^{-/-}$ mice developed larger tumors compared to WT controls. Thus, we could show that increase growth of melanoma in the absence of *Adam-9* was not a cell-type specific effect. We cannot absolutely exclude the effect of the background of the animals used for these studies however; there are some arguments eliminating the background as the reason for the differences between the two studies. First, the mice we have used were the same as those used by Guiaquill et al., (2009). These animals are of a mixed genetic background (129/SvJ and C57BL/6J). To reduce variations in the background and to increase the number of animals needed for the analysis, we have mated one pair of heterozygous *Adam-9*$^{+/-}$ parents to generate WT or *Adam-9*$^{-/-}$ mice. The offsprings of the heterozygous pairing were mated to get *Adam-9*$^{-/-}$ or WT mice that were closely related, as they were derived from the same heterozygous grandparents. Second, we failed to detect altered inflammatory reaction in tumors developed either in *Adam-9*$^{-/-}$ or WT mice to support an altered immunological reaction in response to the different genetic background. Differences that may account for these contradicting results can be technical differences in the

performance and analysis of the animal experiments. While Guaiquil et al., (2009), injected B16F0 cells subcutaneously and measured the weight of the tumors at the end of the experiment; we have injected melanoma cells intradermally and measured the volume of the tumors at different time points using a precision caliper. This raises the possibility that the contribution of ADAM-9 to the tumor progression is dependent on the injection site.

Our data suggest a protective role of host-derived ADAM-9 during melanoma development. Protective functions of proteases have been reported for other ADAMs, for example, growth of subcutaneously injected B16F0 cells was significantly higher in *Adam-8*$^{-/-}$ mice compared to WT controls (Guaiquil et al., 2010). Apart from investigating angiogenesis in these tumors, this study does not address the reason for the increased tumor growth in *Adam-8*$^{-/-}$ mice. In addition, cell-specific expression of matrix metalloproteinases has been shown to have different effects on tumor growth. For example, the expression of MMP-12 by tumor cells (in this case squamous cell carcinoma) correlated with more aggressive and poorly-differentiated tumors, while its expression in macrophages correlated inversely with tumor invasiveness (Kerkelä et al., 2002).

Key events that are known to influence tumor growth include angiogenesis (Ria et al., 2010), inflammation (Coussens and Werb 2002), resistance to apoptosis and replicative potential (Hanahan et al., 2000). When we analyzed inflammatory reaction by determining the number and location of neutrophils, T-/B-cells and macrophages in tumors from *Adam-9*$^{-/-}$ and WT mice, we could not detect any alterations, suggesting that host-derived ADAM-9 is not involved in modulating inflammation. The function of ADAM-9 in inflammatory cells in the context of melanoma progression is unclear. However, up-regulation of ADAMs including ADAM-9 has been reported in peripheral blood mononuclear cells and macrophages during immune-mediated diseases where they are speculated to have a role in leukocyte migration by promoting cellular adhesion (Dehmel et al., 2007; Oksala et al., 2009). Interestingly, the expression of ADAM-9 in blood vessels coincides with that of CD31, where this protein was shown, by *in vitro* assays, to be involved in the shedding of proteins on the surface of endothelial cells (Guaiquil et al., 2009). In our tumor model, this function of ADAM-9 may not be relevant as despite detecting altered intratumoral angiogenesis in tumors from *Adam-9*$^{-/-}$ as compared to WT animals, comparison of vascularization in tumors of similar sizes (from different time point; day 6 *Adam-9*$^{-/-}$

versus day 10 WT), displayed no difference in vessel density. This indicates that altered angiogenesis was a result of increased tumor growth but was not induced by the lack of ADAM-9 in the host.

In vivo, we detected a significant increase in tumor cell proliferation accompanied by a decrease in apoptosis in tumors from *Adam-9*$^{-/-}$ as compared to those from WT animals. This difference was also observed when comparing tumors of similar sizes, albeit different excision time point. This indicates that the increase tumor cell proliferation and decreased apoptosis of melanomas in *Adam-9*$^{-/-}$ mice was due to *Adam-9* ablation. We hypothesize that the resultant increased tumor development in the absence of *Adam-9* is the result of an imbalance between tumor cell proliferation and apoptosis.

4.2   Regulation of tumor metastasis by ADAM-9

Another process, which we have investigated in our mouse model, was melanoma metastasis. Upon growth and migration from the primary site, melanoma cells metastasize to lymph nodes and distant organs. This process is underlined by several steps including intravasation, transport through the blood stream or lymph system, extravasation, arrest at the secondary site and growth (Koblinski et al., 2000; Tarhini and Agarwala 2006). The most common site of visceral metastasis is the lungs (Balch et al., 2003) while the regional lymph nodes are considered to be the first site of metastatic spread because they are the first to come in contact with the fluid draining from the primary tumor (Nathanson 2003). Despite the difference in tumor growth between *Adam-9*$^{-/-}$ and WT mice, there was no difference in metastasis to lungs and lymph nodes. In our melanoma grafting experiment, we observed similar metastasis to lungs and lymph nodes at day 3, 6 and 10. There was a slight decrease in metastasis to lungs and lymph nodes in *Adam-9*$^{-/-}$ mice at day 13, thus inversely correlating with tumor size. Tail vein injection of melanoma cells to assess metastasis of blood borne melanoma cells also did not show any difference in metastasis to lymph nodes and visceral organs. This suggests that the processes involved in metastasis such as chemotaxis, extravasation and intravasation were not affected by the loss of host-derived ADAM-9, and that despite the extensive growth of the tumors in *Adam-9*$^{-/-}$ mice, tumor growth and metastasis, are not strictly dependent on each other.

This is very important, but may consider controversial on the light of common theories of metastasis. Theories of metastasis have been recently revised, the parallel and the linear progression model. In the linear progression model, metastasis is generated by late dissemination of fully malignant cells after rounds of mutation and selection. The parallel progression model states that metastasis is initiated long before the primary tumor is diagnosed and is independent of the size of the tumor (reviewed by Klein 2009). The mouse mammary tumor virus-polyoma middle T antigen transgenic model (MMTV-PyMT) which develops spontaneous breast cancer (Hüseman et al., 2008) supports the parallel progression model. It was shown in this mouse models that disseminated tumor cells were present in the bone marrow and lungs when the primary tumor was in the premalignant phase, and that their number was independent of the size of the primary tumor (Hüsemann et al. 2008). Considering the parallel progression model it is not surprising that even though we detect large tumors, we observed similar metastatic spread to lungs and lymph nodes in *Adam-9*^{-/-} and WT mice.

4.3 Melanoma cell proliferation and apoptosis in the absence of host-derived ADAM-9

Cancer cells modify their pericellular stoma by producing a variety of factors (Mueller and Fusenig 2004). Fibroblasts constitute a great portion of the cellular part of the tumor stoma and contribute to tumor progression by secreting ECM components, proteases that modify the ECM and growth factors/cytokines (Kalluri and Zeisberg 2006).

ADAM-9 was shown to mediate cellular interactions between melanoma cells and fibroblasts (Zigrino et al 2011). To analyze the molecular mechanism, which may lead to altered tumor proliferation and apoptosis in the absence of *Adam-9*, we have therefore focused our studies on the role of fibroblasts-derived ADAM-9 in these processes. Using co-culture system of tumor cells and fibroblasts, we could show that direct contact of mitotically inactive fibroblasts and melanoma cells alone do not influence cell proliferation. Induction of B16F1 cell proliferation was observed when melanoma cells were cultured with *Adam-9*^{-/-} fibroblasts either in transwell or in using *Adam-9*^{-/-} fibroblast supernatant suggesting a soluble-factor mediated mechanism. Interestingly, conditioned media from *Adam-9*^{-/-} fibroblasts could enhance the proliferation of human melanoma and glioma cells, whereas no significant effect was

detected on epithelial tumor cell lines. The effect on glioma cells could be because glioma and melanoma share many similar biological properties as melanocytes and glial cells share a common origin namely the precursor cell type, which differentiate from neural crest cells in the dorsolateral surface (Herlyn et al., 2000). Melanoblast precursors can differentiate into glial precursors and glioblasts can differentiate into melanoblasts (Herlyn et al., 2000; Adameyko et al., 2010).

Studies have documented the regulation of tumor cell proliferation by stromal fibroblasts. For example, serum-free media from breast fibroblasts stimulate the proliferation of breast cancer cell lines; an effect attributed partly to insulin-like growth factors (Kees et al., 1996). Another study ascribed the growth promoting activity of stromal fibroblasts towards breast carcinoma to their ability to secrete stromal cell-derived factor 1 which stimulates tumor growth directly through its receptor, CXCR4 (Orimo et al., 2005).

We analyzed factors present in the supernatant of fibroblasts and tumor lysates from *Adam-9*^{-/-} and WT mice and selected factors which were regulated in both, thereby likely derived from fibroblasts. We identified several soluble factors with roles in apoptosis and growth stimulating activity. Among soluble factors with growth stimulatory activity on melanoma cells were macrophage inflammatory protein -2 (MIP-2/CXCL1) also known as growth-regulated oncogene (Haghnegahdar et al., 2000), stromal cell-derived factor 1 alpha (SDF-1α/CXCL12) (Lui et al., 2011) and TIMP-1 (Hayakawa et al., 1992). However, the most significantly regulated factor was TIMP-1, which was up-regulated 6.72 fold in *Adam-9*^{-/-} fibroblasts and 7.91 fold in tumor lysates from *Adam-9*^{-/-} mice. We could detect increased Timp-1 transcript and protein in fibroblasts from *Adam-9*^{-/-} mice *in vitro* as well as in the stoma surrounding the melanoma tumors *in vivo*. This protein has been described to have both tumor promoting and tumor suppressing activities that could be metalloproteinase-independent or metalloproteinase-dependent (Hornebeck et al., 2005).

TIMP-1 has been shown to possess growth promoting activity for a number of cells (Hayakawa et al., 1992; Sorensen et al., 2008). Its growth promoting activity may explain its presence of the serum used for cell culture (Hayakawa et al., 1992). In a human melanoma cell line, the expression of TIMP-1 has been shown to stimulate growth (Hoashi et al., 2001). Neutralization of TIMP-1 in media from *Adam-9*^{-/-} fibroblasts ablated the increased induction of B16F1 melanoma cell proliferation observed. The growth promoting activity of TIMP-1 was further strengthened by the

fact that, *in vitro* we could show that recombinant TIMP-1 enhances the growth of murine and human melanoma cells. Conflicting views exists on the role of TIMP-1 in tumor growth; TIMP-1 transgenic mouse model, over-expressing TIMP-1 in the liver, showed early subcutaneous growth of melanoma with increased tumor angiogenesis (De Lorenzo et al., 2003). On the other hand, up-regulation of TIMP-1 in B16F10 melanoma cells was shown to suppress tumor growth (Khokha 1994). This implies that TIMP-1 may have a promoting or inhibiting effect on melanoma growth depending on the cellular source or local and systemic expression. TIMP-1 can regulate cell growth in an MMP-dependent and MMP-independent manner. MMP-independent function of TIMP-1 occurs through binding of TIMP-1 to a cell surface receptor, CD63, which is a member of the tetraspanin family (Jung et al., 2006). Binding of TIMP-1 to a CD63/integrin β1 complex is thought to activate integrin-mediated signaling pathway involving focal adhesion kinase, phosphoinositide 3-kinase, extracellular signal-regulated kinase-1 and Akt leading to the regulation of cell proliferation and cell survival (Chirco et al., 2006). It is however unclear whether the proliferative effect of TIMP-1 we detected on B16F1 cell proliferation is mediated by an MMP-dependent or independent manner. The increase in TIMP-1 we observed is possibly due to increase IL-6 and IL-1, which have been shown to induce the synthesis of TIMP-1 (Richard et al., 1993). Both cytokines were up-regulated in fibroblasts and tumors from *Adam-9$^{-/-}$* animals.

In addition to increased proliferation in melanoma grown in *Adam-9$^{-/-}$* mice, we also detected a significant reduction in B16F1 cell apoptosis. Although TIMP-1 also has anti-apoptotic activity (Stetler-Stevenson 2008), neutralization of TIMP-1 in media from *Adam-9$^{-/-}$* fibroblasts prior to B16F1 stimulation did not affect apoptosis. In fibroblasts supernatants and tumor lysates, we identified factors that could modulate apoptosis, such as soluble TNF-α and soluble TNFRI. TNF-α is a cytokine secreted by a variety of cells and signals through two surface receptors, TNFRI and TNFRII. The majority of the biological activity of TNF-α is mediated through binding to TNFRI (Chen and Goeddel 2002). Binding of membrane bound or soluble form of TNF-α, released by shedding (Garton et al., 2006), to TNFRI leads to the activation of pro-apoptotic signaling or expression of anti-apoptotic genes (Baud and Karin 2001). Proteolytic release of TNFR1 generates a soluble receptor (sTNFRI) which binds to TNF-α and inactivates the receptor-mediated signaling (Engelmann et al., 1989). We hypothesize that in the absence of ADAM-9 increased sTNFRI neutralizes TNF-α

resulting in reduced melanoma cell apoptosis. In support of this hypothesis, inhibition of TNFRI shedding in *Adam-9*$^{-/-}$ fibroblasts, prior to melanoma cell stimulation, led to reduced release of TNFRI and increased apoptosis. Furthermore, addition of Enbrel, a recombinant human soluble TNF-α receptor II which is capable of binding TNF-α (Madhusudan et al., 2005), to supernatants from WT fibroblasts also leads to reduced apoptosis. These data confirmed that sTNFRI is responsible for the reduced level of apoptosis observed in B16F1 cells upon culture with media of *Adam-9*$^{-/-}$ fibroblast.

sTNFRI derives from ectodomain shedding by the activity of ADAM-10 and ADAM-17 (Hikita et al., 2009), however, ADAM-17 has been indicated as the main sheddase for the TNFR1 (Bell et al., 2007). We found ADAM-10 and ADAM-17 up-regulated in fibroblasts from *Adam-9*$^{-/-}$ animals suggesting that the increase in sTNFRI maybe due to the activity of these proteases. The increase of sTNFR1 may be due to increase of ADAM-17 rather than ADAM-10 as ADAM-10, but not ADAM-17, is effectively inhibited by TIMP-1 (Amour et al., 2000), which is increased in *Adam-9*$^{-/-}$ fibroblasts. Inhibition of ADAM-17 in *Adam-9*$^{-/-}$ fibroblasts with TAPI-0 led to a reduction of sTNFRI release. TAPI-0 is not specific for the inhibition of ADAM-17 alone but also inhibits MMPs such as MMP-1, -3, -9 and -13 (Roghani et al., 1999). However, among these MMPs only MMP-9 is thought to be involved in the shedding of TNFRI (Masters Thesis; http://www.rescancer.com/bmc-cancer/20570.html). Furthermore TAPI-0 has a higher binding affinity to MMP-9 than to ADAM-17 (K_i values ADAM-17, 8.8 nM; MMP-9 0.5 nM) (Roghani et al., 1999). Despite the fact that we cannot conclusively point to ADAM-17 in releasing TNFR1 upon *Adam-9* knock out in fibroblasts, all together our data support the hypothesis that the decrease in B16F1 apoptosis after stimulation with *Adam-9*$^{-/-}$ fibroblast supernatants is the result of increased enzymatic release of sTNFRI. Interestingly, TNF-α, which we have found increased in fibroblasts and melanomas from *Adam-9*$^{-/-}$ mice, can induce the expression of ADAM-17 (Cessaro et al., 2009), thus suggesting an autocrine regulatory path leading at the end to modulation of apoptosis.

It is still unclear how the lack of ADAM-9 affects the production of cytokines and other soluble factors. ADAM-9 may influence the production of cytokines through signaling via its cytoplasmic tail. The cytoplasmic tail of ADAM-9 has already been documented in the regulation of inside-out signaling where binding of ADAM-9 to PKCδ triggers spatial changes in ADAM-9 and affects the shedding of HB-EGF

(Izumi et al., 1998). In addition, the cytoplasmic tail of ADAM-9 contains two proline-rich sequences, which bind SH3 domains. SH3 domains are is present in several signaling molecules (Weskamp et al., 1996; Pawson 1995). One can speculate that ADAM-9 may interact with SH3 domain-containing signaling molecules in the cytoplasm and in this way influence intracellular signaling, leading to regulation of various soluble factors. Possibly, in the absence of ADAM-9 lack of shedding of cell surface proteins may affect the production of cytokines. One candidate surface protein is delta-like 1 (Dll1). Dll1 is a notch ligand that is constitutively cleaved by ADAM-12 and ADAM-9 (Dyczynska et al., 2007). When Dll1 binds to notch, the ligand bound receptor undergoes proteolytic cleavage in the extracellular and transmembrane domain. The intracellular domain translocates to the nucleus and regulates gene expression (Lai 2004). We could envision that in the absence of ADAM-9 reduced ligand processing may lead to increase notch ligand-receptor interaction and increase notch signaling. Indeed, persistent notch signaling has been shown to affect fibroblasts gene expression (Dees et al., 2011). We found a drosophila homolog of Dll1, Dlk1, significantly up-regulated in $Adam-9^{-/-}$ fibroblast rendering the above speculation feasible. Detailed analysis of this theory was not possible within the frame of this thesis; further investigations are aimed at analyzing the expression and cleavage of Dll1 in $Adam-9^{-/-}$ versus WT fibroblasts. RNA array analysis has identified transcription factors, which are differentially expressed in the absence of ADAM-9 and may be involved in the synthesis of cytokines. One of the transcription factors up-regulated in $Adam-9^{-/-}$ fibroblasts is trans-acting transcription factor 6 (Sp6) also known as Krueppel-like factor 14, a member of the Sp/KLF family of transcription factors (Kacynski et al., 2003). A member of this family, Sp1, is involved in the regulation of TIMP-1 and ADAM-17 (Lee et al., 2004; Szalad et al., 2009). Whether Sp6 is also involved in the regulation of TIMP-1 or ADAM-17 or other cytokines and whether it is itself regulated by ADAM-9 remains to be validated.

4.4 Extracellular matrix proteins in the absence of ADAM-9

The ability of tumor cells to grow and invade the surrounding tissue depends on their ability to communicate with other cells of the tumor microenvironment and to remodel the extracellular matrix (ECM) (Liotta and Kohn 2001). Remodeling of the ECM by proteases alters the matrix and also sets bound growth factors and cytokines free thereby contributing to the regulation of cellular functions such as adhesion,

proliferation and migration (Van Kempen et al., 2003; De wever and Mareel 2003). Proteolytic activity of ADAM-9 towards matrix components such as laminin 111 and fibronectin have been reported (Schwettman and Tschesche 2001; Mazzocca et al., 2005), therefore, we started to explore by proteomic analysis how the enzymatic activity of ADAM-9 may modify the ECM at the tumor-stroma border.

Analysis of matrix purified from the peritumoral stroma area of tumors from WT and *Adam-9$^{-/-}$* animals, revealed differential expression of some ECM proteins and cellular components, the latter was due to the presence of peritumoral cells in the analyzed specimen. ECM proteins such as decorin, collagen type V and collagen type I were up-regulated at the tumor-stroma border of tumors from *Adam-9$^{-/-}$* mice. The up-regulation of both collagen type I and V, is somehow not surprising as collagen type V has been often associated with collagen type I and is involved in fibrillogenesis (Wenstrup et al., 2004). Increased collagen type V has been associated with the promotion of epidermal tumors (Marian 1987), but a role for this collagen in melanoma development has not been explored. Increase synthesis of collagen type I by stromal cells has been reported in melanoma (Smolle et al., 1996). In skin, fibroblasts are the major cell types that synthesize collagen type I and other ECM components (Kielty et al., 1993). *In vitr*o, analysis of fibroblasts or fibroblasts stimulated with murine melanoma cells media confirmed increase in collagen type I and decorin secretion. No changes were detected in the other analyzed matrix proteins. Further investigations showed that decorin but not collagen type I was transcriptionally induced in *Adam-9$^{-/-}$* fibroblasts, indicating that increase of decorin was as a result of increased *de novo* synthesis. However, the increase in decorin protein secretion by fibroblasts alone is too small to account for the 2-fold increase we observe at the tumor-stroma border in tumors from Adam-9$^{-/-}$ mice. Other cell types for example endothelial cells (Järveläinen et al., 1992) could therefore be involved in the secretion of decorin *in vivo*. As decorin is involved in collagen fibrillogenesis (Weber et al., 1995; Iozzo et al., 1998), it is tempting to speculate that its expression is increased to reorganize the increasingly secreted collagen type I.

In the case of collagen type I, its production was not regulated at the transcriptional level indicating that post-transcriptional mechanisms are involved. Increased collagen type I *in vivo* and *in vitro*, may result from decreased degradation. Some MMPs known to degrade collagen type I e.g. MMP-13 (Nagase and Murphy 2008), can be inhibited by the high amount of TIMP-1 present in the peritumoral areas when ADAM-

9 is ablated. However, this would not explain an ADAM-9-dependent proteolytic effect, as ADAM-9 is not inhibited by TIMP-1 (Amour et al., 2002). Apart from the accumulation of collagen type I in *Adam-9*^{-/-} fibroblasts, another interesting observation was the significant reduction of a low molecular weight fragment of collagen type I of about 70KDa in *Adam-9*^{-/-} fibroblasts. Enzymatic assays using recombinant ADAM-9 indicated that active soluble ADAM-9 but not its proteolytically inactive form could cleave collagen type I generating a fragment of about 70KDa. Mass peptide finger printing identified this fragment as a fragment of collagen alpha 1 (I) chain. Whether this fragment is of biological significance will be a matter of future investigations. Although ADAM-9 could cleave collagen type I, the amount of intact collagen type I was not visibly reduced (figure 37). This could mean that the accumulation of collagen type I in fibroblasts and melanoma from *Adam-9*^{-/-} mice is because of reduced expression of other collagenases or increase expression of collagenase inhibitors in the absence of ADAM-9.

In a study using an *in vitro* model that reconstitutes the fibrillar collagen type I structure, Henriet et al., (2000) showed that the proliferation of melanoma cells in contact with collagen was dependent on the organization of the collagen fibrils. High collagen type I density also enhances the growth of mammary tumors (Provenzano et al., 2008). Furthermore, interaction of melanoma cells with collagen type I have been shown to reduce drug-induced apoptosis (reviewed by Aoudjit and Vuori 2012). In agreement with this, *in vivo* analysis of B16F1 cell proliferation in tumors from *Adam-9*^{-/-} animals showed higher number of proliferating melanoma cells at the tumor periphery, in close vicinity to areas with high collagen density compared to tumors from WT. In support of a pro-proliferative activity of collagen type I we could also demonstrate *in vitro*, that B16F1 melanoma cell proliferation is increased with increase collagen type I concentration reaching a plateau above which proliferation reduces steadily. Higher amount of collagen type I may lead to the formation of networks around the tumor cells, which are too stiff or tense and impede cell proliferation. Changes in the stiffening of the ECM are observed in the progression of cancer (Butcher et al., 2009; Levental et al., 2009). Matrix stiffness plays a role in cell proliferation; this may depend on the type of cancer as glioma cells were shown to proliferate more on rigid ECM possibly by altering the mechanochemical feedback during mitosis hence altering the cells progression through the cell cycle (Ulrich et al., 2009). Another explanation is that stiff matrix triggers mitogenic signaling pathways

through integrins (Paszek et al., 2005). The increased tumor cell proliferation maybe the result of two events; increased TIMP-1 and collagen type I at the tumor-stroma border.

In summary, we showed that the expression of ECM components during melanoma development is altered in the absence of ADAM-9. We observed increase expression of decorin and collagen type I at the tumor-stroma border of melanomas from *Adam-9$^{-/-}$* animals and *in vitro* in Adam-*9$^{-/-}$* dermal fibroblasts. We identified collagen type I as a new ADAM-9 substrate and provide evidence that the collagen type I concentration is important in B16F1 melanoma development.

4.5 Melanoma fish model

Among models available for the study of melanoma, a few spontaneous mouse models have been characterized (Pollock et al., 2003; Tormo et al., 2006) and the addition of spontaneous fish models has enlarged the possibilities for *in vivo* studies. Fish models for melanoma include the Xiphophorus model (Meierjohann et al., 2004); the zebrafish model (Patton et al., 2005) and the medaka model (Meierjohann et al., 2004). The Medaka fish melanoma model spontaneously develops tumors in the pigment cells due to over-expression of Xmrk receptor under control of a pigment cell specific promoter (Meierjohann et al., 2004). Some molecular peculiarities of human and murine melanoma have been characterized in this model (Meierjohan and Schartl 2006). Although MMPs and ADAMs have been identified in the medaka genome (http://www.ensembl.org/Oryzias_latipes/Info/Index) their characterization in skin and melanoma in terms of expression and function has not been investigated. One aspect we investigated in this study was the expression of proteolytic enzymes, which are necessary to generate an environment that helps tumor cells to invade the surrounding tissue and to cross physical barriers (Stewart et al., 2004). We have analyzed the expression and localization of various metalloproteinases in medaka melanoma tissue as compared to healthy unaffected skin. We have shown increased expression of Adam-9, -10, Mmp-2, -13 and -14, specifically in melanoma and exyophytic erythrophoroma as compared to healthy skin at transcript level. Similar to human melanoma (Zigrino et al., 2005) we have detected ADAM-9 protein in the stoma compartment in medaka melanoma (figure 41). ADAM-10 was highly expressed in medaka melanoma cells, likewise in human melanoma (Lee at al., 20010). MMP-14 was localized in tumor and stromal cells, an expression pattern,

which resembles that observed in humans (Anderegg et al., 2009). Other metalloproteases, which have been shown to be expressed in melanoma like ADAM-12, -15, -17 and MMP-13 were not detected with the antibodies used, probably due lack of cross-react with this specie.

We show here for the first time the expression pattern of some metalloproteases in a melanoma spontaneously developed in fish. The similarities in the expression pattern of the ADAMs and the MMPs in the medaka and human melanoma makes the medaka melanoma model a promising tool for the analyzing the expression and role of metalloproteases in melanoma progression and screening of metalloprotease inhibitors.

5   Conclusion and perspectives

This study provides insight into the molecular mechanisms involved in the regulation of tumor growth and modification of the peritumoral microenvironment by fibroblast-derived ADAM-9. This is important as it shows that proteases may exert functions that may be beneficial to counteract cancer. We provide data showing that during melanoma development, stroma-derived ADAM-9 is involved in the regulation of TIMP-1 and sTNFR1 in fibroblasts, which in turn affect tumor cell proliferation and apoptosis. The mechanism of how ADAM-9 regulates the production of cytokines is still unclear; whether it involves cleavage of a cell surface protein which then affects downstream signaling or whether it involves signaling through its cytoplasmic tail will be addressed in future studies. The use of recombinant ADAM-9 with specific deletion of the metalloprotease domain or cytoplasmic tail in cell base assays will indicate which domain is important in the regulation of cytokines by ADAM-9.

Enhanced tumor growth in *Adam-9*$^{-/-}$ mice was accompanied by accumulation of collagen type I around the tumors. The fact that collagen type I enhances tumor cell proliferation in a concentration dependent manner, depicts the significance of the composition and integrity of the ECM in controlling growth of tumor cells. ADAM-9 could cleave and released a 70 KDa fragment from collagen type I, which represents a new ADAM-9-proteolytic product.

In a side project, we show that the expression profile of MMPs and ADAMs in the medaka melanoma is similar to that of human melanoma, providing a new model for the future study of metalloproteases in melanoma progression.

6 References

Adameyko I, Lallemend F, Aquino JB, Pereira JA, Topilko P, Müller T. (2009) Schwann cell precursors from nerve innervation are a cellular origin of melanocytes in skin. Cell. 139(2):366-79.

Adameyko I, Lallemend F. (2010) Glial versus melanocyte cell fate choice: Schwann cell precursors as a cellular origin of melanocytes. Cell Mol Life Sci. 67(18):3037-55.

Aicher WK, Alexander D, Haas C, Kuchen S, Pagenstecher A, Gay S, et al. (2003) Transcription factor early growth response 1 activity up-regulates expression of tissue inhibitor of metalloproteinases 1 in human synovial fibroblasts. Arthritis Rheum 48: 348–359.

Airola K, Karonen T, Vaalamo M, Lehti K, Lohi J, Kariniemi AL, et al. (1999) Expression of collagenases-1 and -3 and their inhibitors TIMP-1 and -3 correlates with the level of invasion in malignant melanoma. Br J Cancer 80: 733–743.

Alonso SR, Tracey L, Ortiz P. (2007) A high-throughput study in melanoma identifies epithelial-mesenchymal transition as a major determinant of metastasis. Cancer Res 67: 3450-3460.

Amour A, Slocombe PM, Webster A, Butler M, Knight CG, Smith BJ, et al. (1998) TNF-alpha converting enzyme (TACE) is inhibited by TIMP-3. FEBS Lett. 11;435(1):39-44.

Amour A, Knight CG, Webster A, Slocombe PM, Stephens PE, Knäuper V, et al. (2000) The in vitro activity of ADAM-10 is inhibited by TIMP-1 and TIMP-3. FEBS Lett 473:275-279.

Amour A, Knight CG, English WR, Webster A, Slocombe PM, Knäuper V, et al. (2002 The enzymatic activity of ADAM8 and ADAM9 is not regulated by TIMPs. FEBS Lett. 31;524(1-3):154-8.

Anderegg U, Eichenberg T, Parthaune T, Haiduk C, Saalbach A, Milkova L, et al., (2008). ADAM10 is the constitutive functional sheddase of CD44 in human melanoma cells. J Invest Dermatol 129: 1471-82.

Ansorge HL, Meng X, Zhang G, Veit G, Sun M, Klement JF, et al. (2009) Type XIV Collagen Regulates Fibrillogenesis: premature collagen fibril growth and tissue dysfunction in null mice. J Biol Chem 284: 8427-38.

Antonicelli F, Bellon G, Debelle L, Hornebeck W. (2007) Elastin-elastases and inflamm-aging. Curr Top Dev Biol. 79:99-155.

Aoudjit F, Vuori K (2012) Integrin Signaling in Cancer Cell Survival and Chemoresistance. Chemotherapy Research and Practice 283181: 16 pages

Badylak SF. (2002) The extracellular matrix as a scaffold for tissue reconstruction. Semin Cell Dev Biol. 3(5):377-83.

Balbín M, Fueyo A, Tester AM, Pendás AM, Pitiot AS, Astudillo A, et al. (2003) Loss of collagenase-2 confers increased skin tumor susceptibility to male mice. Nat Genet 35:252-257.

Balch CM, Houghton AN, Sober AJ, Soong S. (2003) Cutaneous Melanoma, 4th edition; Quality Medical Publishing: St. Louis MO USA.

Bandarchi B, Ma L, Navab R, Seth A, Rasty G. (2010) From melanocyte to metaststic malignant melanoma. Dermatol Res Pract 2010: 583748.

Baud V, Karin M. (2001) Signal transduction by tumor necrosis factor and its relatives. Trends Cell Biol. 11(9):372-7.

Beacham DA, Amatangelo MD, Cukierman E. (2007) Preparation of Extracellular Matrices Produced by Cultured and Primary Fibroblasts In: Current Protocols in Cell Biology. Chapter 10:Unit 10.9.

Bell JH, Amy HH, Li Y, Walcheck B. (2007) Role of ADAM17 in the ectodomain shedding of TNF-α and its receptors by neutrophils and macrophages. J Leukoc Biol. 82:173-176

Bergers G, Benjamin LE. (2003) Angiogenesis: Tumorigenesis and the angiogenic switch. Nat Rev Cancer 3:401-410.

Bigler D, Takahashi Y, Chen MS, Almeida EA, Osbourne L, et al. (2000) Sequence-specific interaction between the disintegrin domain of mouse ADAM 2 (fertilin β)and murine eggs. J. Biol. Chem. 275: 11576–11584.

Black RA, Rauch CT, Kozlosky CJ, Peschon JJ, Slack JL, Wolfson MF, (1997) A metalloproteinase disintegrin that releases tumour-necrosis factor-alpha from cells. Nature 385:729–733

Blobel CP (2005) ADAMs: key components in EGFR signalling and development. Nat Rev Mol Cell Biol. 6(1):32-43.

Boukamp P, Breitkreutz D, Stark HJ, Fusenig NE (1990) Mesenchyme-mediated and endogenous regulation of growth and differentiation of human skin keratinocytes derived from different body sites. Differentiation. 44: 150-61.

Birdwell CR, Gospodarowicz D, Nicolson GL (1978) Identification, localization and role of fibronectin in cultured endothelial cells. Proc Natl Acad Sci U S A 75: 3273-3277.

Brou C, Logeat F, Gupta N, Bessia C, LeBail O, Doedens JR, et al. (2000) A novel proteolytic cleavage involved in Notch signaling: the role of the disintegrin-metalloprotease TACE. Mol Cell 5: 207-216.

Butcher DT., Alliston T, Weaver VM. (2009). A tense situation: forcing tumour progression. Nat. Rev. Cancer 9, 108–122.

Calzascia T, Pellegrini M, Hall H, Sabbagh L, Ono N, Elford AR, et al. (2007) TNF-α is critical for antitumor but not antiviral T cell immunity in mice. The Journal of Clinical Investigation 117: 3833-3845.

Carey TE, Takahashi T, Resnick LA, Oettgen HF, Old LJ. (1976) Cell surface antigens of human malignant melanoma: mixed hemadsorption assays for humoral immunity to cultured autologous melanoma cells. Proc Natl Acad Sci U S A. 73(9):3278-82.

Cesaro A, Abakar-Mahamat A, Brest P, Lassalle S, Selva E, Filippi J et al. Differential expression and regulation of ADAM17 and TIMP3 in acute inflamed intestinal epithelia. Am J Physiol Gastrointest Liver Physiol 2009;296:1332-1343.

Chen G and Goeddel DV. (2002) TNF-R1 signaling: a beautiful pathway. Science 296: 1634-1635.

Chin L, Pomerantz J, Polsky D, Jacobson M, Cohen C, Cordon-Car. (1997) Cooperative effects of INK4a and ras in melanoma susceptibility in vivo. Genes Dev 11: 2822–2834.

Chirco R, Liu XW, Jung KK, Kim HR (2006) Novel functions of TIMPs in cell signaling. Cancer Metastasis Rev. 25(1):99-113.

Clark WH Jr, Elder DE, Guerry D, Epstein MN, Greene MH, Van Horn M (1984) A study of tumor progression the precursor lesions of superficial spreading and nodular melanoma. Hum Pathol 15: 1147-1165.

Cohen C, Zavala-Pompa A, Sequeira JH, Shoji M, Sexton DG, Cotsonis G, et al. (2002) Mitogen-acted Protein Kinase Activation Is an Early Event in Melanoma Progression. Clin Cancer Res 8: 3728-3733.

Cong L, Jia J (2011) Promoter polymorphisms which regulate ADAM9 transcription are protective against sporadic Alzheimer's disease. Neurobiol Aging. 32(1):54-62.

Coussens LM, Werb Z (2002) Inflammation and cancer. Nature 420: 860-861.
Dankort D, Curley DP, Cartlidge RA, Nelson B, Karnezis AN, Damsky WE Jr, (2009) Braf(V600E) cooperates with Pten loss to induce metastatic melanoma. Nat Genet 41: 544–552.

Davies H, Bignell GR, Cox C, Stephens P, Edkins S, Clegg S, et al. (2002) Mutations of the BRAF gene in human cancer. Nature 417: 949-54.

Dees C, Tomcik M, Zerr P, Akhmetshina A, Horn A, Palumbo K, et al. (2011) Notch signalling regulates fibroblast activation and collagen release in systemic sclerosis. Ann Rheum Dis. 70(7):1304-10.

Dehmel T, Janke A, Hartung HP, Goebel HH, Wiendl H, Kieseier BC. (2007) The cell-specific expression of metalloproteinase-disintegrins (ADAMs) in inflammatory myopathies. Neurobiol Dis. 25(3):665-74.

De Lorenzo MS, Ripoll GV, Yoshiji H, Yamazaki M, Thorgeirsson UP, Alonso DF et al. (2003) Altered tumor angiogenesis and metastasis of B16 melanoma in transgenic mice overexpressing tissue inhibitor of metalloproteinases-1. In Vivo. 17(1):45-50.

De Wever O and Mareel M (2003) Role of tissue stroma in cancer cell invasion J Pathol 200: 429-447.

De Young BR, Wick MR, Fitzgibbon JF, Sirgi KE, Swanson PE, (1993) CD31: an immuno-specific marker for endothelial differentiation in human neoplasms. Appl Immunohistochem 1:97–100.

Doedens JR, Black R. (2000) Stimulation-induced down-regulation of tumor necrosis factor-α converting enzyme. J. Biol. Chem. 275, 14598–14607.

Duffy MJ, McKiernan E, O´Donovan N, McGowan PM. (2009) Role of ADAMs in cancer formation and progression. Clin Cancer 15: 1140-1144.

Duffy MJ, Mullooly M, O'Donovan N, Sukor S, Crown J, Pierce A et al. (2011) The ADAMs family of proteases: new biomarkers and therapeutic targets for cancer? Clin Proteomics. 8(1):9.

Dyczynska E, Sun D, Yi H. (2007). Proteolytic processing of Delta-like 1 by ADAM proteases. J Biol Chem 282: 436-444.

Egeblad M, Werb Z. (2002) New functions for the matrix metalloproteinases in cancer progression. Nat Rev Cancer 2: 161–74.

Engelmann H, Aderka D, Rubinstein M, Rotman D, Wallach D. (1989). A tumor necrosis factor-binding protein purified to homogeneity from human urine protects cells from tumor necrosis factor toxicity. J Biol Chem 264: 11974-11980.

Eto K, Puzon-McLaughlin W, Sheppard D, Sehara-Fujisawa A, Zhang XP, Takada Y. (2000) RGD-independent binding of integrin α9β1 to the ADAM-12 and -15 disintegrin domains mediates cell–cell interaction. J Biol Chem 275: 34922–34930.

Fidler IJ. (1973) Selection of successive tumour lines for metastasis. 242: 148-9.

Fidler IJ. (1975) Biological behavior of malignant melanoma cells correlated to their survival in vivo. Cancer Res 35: 218-24.

Fox JW, Serrano SM. (2005) Structural considerations of the snake venom metalloproteinases, key members of the M12 reprolysin family of metalloproteinases. Toxicon. 45: 969-85.

Franzke C, Bruckner-Tuderman L, Blobel CP (2009) Shedding of collagen XVII/BP180 in skin depends on both ADAM10 and ADAM9. J Biol Chem 284: 23386-23396.

Fritzsche FR, Wassermann K, Jung M, Tölle A, Kristiansen I, Lein M, et al. (2008) ADAM9 is highly expressed in renal cell cancer and is associated with tumour progression. BMC Cancer 8:179.

Fridman JS, Scherle PA, Liu X, et al. Preclinical characterization of INCB7839, a potent and selective inhibitor of ErbB ligand and HER2 receptor shedding: inhibition of ADAM10 and ADAM17 for the treatment of breast cancer. Breast Cancer Res Treat 2007;106:S82.

Frohlich E, Schlagenhauff B, Mohrle M, Weber E, Klessen C, Rassner G. (2001) Activity, expression and transcription rate of the cathepsins B, D, H and L in cutaneous malignant melanoma. Cancer 91: 972-982.

Fry LY, Toker A. (2010) Secreted and membrane-bound isoforms of protease ADAM9 have opposing effects on breast cancer cell migration. Cancer Res 70: 8187-98.

Gandy, S. and Petanceska, S (2000) Regulation of Alzheimer-amyloid precursor trafficking and metabolism. Biochim. Biophys. Acta 1502: 44–52.

Garton KJ, Gough PJ, Raines EW. (2006) Emerging roles for ectodomain shedding in the regulation of inflammatory responses. J Leokoc Biol. 79(6):1105-1116.

Giard DJ, Aaronson SA, Todaro GJ, Arnstein P, Kersey JH, Dosik H, et al. (1973) In vitro cultivation of human tumors: Establishment of cell lines derived from a series of solid tumors. J Natl Cancer Inst 51: 1417–1423.

Gruber CJ, Gruber DM, Gruber IM, Wieser F, Huber JC. (2004) Anatomy of the estrogen response element. Trends Endocrinol. Metab. 15: 73-78.

Guaiquil V, Swendeman S, Yoshida T, Chavala S, Campochiaro PA, Blobel CP. (2009) ADAM9 Is Involved in Pathological Retinal Neovascularization. Molecular and Cellular Biology 29: 2694-2703.

Gluzman Y (1981) SV40-transformed simian cells support the replication of early SV40 mutants. Cell 23: 175-82.

Ha L, Noonan FP, De Fabo EC, Merlino G. (2005) Animal models of melanoma. J Investig Dermatol Symp Proc. 10(2):86-8.

Haghnegahdar H, Du J, Wang D, Burdick MD, Nanney LB, (2000) The tumorigenic and angiogenic effects of MGSA/GRO proteins in melanoma. J Leukoc Biol. 67(1):53-62.

Hanahan D, Weinberg RA. (2000) The hallmarks of cancer. cell 100: 57-70.

Hattori M, Osterfield M, Flanagan JG (2000) Regulated cleavage of a contact-mediated axon repellent. Science 289: 1360–1365.

Hawari FI, Rouhani FN, Cui X, et al (2004). Release of full-length 55KDa TNF receptor 1 in exosome-like vesicles: A mechanism for generation of soluble cytokine receptors. Proc Natl Acad Sci U S A 101: 1297-1302.

Hayakawa T, Yamashita K, Tanzawa K, Uchijima E, Iwata K (1992) Growth-promoting activity of tissue inhibitor of metalloproteinases-1 (TIMP-1) for a wide range of cells. FEBS 298: 29-32.

Herlyn D, Iliopoulos D, Jensen PJ, Parmiter A, Baird J, Hotta H, et al. (1990) In vitro properties of human melanoma cells metastatic in nude mice. Cancer Res 50: 2296-302.

Herlyn M, Berking C, Li G, Satyamoorthy K. (2000) Lessons from melanocyte development for understanding the biological events in naevus and melanoma formation. Melanoma Res. 10: 303-12.

Hikita A, Tanaka N, Yamane S, Ikeda Y, Furukawa H, Tohma S, et al. (2009) Involvement of a disintegrin and metalloproteinase 10 and 17 in shedding of tumor necrosis factor-alpha. Biochem Cell Biol 87: 581-93.

Hoashi T, Kadono T, Kikuchi K, Etoh T, Tamaki K. (2001) Differential growth regulation in human melanoma cell lines by TIMP-1 and TIMP-2. Biochem Biophys Res Commun. 288:371–379.

Hofmann UB, Westphal JR, Van Muijen GN, Ruiter DJ. (2000) Matrix metalloproteinases in human melanoma. J Invest Dermatol. 115(3):337-44.

Horiuchi K, Kimura T, Miyamoto T, Takaishi H, Okada Y, Toyama Y, et al. (2007) Cutting edge: TNF-alpha-converting enzyme (TACE/ADAM17) inactivation in mouse myeloid cells prevents lethality from endotoxin shock.J Immunol. 179:2686-9.

Hotoda N, Koike H, Sasagawa N, Ishiura S (2002) A secreted formof human ADAM9 has an α-secretase activity for APP. Biochem Biophys Res Commun 293: 800–805.

Howard L, Nelson KK, Maciewicz RA, Blobel CP (1999) Interaction of the metalloprotease disintegrins MDC9 and MDC15 with two SH3 domain-containing proteins, endophilin I and SH3PX1. J Biol Chem 274: 31693–31699.

Howard, L., Maciewicz, R.A., and Blobel, C.P. 2000. Cloning and characterization of ADAM28: Evidence for autocatalytic pro-domain removal and for cell surface localization of mature ADAM28. Biochem. J. 348: 21–27

Hsu MY, Wheelock M.J, Johnson KR, Herlyn M (1996). Shifts in cadherin profiles between human normal melanocytes and melanomas. J. Invest. Dermatol. Symp. Proc. 1: 188-194.

Hsu MY, Andi T, Meinkoth JL, Herlyn M. (2002) Cadherin repertoire determines partner-specific gap junctional communication during melanoma progression. J Cell Sci. 113 (Pt 9):1535-42.

Hüseman Y, Geigi JB, Schubert F, Musiani P, Meyer M, Burghart E, et al. (2007) Systemic spread is an early step in breast cancer. Cancer Cell 13: 58-68.

Iba K, Albrechtsen R, Gilpin B, Frohlich C, Loechel F, Zolkiewska A, et al. (2000) The cysteine-rich domain of human ADAM 12 supports cell adhesion through syndecans

and triggers signaling events that lead to β1 integrin-dependent cell spreading. J Cell Biol 149: 1143–1156.

Iozzo, RV (1998) Matrix proteoglycans: from molecular design to cellular function. Annu Rev Biochem 67: 609-652.

Izumi Y, Hirata M, Hasuwa H, Iwamoto R, Umata T, Miyado K, et al. (1998) A metalloprotease-disintegrin, MDC9/meltrin-gamma/ADAM9 and PKCdelta are involved in TPA-induced ectodomain shedding of membrane-anchored heparin-binding EGF-like growth factor. EMBO J 17: 7260-72.

Järveläinen HT, Iruela-Arispe ML, Kinsella MG, Sandell LJ, Sage EH, Wight TN (1992) Expression of decorin by sprouting bovine aortic endothelial cells exhibiting angiogenesis in vitro. Exp Cell Res 2: 395-401.

Jung KK, Liu XW, Chirco R, Fridman R, Kim HR. (2006) Identification of CD63 as a tissue inhibitor of metalloproteinase-1 interacting cell surface protein. EMBO J. 25(17):3934-42.

Kadler KE, Baldock C, Bella J, Boot-Handford RP. (2007) Collagens at a glance. J Cell Sci. 120(Pt 12):1955-8.

Kalluri R, Zeisberg M. (2006) Fibroblasts in cancer. Nat Rev Cancer 6: 392-401.

Karadag A, Zhou M, Croucher PI (2006) ADAM-9 (MDC-9/meltrin-γ), a member of the a disintegrin and metalloproteinase family, regulates myeloma-cell–induced interleukin-6 production in osteoblasts by direct interaction with the αvβ5 integrin. Blood 107: 3271-3278.

Kashima T, Vinters HV, Campagnoni AT. (1995) Unexpected expression of intermediate filament protein genes in human oligodendroglioma cell lines. J. Neuropathol. Exp. Neurol. 54: 23–31.

Keating GM, Santoro A. (2009) Sorafenib: a review of its use in advanced hepatocellular carcinoma. Drugs. 69(2):223-40.

Kees EP, Klun J, Bart Van Odijen, Claassen C, Eggermont AMM, Henzen-Logmans S, et al. (1996) Differential regulation of breast tumor cell proliferation by stromal fibroblasts of various breast tissue sources. Int J Cancer 65: 120-125.

Kerkelä E, Ala-aho R, Klemi P, Grénman S, Shapiro SD, Kähäri VM, et al. (2002) Metalloelastase (MMP-12) expression by tumour cells in squamous cell carcinoma of the vulva correlates with invasiveness, while that by macrophages predicts better outcome. J Pathol198: 258-69.

Kielty MP, Hopkinson I, Grant ME (1993) The Collagen Family: Structure, Assembly, and Organization in the Extracellular Matrix. In: Royce PM, Steinmann B, eds. Connective tissue and its inheritable disorders. New York: Wiley-Liss, 1993:103-47.

Klein CA (2009) Parallel progression of primary tumours and metastases. Nat Rev Cancer 9: 302-12.

Khokha R. (1994) Suppression of the tumorigenic and metastatic abilities of murine B16-F10 melanoma cells in vivo by the overexpression of the tissue inhibitor of the metalloproteinases-1. J Natl Cancer Inst. 86(4):299-304.

Kohga K, Takehara T, Tatsumi T, Ishida H, Miyagi T, Hosui A, et al. (2010) Sorafenib inhibits the shedding of major histocompatibility complex class I-related chain A on hepatocellular carcinoma cells by down-regulating a disintegrin and metalloproteinase 9. Hepatology. 51(4):1264-73.

Lai EC. (2004) Notch signaling: control of cell communication and cell fate. Development. 131(5):965-73.

Lakhani SA, Masud A, Kuida K, Porter GA Jr, Booth CJ, Mehal WZ, et al. (2006) Caspases 3 and 7: Key Mediators of Mitochondrial Events of apoptosis. Science 311: 785-6.

Lambert E, Boudot C, Kadri Z, Soula-Rothhut M, Sowa ML, Mayeux P, et al. (2003) Tissue inhibitor of metalloproteinases-1 signalling pathway leading to erythroid cell survival. Biochemical Journal. 372: 767-774.

Lantz M, Gullberg U, Nilsson E, Olssom I. (1990). Characterization in vitro of a human tumor necrosis factor-binding protein: A soluble form of tumor necrosis factor receptors. J. Clin Invest. 86: 1396-1402.

Lee SB, Schramme A, Doberstein K, Dummer R, Abdel-Bakky MS, Keller S, et al. (2010). ADAM10 is upregulated in melanoma metastasis compared with primary melanoma. J Invest Dermatol 130: 763-73.

Lendeckel U, Kohl J, Arndt M, Carl-McGrath S, Donat H, Röcken C. (2005) Increased expression of ADAM family members in human breast cancer and breast cancer cell lines. J Cancer Res Clin Oncol 131: 41–8.

Levental KR, Yu H, Kass L, Lakins JN, Egeblad M, Erler JT, et al. (2009) Matrix crosslinking forces tumor progression by enhancing integrin signaling. Cell. 139:891–906.

Li G, Fridman R, Kim HRC. (1999) Tissue inhibitor of metalloproteinase-1 inhibits apoptosis of human breast epithelial cells. Cancer Res. 59:6267–6275.

Li G, Satyamoorthy K, Meier F, Berking C, Bogenrieder T, Herlyn M (2003) Function and regulation of melanoma-stromal fibroblast interactions: when seeds meet soil. Oncogene. 22(20):3162-71.

Liotta LA and Kohn EC (2001) The microenvironment of the tumor-host interface. Nature 411: 375-379.

Loechel F, Fox JW, Murphy G, Albrechtsen R, Wewer UM. (2000) ADAM 12-S cleaves IGFBP-3 and IGFBP-5 and is inhibited by TIMP-3. Biochem Biophys Res Commun. 278(3):511-5.

Ludwig A, Hundhausen C, Lambert MH, Broadway N, Andrews RC, Bickett DM. (2005) Metalloproteinase inhibitors for the disintegrin-like metalloproteinases ADAM10 and ADAM17 that differentially block constitutive and phorbol ester-inducible shedding of cell surface molecules. Comb Chem High Throughput Screen. 8(2):161-71.

Lukashev ME, Werb Z. (1998). ECM signalling: orchestrating cell behaviour and misbehaviour. Trends Cell Biol. 8, 437-41.

Luzzi K. (1998) Multistep nature of metastatic inefficiency:dormancy of solitary cells after successful extravasation and limited survival of early micrometastasis. Am J Pathol 153: 865-873.

Martin J, Eynstone LV, Davies M, Williams JD, Steadman R. (2002). The role of ADAM 15 in glomerular mesangial cell migration. J Biol Chem 277: 33683–33689.

Mazzocca A, Coppari R, De Franco R, Cho JY, Libermann TA, Pinzani M et al. (2005) A secreted form of ADAM9 promotes carcinoma invasion through tumor–stromal interactions. Cancer Res 65: 4728–38.

Madhusudan S, Muthuramalingam SR, Braybrooke JP, Wilner S, Kaur K, Han C, et al. (2005) Study of etanercept, a tumor necrosis factor-alpha inhibitor, in recurrent ovarian cancer. J Clin Oncol 23: 5950-9.

Marian B, Danner MW. (1987) Skin tumor promotion is associated with increased type V collagen content in the dermis. Carcinogenesis. 8(1):151-4.

Mauch C, Zamek J, Abety AN, et al (2010). Accelerated wound repair in ADAM-9 knockout animals. J Invest Dermatol. 130: 2120-2130.

Mccarthy K, Maguire T, McGreal G, McDermott E, O'Higgins N, Duffy MJ. (199) High levels of tissue inhibitor of metalloproteinase-1 predict poor outcome in patients with breast cancer. Int J Cancer 84: 44–48.

McGowan PM, Ryan BM, Hill AD, McDermott E, O'Higgins N, Duffy MJ. (2007) ADAM-17 expression in breast cancer correlates with variables of tumor progression. Clin Cancer Res. 13(8):2335-43.

MacKie RM, Hauschild A, Eggermont AM. (2009) Epidemiology of invasive cutaneous melanoma. Ann Oncol. Suppl 6:vi1-7.

Meierjohann S, Schartl M, Volff JN. (2004). Genetic, biochemical and evolutionary facets of Xmrk-induced melanoma formation in the fish Xiphophorus. Comp Biochem Physiol C Toxicol Pharmacol 138: 281-9.

Meierjohann S. Schartl M. (2006). From mendelian to molecular genetics: the xiphophorus melanoma model. Trends Genet 22: 654-61.

Millichip MI, Dallas DJ, Wu E, Dale S, McKie N. (1998) The metallo-disintegrin ADAM10 (MADM) from bovine kidney has type IV collagenase activity in vitro. Biochem Biophys Res Commun 245: 594–598.

Mochizuki S and Okada Y (2007) ADAMs in cancer cell proliferation and progression. Cancer Sci 98: 621–628.

Moller Sorensen N, Vejgaard Sorensen I, Ornbjerg Wurtz S, Schrohl AS, Dowell B, Davis G, et al. (2008) Biology and potential clinical implications of tissue inhibitor of metalloproteinases-1 in colorectal cancer treatment. Scand J Gastroenterol 43: 774-786.

Monfort J, Tardif G, Reboul P, Mineau F, Roughley P, Pelletier JP et al. (2006) Degradation of small leucine-rich repeat proteoglycans by matrix metalloprotease-13: identification of a new biglycan cleavage site. Arthritis Res Ther. 8(1):R26. Epub 2006 Jan 3.

Mori S, Tanaka M, Nanba D, Nishiwaki E, Ishiguro H, Higashiyama S, et al. (2003) PACSIN3 binds ADAM12/meltrin alpha and up-regulates ectodomain shedding of heparin-binding epidermal growth factor-like growth factor. J Biol Chem. 278(46):46029-34.

Mueller MM, Fusenig NE. (2004) Friends or foes - bipolar effects of the tumour stroma in cancer. Nat Rev Cancer. 4(11):839-49.

Murphy G (2008) The ADAMs: signalling scissors in the tumour microenvironment. Nat Rev Cancer 12:929–941.

Nagase H (1997) Activation mechanisms of matrix metalloproteinases. Biol Chem 378:151–160.

Nath D, Slocombe PM, Webster A, Stephens PE, Docherty AJ, Murphy G (2000) Meltrin gamma (ADAM-9) mediates cellular adhesion through alpha(6)beta(1)integrin, leading to a marked induction of fibroblast cell motility. J Cell Sci 113: 2319–2328.

Nathanson SD (2003) Insights into the mechanisms of lymph node metastasis. Cancer 98: 413-423.

Navarini-Meury AA, Conrad C (2009) Melanoma and innate immunity--aActive inflammation or just erroneous attraction? Melanoma as the source of leukocyte-attracting chemokines. Semin Cancer Biol 19: 84-91.

Nelson KK, Schlondorff J, Blobel CP, (1999) Evidence for an interaction of the metalloprotease-disintegrin tumour necrosis factor α convertase (TACE) with mitotic arrest deficient 2 (MAD2), and of the metalloprotease-disintegrin MDC9 with a novel MAD2-related protein, MAD2β. Biochem. J. 343: 673–680.

Oksala N, Levula M, Airla N, Pelto-Huikko M, Ortiz RM, Järvinen O et al. (2009) ADAM-9, ADAM-15, and ADAM-17 are upregulated in macrophages in advanced human atherosclerotic plaques in aorta and carotid and femoral arteries--Tampere vascular study. Ann Med. 41(4):279-90.

Orimo A (2001) Cancer-associated myofibroblasts possess various factors to promote endometrial tumor progression. Clin Cancer Res 7: 3097-3105.

O'Shea C, McKie N, Buggy Y (2003) Expression of ADAM-9 mRNA and protein in human breast cancer. Int J Cancer, 105:754–61.

Otsuka T, Takayama H, Sharp R, Celli G, LaRochelle WJ, Bottaro DP. (1998) c-Met autocrine activation induces development of malignant melanoma and acquisition of the metastatic phenotype. Cancer Res 58:5157–5167.

Overwijk WW, Restifo NP. (2001) B16 as a mouse model for human melanoma. Curr Protoc Immunol. Chapter20:Unit 20.1.

Pan D, Rubin GM. (1997) Kuzbanian controls proteolytic processing of Notch and mediates lateral inhibition during Drosophila and vertebrate neurogenesis. Cell 90(2):271-80.

Parkin E, Harris B. (2009) A disintegrin and metalloproteinase (ADAM)-mediated ectodomain shedding of ADAM10. J Neurochem 108: 1464-79.

Parry DA, Toomes C, Bida L, Danciger M, Towns KV, McKibbin M et al. (2009) Loss of the metalloprotease ADAM9 leads to cone-rod dystrophy in humans and retinal degeneration in mice. Am J Hum Genet. 84(5):683-91.

Paszek MJ, Zahir N, Johnson KR, Lakins JN, Rozenberg GI, Gefen A. et al. (2005) Tensional homeostasis and the malignant phenotype. Cancer Cell 8: 241-254.

Patton EE, Nairn RS. (2010) Xmrk in medaka: a new genetic melanoma model. J Invest Dermatol. 130(1):14-7.

Patton EE, Mitchell DL, Nairn RS. (2010) Genetic and environmental melanoma models in fish. Pigment Cell Melanoma Res. 23(3):314-37.

Peduto L, Reuter VE, Shaffer DR, Scher HI, Blobel CP. (2005) Critical function for ADAM9 in mouse prostate cancer. Cancer Res 65.(20):9312-9.

Peduto L (2009) ADAM9 as a potential target molecule in cancer. Curr Pharm Des. 15:2282-7.

Poghosyan Z, Robbins SM, Houslay MD, Webster A, Murphy G, Edwards DR (2001) Phosphorylation-dependent interactions between ADAM15 cytoplasmic domain and Src family protein tyrosine kinases. J Biol Chem 277: 4999–5007.

Pollock PM, Cohen-Solal K, Sood R, Namkoong J, Martino JJ, Koganti A et al. (2003) Melanoma mouse model implicates metabotropic glutamate signaling in melanocytic neoplasia. Nat Genet 34: 108–112.

Provenzano PP, Inman DR, Eliceiri KW, Knittel JG, Yan L, Rueden CT et al. (2008) Collagen density promotes mammary tumor initiation and progression. BMC Med. 28:6-11.

Qi H, Rand MD, Wu X, Sestan N, Wang W, Rakic P, et al. (1999) Processing of the notch ligand delta by the metalloprotease Kuzbanian. Science. 283(5398):91-4.

Rath PC, Aggarwal BB. (1999) TNF-induced signaling in apoptosis. J Clin Immunol. 19(6):350-64.

Ray A, Schatten H, Ray BK, (1999) Activation of Sp1 and its functional co-operation with serum amyloid A-activating sequence binding factor in synoviocyte cells trigger synergistic action of interleukin-1 and interleukin-6 in serum amyloid A gene expression. J Biol Chem. 274(7):4300-8.

Refaeli Y, Bhoumik A, Roop DR, Ronai ZA. (2009) Melanoma-initiating cells: a compass needed. EMBO Rep. 0(9):965-72.

Ricca TI, Liang G, Suenaga AP, Han SW, Jones PA, Jasiulionis MG. (2009) Tissue inhibitor of metalloproteinase 1 expression associated with gene demethylation confers anoikis resistance in early phases of melanocyte malignant transformation. Transl Oncol 2:329-40.

Richard CD, Shoyab M, Brown TJ Gauldie J. (1993). Selective regulation of metalloproteinase inhibitor (TIMP-1) by oncostatin M in fibroblasts in culture. J Immunol 150: 5596-5603.

Richmond A, Su Y. (2008) Mouse xenograft models vs GEM models for human cancer therapeutics. Dis Model Mech. 1(2-3):78-82.

Roghani M, Becherer JD, Moss ML, Atherton RE, Erdjument-Bromage H, Arribas J, et al. (1999) Metalloprotease-disintegrin MDC9: Intracellular maturation and catalytic activity. J Biol Chem 274: 3531–3540.

Sahin U, Weskamp G, Zhou HM. (2004) Distinct roles for ADAM10 and ADAM17 in ectoddomain shedding of six EGFR-ligands. J cell Biol 164:769-79. 65(20):9312-9.

Satyamoorthy K, Li G, Gerrero MR. (2003) Constitutive Mitogen-activated Protein Kinase activation in melanoma is mediated by Both BRAF mutations and autocrine growth factor stimulation. Cancer Res 63: 756-759.

Schartl M, Wilde B, Laisney JA, Taniguchi Y, Takeda S, Meierjohann S. (2009) A mutated EGFR is sufficient to induce malignant melanoma with genetic background-dependent histopathologies. J Invest Dermatol130: 249-58.

Schopfer V, Weilbrock C, Marais R. (2007) Melanoma biology and new targeted therapy. Nature 445: 851-857.

Schwettmann L, Tschesche H. (2001) Cloning and expression in Pichia pastoris of metalloprotease domain of ADAM 9 catalytically active against fibronectin Protein. Expr Purif 21: 65–70.
Seals DF, Courtneidge SA. (2003) The ADAMs family of metalloproteases: multidomain proteins with multiple functions. Genes Dev. 17(1):7-30.

Slack BE, Ma LK, Seah CC. (2001) Constitutive shedding of the amyloid precursor protein ectodomain is up-regulated by tumour necrosis factor-α converting enzyme. Biochem. J. 357: 787–794.

Smith MR, Kung H, Durum SK, Colburn NH, Sun Y. (1997) TIMP-3 induces cell death by stabilizing TNF-alpha receptors on the surface of human colon carcinoma cells. Cytokine. 9: 770-80.

Soloway PD, Alexander CM, Werb Z, et al. (1996). Targeted mutagenesis of Timp-1 reveals that lung tumor invasion is influenced by Timp-1 genotype of the tumor but not by that of the host. Oncogene 13: 2307-2314.

Sorensen NM, Sorensen IV, Wurtz SO, et al. (2008). Biology and potential clinical implications of tissue inhibitor of metalloproteinases-1 in colorectal cancer treatment. Scand J Gastroenterol 43: 774-786.

Stetler-Stevenson WG. (1999) Matrix metalloproteinases in angiogenesis: a moving target for therapeutic intervention. J. Clin. Investig., 103:1237–1241.

Stewart, D. A., Cooper, C. R. and Sikes, R. A. (2004) Changes in extracellular matrix (ECM) and ECM-associated proteins in the metastatic progression of prostate cancer. Reprod. Biol. Endocrinol. 2: 2.

Szalad A, Katakowski M, Zheng X, , Chopp M. (2009) Transcription factor Sp1 induces ADAM17 and contributes to tumor cell invasiveness under hypoxia. J Exp Clin Cancer Res. 28:129.

Takeda S, Igarashi T, Mori H, Araki S. (2006) Crystal structures of VAP1 reveal ADAMs' MDC domain architecture and its unique C-shaped scaffold. EMBO J 25: 2388-96.

Tang A, Eller MS, Hara M, Yaar M, Hirohashi S, Gilchrest BA. (1994) E-cadherin is the major mediator of human melanocyte adhesion to keratinocytes in vitro. J Cell Sci. 107 (Pt 4):983-92.

Tormo D, Ferrer A, Gaffal E, Wenzel J, Basner-Tschakarjan E, Steitz J, et al. (2006) Rapid growth of invasive metastatic melanoma in carcinogen-treated hepatocyte growth factor/scatter factor-transgenic mice carrying an oncogenic CDK4 mutation. Am J Pathol 169: 665-672.

Turner SL, Mangnall D, Bird NC, Blair-Zajdel ME, Bunning RA. (2010) Effects of pro-inflammatory cytokines on the production of soluble fractalkine and ADAM17 by HepG2 cells. J Gastrointestin Liver Dis. 19(3):265-71.

Ulrich TA, de Juan Pardo EM, Kumar S. (2009) The mechanical rigidity of the extracellular matrix regulates the structure, motility, and proliferation of glioma cells. Cancer Res. 69(10):4167-74.

Ungerer C, Doberstein K, Bürger C, Hardt K, Boehncke WH, Böhm B et al. (2010) ADAM15 expression is downregulated in melanoma metastasis compared to primary melanoma. Biochem Biophys Res Commun. 401(3):363-9.

Urruticoechea A, Ian E Smith, Dowsett M. (2005) Proliferation Marker Ki-67 in Early Breast Cancer Journal of Clinical Oncology, 23: 7212-7220.

Valkovskaya NV. (2008) Hypoxia-dependent expression of ADAM8 in human pancreatic cancer cell lines. Exp Oncol. 30(2):129-32.

Van Kempen LC, Rijntjes J, Mamor-Cornelissen I, Vincent-Naulleau S, Gerritsen MJ, Ruiter DJ, et al. (2008) Type I collagen expression contributes to angiogenesis and the development of deeply invasive cutaneous melanoma. Int J Cancer 122: 1019-1029.

Van Muijen GNP, Cornelissen LM, Jansen CF, Figdor CG, Johnson JP, Brocker EB et al. (1991) Antigen expression of metastasizing and non-metastasizing human melanoma cells xenografted into nude mice. Clin Exp Metastasis 9 (3):259-72.

Van Raamsdonk CD, Bezrookove V, Green G, Bauer J, Gaugler L, O'Brien JM, et al. (2009) Frequent somatic mutations of GNAQ in uveal melanoma and blue naevi. Nature 457: 599–602.

Van Wart HE, Birkedal-Hansen H. (1990) The cysteine switch: a principle of regulation of metalloproteinase activity with potential applicability to the entire matrix metalloproteinase gene family. Proc Natl Acad Sci U S A. 87: 5578-82.

Visse R, Nagase H. (2003) Matrix metalloproteinases and tissue inhibitors of metalloproteinases: structure, function, and biochemistry. Circ Res. 92(8):827-39.

Vitale A, Denecke J. (1999) The endoplasmic reticulum-gateway of the secretory pathway. Plant Cell. 11: 615-28.

Ward M, Marcey D. (2001) Fibronectin, an Extracellular Adhesion Molecule. http://biology.kenyon.edu/BMB/Chime/Fibronectin/frames/fibrotxt.htm

Wang Q, Kaan HYK, Hooda RN, Goh SL, Sondermann H. (2008) Structure and plasticity of endophilin and sorting nexin 9. Structure 1: 1574-1587.

Weber IT, Harrison RW, Iozzo RV (1996) Model structure of decorin and implications for collagen fibrillogenesis. J Biol Chem. 271(50):31767-70.

Wenstrup RJ, Florer JB, Brunskill EW, Bell SM, Chervoneva I, Birk DE. (2004) Type V collagen controls the initiation of collagen fibril assembly. J Biol Chem. 279(51):53331-7.

Weskamp G, Kratzschmar J, Reid MS, Blobel CP. (1996) MDC9, a widely expressed cellular disintegrin containing cytoplasmic SH3 ligand domains. J Cell Biol.132: 717–726.

Weskamp G, Cai H, Brodie TA, Higashyama S, Manova K, Ludwig T, et al. (2002) Mice lacking the metalloprotease-disintegrin MDC9 (ADAM9) have no evident major abnormalities during development or adult life. Mol Cell Biol 22: 1537–1544.

White JM. (2003) ADAMs: modulators of cell-cell and cell-matrix interactions. Current Opinion in Cell Biology 15: 598-606.

Wurtz SO, Moller S, Mouridsen H. (2008) Plasma and serum levels of tissue inhibitor of metalloprrteinases-1 are associated with prognosis in node-negative breast cancer a prospective study. Mol Cell Proteomics 7: 424–430.

Yagami-Hiromasa T, Sato T, Kurisaki T, Kamijo K, Nabeshima Y, Fujisawasehara A. (1995) A metelloprotease-disintegrin participating in myoblast fusion. Nature 1995, 377:652-656.

Yoshiji H, Harris SR, Raso E, Gomez DE, Lindsay CK, Shibuya M, et al. (1998) Mammary carcinoma cells over-expressing tissue inhibitor of metalloproteinase-1 show enhanced vascular endothelial growth factor expression. Int J Cancer 75: 81-87.

Zheng Y, Saftig P, Hartmann D, Blobel C. (2004) Evaluation of the contribution of different ADAMs to tumor necrosis factor α (TNFα) shedding and of the function of the TNFα ectodomain in ensuring selective stimulated shedding by the TNFα convertase (TACE/ADAM17. J cell Biol 279: 42898-42906.

Zhu X, Bansal NP, Evans JP. (2000) Identification of key functional amino acids of the mouse fertilin β (ADAM2) disintegrin loop for cell–cell adhesion during fertilization. J. Biol. Chem. 275: 7677–7683.

Zigrino P, Mauch C, Fox JW, Nischt R. (2005) ADAM-9 expression and regulation in human skin melanoma and melanoma cell lines. Int J Cancer: 116:853–859.

Zigrino P, Steiger J, Fox JW, Löffek S, Schild A, Nischt R, et al. (2007) Role of ADAM-9 Disintegrin-cysteine-rich domains in human keratinocyte migration. J Biol Chem 282: 30785-30793.

Zigrino P, Kuhn I, Bäuerle T, Zamek J, Fox JW, Neuman S, et al. (2009) Stromal expression of MMP-13 is required for melanoma invasion and metastasis. J Biol Chem 129: 2686-2693.

Zigrino P, Nischt R, Mauch C. (2011). The disintegrin-like and cysteine-rich domains of ADAM-9 mediate interactions between melanoma cells and fibroblasts. J Biol Chem 286: 6801-6807.

Zigrino P and Mauch C. (2011) Proteases in Melanoma. Melanoma Development. 1st Edition, Vienna Springer, page 165-179, ISBN: 978-3-7091-0370-8.

Abbreviation

ADAM	a disintegrin and metalloprotease domain
BSA	bovine serum albumin
cDNS	complimentary deoxyribonucleic acid
c.m.	conditioned medium
Dll1	delata-like 1
DNA	deoxyribonucleic acid
dNTP	2'-Deoxynucleosine-5'-triphosphate
EDTA	ethylenediamine tetraacetic acid
ERE	estrogen response element
FCS	fetal calf serum
g	gram
H&E	hematoxylin and eosin
IF	immnunofluorescence
IHC	immunohistochemistry
IL	interleukin
kDa	kilodalton
NGS	normal goat serum
No.	number
M	meter
mM	millimolar
mm	millimetre
Mmp	matrix metalloproteinase
nm	nanometer
PFA	parafomaldehyde
PAGE	polyacrylamide gel electrophoresis
PBS	phosphate buffered saline
PCR	polymerase chain reaction
RNA	ribonucleic acid
rpm	rounds per minute
RT	reverse transcriptase
SD	standard deviation
SDS	sodium dodecylsulphate
SDS-PAGE	denaturant polyacrylamide gel electrophoresis
TIMP	tissue inhibitor of metalloprotease
TNF-α	tumor necrosis factor alpha
TNF RI	tumor necrosis factor receptor type I
TNF RII	tumor necrosis factor receptor type II
Tris	tri (hydroxymethyl)-aminomethane
U	unit
v/v	volume percentage
w/v	weight percentage
WB	western blot
WT	wild type
µ	micro
°C	degrees centigrade

Acknowledgement

Erklärung

Ich versichere, dass ich die von mir vorgelegte Dissertation selbstständig angefertigt, die benutzten Quellen und Hilfsmittel vollständig angegeben und die Stellen der Arbeit- einschließlich Tabellen, Karten und Abbildungen-, die anderen Werken im Wortlaut oder dem Sinn nach entnommen sind, in jedem Einzelfall als Entlehnung kenntlich gemacht habe; dass diese Dissertation noch keiner anderen Fakultät oder Universität zur Prüfung vorgelegen hat; dass sie - abgesehen von den unten angegebenen Teilpublikationen - noch nicht veröffentlich worden ist sowie, dass ich eine solche Veröffentlichung vor Abschluss des Promotionsverfahrens nicht vornehmen werde.

Die Bestimmungen der Promotionsordnung sind mir bekannt. Die von mir vorgelegte Dissertation ist von Frau Dr. Paola Zigrino und Frau Prof. Dr. Dr. Mauch betreut worden.

Ich versichere, dass ich alle Angaben wahrheitsgemäß nach bestem Wissen und Gewissen gemacht habe und verpflichte mich, jedmögliche, die obigen Angaben betreffenden Veränderungen, dem Dekanat unverzüglich mitzuteilen.

Teilpublikationen:

A.N. Abety, J. W. Fox, A. Schönefuß, J. Zamek, J. Landsberg, T. Krieg, C. Blobel, C. Mauch, and P. Zigrino. (2012)   Protective role of host-derived ADAM-9 in the progression of malignant melanoma *J Invest Dermatol in press*.

C. Mauch, J. Zamek, **A.N. Abety**, G. Grimberg, J.W. Fox, P. Zigrino. (2010) Role of ADAM-9 during wound repair. *J Invest Dermatol* 130(8): 2120-2130.

Zusätzliche Angaben, die nicht in dieser Arbeit enthalten:

Schönefuß A, **Abety AN**, Zamek J, Mauch C, Zigrino P. (2012) Role of ADAM-15 in wound healing and melanoma development *Exp Dermatol* 21(6):437-42.

Köln, den
Ngum Anna Abety

Curriculum vitae

Persönliche Daten:

Name: Ngum Anna Abety

Geburtsdatum: 13.07.1982

Geburstsort: Bafou-Djuttitsa, Cameroon

Staatsangehörigkeit: German

Wohnort: Nideggerstr. 4, 53115 Bonn

Schulausbildung:

1986-1993   Grundschule, Government Primary School, Cameroon

1993-1996   Mittlerereife, Our Lady of Lourdes Secondary School

1996-2000   Hochschulereife, Saker Baptist College, Limbe, Cameroon

2002-2005   Bachelor of Science in Biology

                            Fachhochschule Bonn-Rhein-Sieg

                            Bachelor-Arbeit: "Biofilms on oral surfaces: Aggregation of
                            Streptococcus Mutans using the human diabody derivative
                            of murine monoclonal antibody Guy´s 13"

2005-2007   Master of Science in Biology with Biomedical Sciences

                            Fachhochschule Bonn-Rhein-Sieg

                            Master-Arbeit: "MAPK p38 plays an essential role in NFκB
                            activation and gene transcription"

Promotion:

2008   Beginn der Promotion in der Klinik und Poliklinik für
                            Dermatologie und Venerologie der Uniklinik Köln

                            Arbeitsgruppe: Dr. Paola Zigrino/Prof. Dr. Cornelia Mauch

                            Thema der Promotion: "Role of host-derived ADAM-9 in
                            tumor invasion and metastasis of malignant melanoma"